

A mining research contract report  
OCTOBER 1984

# EM RESCUE (LOCATION) SYSTEM FOR DEEP MINES PHASE II – BUILD AND TEST BREADBOARD EQUIPMENT

Contract No. J0199009  
Develco, Inc.

BUREAU OF MINES  
UNITED STATES DEPARTMENT OF THE INTERIOR



<b>REPORT DOCUMENTATION PAGE</b>	<b>1. REPORT NO.</b>	<b>2.</b>	<b>3. Recipient's Accession No.</b>
<b>4. Title and Subtitle</b> EM Rescue (Location) System for Deep Mines Phase II - Build and Test Breadboard Equipment			<b>5. Report Date</b> October 1984
<b>7. Author(s)</b> F.B. Curry, T.C. Moore, L.H. Rorden, I.D. Schleicher			<b>8. Performing Organization Rep. No.</b> 1394-841015
<b>9. Performing Organization Name and Address</b> Develco, Inc. 404 Tasman Drive Sunnyvale, CA 94086			<b>10. Project/Task/Work Unit No.</b> 1394
			<b>11. Contract(C) or Grant(G) No.</b> (C) J0199009 (G)
<b>12. Sponsoring Organization Name and Address</b> U.S. Department of the Interior Bureau of Mines Washington, DC 20241			<b>13. Type of Report &amp; Period Covered</b> Final SEP 1981-OCT 1984
<b>15. Supplementary Notes</b>			<b>14.</b>
<b>16. Abstract (Limit: 200 words)</b>			
<b>ABSTRACT</b>			
<p>The purpose of this program is to extend electromagnetic (EM) techniques for use in locating miners trapped in mines as deep as 1000 m. A previously developed EM system is considered adequate for use at mines less than 300 m deep where it has a probability of detection of 54%. A system for deep mines must keep underground equipment simple, and use extremely low frequencies (ELF), sensitive receivers, and noise cancellation. The proposed location method, developed by Develco for other applications, is based on vector field measurements from two or more static sensors and computation of source location by iterative techniques. During Phase II, very sensitive search coil sensors were built and used in a separate test to verify the feasibility of atmospheric noise cancellation. A "Breadboard" location system version without cancellation, which is a fieldable test bed to evaluate receiving and location functions, was tested and supplied. Very good results were achieved from the first in-mine test with the transmitter at a depth of 380 m. It is expected the results of this work, and additional evaluation tests in the future, will be used to define the requirements for a prototype operational system.</p>			
<b>17. Document Analysis a. Descriptors</b>			
Deep mine rescue		Noise cancellation	
Trapped miner location		Extremely low-frequency noise	
Through-the-earth communication			
Quasi-static magnetic fields			
<b>b. Identifiers/Open-Ended Terms</b>			
Electromagnetic location methods			
Search coil sensors			
Atmospheric noise			
<b>c. COSATI Field/Group</b>			
<b>18. Availability Statement</b>		<b>19. Security Class (This Report)</b>	<b>21. No. of Pages</b>
Approved for public release, distribution unlimited		Unclassified	
		<b>20. Security Class (This Page)</b>	<b>22. Price</b>
		Unclassified	

## FOREWORD

This report was prepared by Develco, Inc., Sunnyvale, California under Contract J0199009. This contract was initiated under the Industrial Hazards and Communications program. It was administered under the technical direction of the U.S. Bureau of Mines Pittsburgh Research Center with John Durkin, Harry Dobroski, and Steve Shope acting as successive Technical Project Officers. Janice Johnson was the contract administrator for the Bureau of Mines. This report is a summary of the work recently completed as a part of this contract during the period September 1981 - October 1984. This report was submitted by the authors in December 1984.

There were no inventions or patents disclosed as a result of work performed on this contract.

We would like to thank the Kerr-McGee Chemical Corporation for permission to use their Hobbs Potash Facility for the in-mine tests on this program. Walter Case, Jr., Facility Manager; Mel Pyeatt, General Superintendent - Underground; John Philippus, Mines Engineer; and Bill Henderson - among others - provided valuable assistance for the tests. Rodger Sturgeon of Kerr-McGee, Oklahoma City, assisted in the planning stage. Steve Shope of the USBM Pittsburgh Research Center assisted with the underground operations. We would also like to thank Herb Mills and Calvin Walkingstick of the U.S. Geological Survey for their permission and assistance in using the Stonecanyon Seismological Observatory near Hollister, California for the noise cancellation tests project.

# CONTENTS

Page

Report Documentation Page .....	3
Foreward .....	4
1.0 Introduction .....	5
2.0 Breadboard Location System Equipment .....	9
2.1 Search Coil Sensors .....	11
2.2 Sensor Data Unit and Preamplifier .....	16
2.3 Location Analysis Unit .....	22
2.4 Beacon Transmitter .....	26
3.0 3-Axis Search Coil Calibration .....	29
A. Method of Measuring Voltages .....	31
B. Helmholtz Coil Adjustment .....	32
C. Search Coil Calibration .....	35
4.0 Test of Atmospheric Noise Cancellation by Using a Remote Sensor .....	44
4.1 Location and Set Up .....	44
4.2 Data Analysis .....	45
4.3 Conclusion .....	54
5.0 In-Mine Location Test .....	55
5.1 Site Description .....	55
5.2 Sensor System Installation .....	55
5.3 Transmitter Installation .....	61
5.4 System Functional Checkout .....	61
5.5 Location Test Data .....	65
5.6 Location Results .....	66
5.7 Discussion of Results .....	71
6.0 Conclusions and Recommendations .....	74
Appendix I. Summary of Method Used to Determine Power Spectral Density for Cancellation Tests .....	76
Appendix II. Location Test Data Sheets .....	77
References .....	106

# TABLES

	<u>Page</u>
2-1 Specifications - Develco Model 107310 3-Axis Search Coil Sensor .....	12
2-2 Specifications - Develco Model 107145-02 Data Unit ...	18
2-3 Sensor data unit and preamplifier calibration ratios..	21
2-4 Location analysis unit hardware .....	23
3-1 Helmholtz coil transfer function calibration .....	30
3-2 Orthogonality measurement before adjust cross trim ...	37
3-3 Final orthogonality measurements .....	38
3-4 Total search coil and Helmholtz alignment error after trim .....	39
3-5 Calibrated scale factor - search coil and post detection amplifier .....	41
3-6 Post detection amplifier .....	42
3-7 Scale factor referred to search coil output .....	43
4-1 Summary of cancellation results .....	50
5-1 Sensor positions and aximuthal orientations .....	59
5-2 Transmitter parameter measurement summary .....	63
5-3 Transmitter-loop parameters and moments .....	63
5-4 Typical measured atmospheric noise levels at 8Hz .....	64
5-5 Location results from in-mine field test .....	70
5-6 System signal-to-noise ratio vs. time .....	72

# ILLUSTRATIONS

		<u>Page</u>
2-1	Breadboard Location System .....	10
2-2	3-Axis Search Coil Sensor .....	13
2-3	Block Diagram - Search Coil and Post Detection Amplifier .....	14
2-4	Search Coil Frequency Response .....	15
2-5	Sensor Data Unit Block Diagram .....	17
3-1	Calibration Voltage Measurements .....	31
3-2	Helmholtz Crosscoupling Network .....	33
3-3A/B	Helmholtz Calibration Measurements .....	34
3-4	Search Coil in Test Stand .....	36
4-1	Noise Data Transmission Setup .....	46
4-2	Noise Data Receiving and Recording Setup .....	47
4-3	Relative Gain .....	48
4-4	Typical Spectral Display for a Horizontal Coil A. Individual Coil - Remote Site .....	51
	B. Noise Residue after Cancelling .....	51
4-5	Typical Spectral Display for Vertical Coils A. Local Site .....	52
	B. Remote Site .....	52
4-6	Comparison of Results with Theoretical Noise Limit .....	53
5-1	Plan View of In-mine Test Location .....	56
5-2	3-Axis Search Coil Surface Sensor Measures Signals from Transmitter-Loop in Mine .....	58
5-3	Sensor Data Unit Processes Signals and Displays Amplitude and Phase Information .....	58
5-4	Equipment Van Holds (left to right) Computer System, Sensor Data Units, and Tape Recorder..	60
5-5	Computer Calculates Transmitter Location Based on Information from the 3 Sensor Data Units...	60
5-6	Location Results from In-mine Field Test .....	62
5-7	Location Results from Data Sets 1-6.....	67
5-8	Location Results from Data Sets 12 and 13 .....	69
5-9	Location Results from Data Sets 15-20 .....	69

## 1.0 INTRODUCTION

The primary objective of this program is to extend electromagnetic (EM) techniques for use in locating miners trapped in deep mines through 1,000 m of overburden with bulk conductivities less than 0.01 Siemens/meter. In terms of signal energy, for a given practical underground transmitter size, this problem is on the order of 1,000 times more difficult - in regard to accuracies on the order of 1% - than has been demonstrated to date in shallower mines less than 300 m deep.

The U.S. Bureau of Mines has sponsored the development and testing of a VF (kHz frequencies) electromagnetic system for detection and location of miners trapped underground, which is considered adequate for use at those mines less than 300 m deep.<sup>1</sup> Recent field studies of this system in coal mines throughout the United States have shown that the probability of detecting a miner's signal from depths of 150 m and 300 m is about 95% and 54%, respectively.<sup>2</sup>

In the existing VF system approach the miner carries a small beacon transmitter that is powered for two to four days by a cap-lamp battery when operated in a pulse square wave mode (10% duty cycle). In the event of an emergency the miner deploys the transmitter's antenna, which consists of 300 feet (91 m) of 18-gauge copper wire, in as large a horizontal loop as possible. When the transmitter is turned on, the loop produces a quasistatic magnetic field similar in shape to the field from a nominally vertical bar magnet. A portable surface receiver and single axis loop antenna is used to locate the surface point approximately over the transmitter by searching for the horizontal magnetic field null which is located at a point perpendicular to the plane of the loop.

In order to conduct similar location operations in deeper mines, which comprise about 10% of the coal mines in the U.S. and have 20% of the miners, or to increase detection in the shallow mines, improvements are necessary.

During Phase I of this contract, the requirements for successful operation in deep mines were considered and various alternatives for transmitters, sensors, receivers, noise processing and determination of location were evaluated.<sup>3</sup>

There are practical physical limits on the size of transmitting antenna that can be conveniently carried, deployed in confined circumstances, energized in an intrinsically safe manner and used for accurate location. Thus it appears that the sizes of portable transmitter and antennas developed to date are close to optimum. Further gains in beacon performance will only be made by a combination of larger antenna wire, lighter conductor material, high efficiency transmitters and better batteries. Moderate increases in signal strength and in battery capacity can be achieved.

The key problem to be solved is the difficult one of detecting very small signals in the presence of high noise levels and obtaining enough information to accurately locate the beacons under difficult emergency conditions.

Advanced communication techniques such as impulsive noise processing, continuous (cw) signalling, and coherent detection methods must be utilized. Also, long-term integration (up to an hour or more in some cases) of the signal is essential to provide the accurate measurements needed to determine location of the transmitter. Most of the sophistication must be built into the surface receivers, using microprocessors for automatic processing, in order to keep the transmitters low cost and light weight.

The need for the strongest practical signal and continuous operation during the receiving process is essential for detection, but will considerably reduce battery life (by 1/2 to 1/4) compared with that obtained in the present system. The reduction can be minimized by using the techniques indicated above. The tradeoff of battery life versus signal strength should be considered in the future.

A precise, very low noise (high sensitivity) magnetic field sensor is the most important system component. The only two choices currently available that can approach the required sensitivity are cryogenic superconducting detectors (SQUID's) and search coils (induction coils). The cryogenic detectors require liquid helium, among other drawbacks, which is inappropriate for this type of field application. Using techniques developed by Develco, compact portable search coils with sensitivities better than SQUID's at frequencies above a few hertz have been designed for general field use.

The sensor must be stationary to prevent even very low-level vibration-induced rotations in the earth's magnetic field from inducing additional electrical interference in the signal band. Because of this stability requirement and the considerable time that may be needed for accurate signal measurement, a physical search for signal minimums is not feasible. Therefore, it is necessary to make vector field measurements with 3-axis sensors at two or more (depending on the geometry of the problem) known surface locations; iterative computational techniques are used to solve for the source location as Develco has done in previous applications.<sup>4</sup> This is quite an involved process but can be automated in practical field equipment.

Operation at frequencies between one and 10 Hz is dictated to optimize system performance as a function of noise, propagation and field scattering effects. At these frequencies, a practical transmitter at depths greater than 400 meters or so produces signal levels at the surface that are on the same order as, or less than, the natural atmospheric noise levels. Thus, some form of spatial or spectral noise cancellation technique is essential for signal detection and measurement at the deeper mines. (A 10 dB



reduction of noise reduces location time by a factor of 10.) Cancellation by using a remote sensor to sample essentially pure noise to be subtracted from the contaminated signal has been selected for initial evaluation since there is some evidence it does work, at least in some circumstances.<sup>5</sup>

There are two key areas that have not been addressed in detail to date because of a lack of data. Man-made noise at frequencies below 20 Hz (such as powerline switching transients) can be expected to be significant in some instances and may predominate after application of cancellation and processing. Propagation effects such as multipath signals, or scattering from conducting and magnetic inhomogeneities can result in significant signal errors. There is limited in-mine experience<sup>6</sup> that suggests scattering is not a serious problem at low frequencies, but this must be checked under conditions more representative of this application. Extensive field experience is needed to determine if these potential problems do have a significant effect on system operation and, if so, what the best solutions are.

The objective of the recently completed Phase II contract work was to construct a "breadboard" location system and conduct preliminary tests with it. This preliminary system is a fieldable test bed to evaluate the receiving and locating functions and to collect additional data. The primary Phase II test goals were to verify the sensor sensitivity, noise cancellation (in a separate test), noise processing, and location method operation (including in a mining environment). It is expected the Bureau will conduct additional tests at a number of other mines in order to evaluate the system under various conditions and, ultimately, define the requirements for a prototype operational system.

Four triaxial search coil sensors were built and tested to verify the required sensitivity and accuracy could be achieved. The first two were used in a preliminary long baseline (5-10 km) noise cancellation experiment to confirm feasibility and determine how (and whether) to implement cancellation in a fully operational prototype system. In general, three sensors will be used in a triangular array, with a spacing on the same order as the transmitter depth to provide resolution and area coverage. A three-sensor co-linear array, which may be useful for some mine or terrain situations, was used for the in-mine test. The fourth sensor will be used for additional cancellation tests in the future.

Three microprocessor-based Develco Model 107145 Sensor Data Units (SDUs -used in an EM navigation system for horizontal drilling), which incorporate automatic signal processing, were adapted for use as the receivers in this application. A GRID Compass portable personal computer was used as the Location Analysis Unit (LAU) to perform the location calculations for the preliminary field tests using the copyrighted location software developed by Develco. Data entry is accomplished manually in this system version. Two standard VF transmitters (GI P/N 852-1476) were modified to operate at low frequency for the location

tests, but there was no attempt to improve their efficiency. Finally, an in-mine test was conducted at moderate depths (approximately 400 m) to evaluate the system operation under nominal conditions without the added complexity of noise cancellation in this initial test phase.

This report discusses the Phase II work with emphasis on the test results.

## 2.0 BREADBOARD LOCATION SYSTEM EQUIPMENT

The "Breadboard" system components, shown in Figure 2-1, were used to test key functions of the location method concept that had been proposed for use in deep mines (up to 1 km depth), in order to completely specify the design requirements for an operational prototype version of the EM Rescue System.

The signals for the system are generated by an underground beacon transmitter, with a 300-foot (or greater) circumference loop antenna laid out in an approximately horizontal plane. This produces a low frequency alternating magnetic field equivalent to that of a nearly vertical magnetic dipole perpendicular to the plane of the loop. The field is quasi-static, i.e., nonradiating, and decays rapidly with distance from the transmitter. A version of the present miner location VF transmitter was modified to produce low frequency signals for the "Breadboard" system tests. Since this transmitter version is unregulated, it was powered by two cap-lamp batteries in parallel to achieve better amplitude stability and longer operational time for the purpose of the tests.

The "Breadboard" EM location system uses an array of three triaxial sensors on the surface to make vector field measurements of the signals produced by the transmitter. They are set up in known positions and orientations that are in the general area nearly over the probable transmitter location. The array pattern may be either linear or, more generally, triangular (depending on the mine configuration) with a spacing between sensors and maximum offset of the array on the order of the depth to the transmitter. (Lateral offset of a linear array should be less.) The plane (or line) containing the sensors (or loop antenna) does not have to be level, but severe tilts may require operator assistance to achieve the correct location.

Three sensors will often be sufficient for use at mines on the order of 300 to 400 m deep, which was the goal for preliminary tests of the "Breadboard" system location (only) functions. At mines up to 1,000 m in depth, an additional sensor is required for noise cancellation in operational systems. This results from the fact that natural atmospheric noise levels, at the low operating frequencies required to minimize the effects of earth conductivity, are very high compared to the weak surface signals from transmitters at the greater depths. Under these conditions, the time required for signal integration to achieve a suitable signal-to-noise ratio (SNR) for accurate location is unacceptable. Since the propagating atmospheric noise fields change slowly over reasonably uniform earth, it is possible to coherently cancel most of the noise at the local sensors by sensing noise only at a remote location. A separate test of this method was conducted as described in Section 4.

The search coil sensors used in the "Breadboard" system tests have an intrinsic system noise level slightly lower than the expected atmospheric

BREADBOARD LOCATION SYSTEM EQUIPMENT

The breadboard system components, shown in Figure 2-1, were used to test key functions of the location method concept that had been programmed for use in step three (up to 1 km accuracy) in order to compare, specifically, the basic requirements for an operational prototype version of the EM location system.

The signals for the transmitter, with a 100 kHz carrier frequency, are produced by a low frequency oscillator. The oscillator is a simple LC circuit with a variable capacitor and a coil. The field is quasi-static, and the signals are transmitted from the transmitter to the receiver. The receiver was modified to produce a signal that is proportional to the distance between the transmitter and receiver. This signal is then processed by the computer to determine the location of the transmitter and receiver.

The breadboard system is shown in Figure 2-1. It consists of a transmitter, a receiver, a computer, and a power supply. The transmitter and receiver are connected to the computer via cables. The power supply provides power to the transmitter and receiver. The computer is used to process the signals from the transmitter and receiver to determine the location of the transmitter and receiver.

The breadboard system is shown in Figure 2-1. It consists of a transmitter, a receiver, a computer, and a power supply. The transmitter and receiver are connected to the computer via cables. The power supply provides power to the transmitter and receiver. The computer is used to process the signals from the transmitter and receiver to determine the location of the transmitter and receiver.

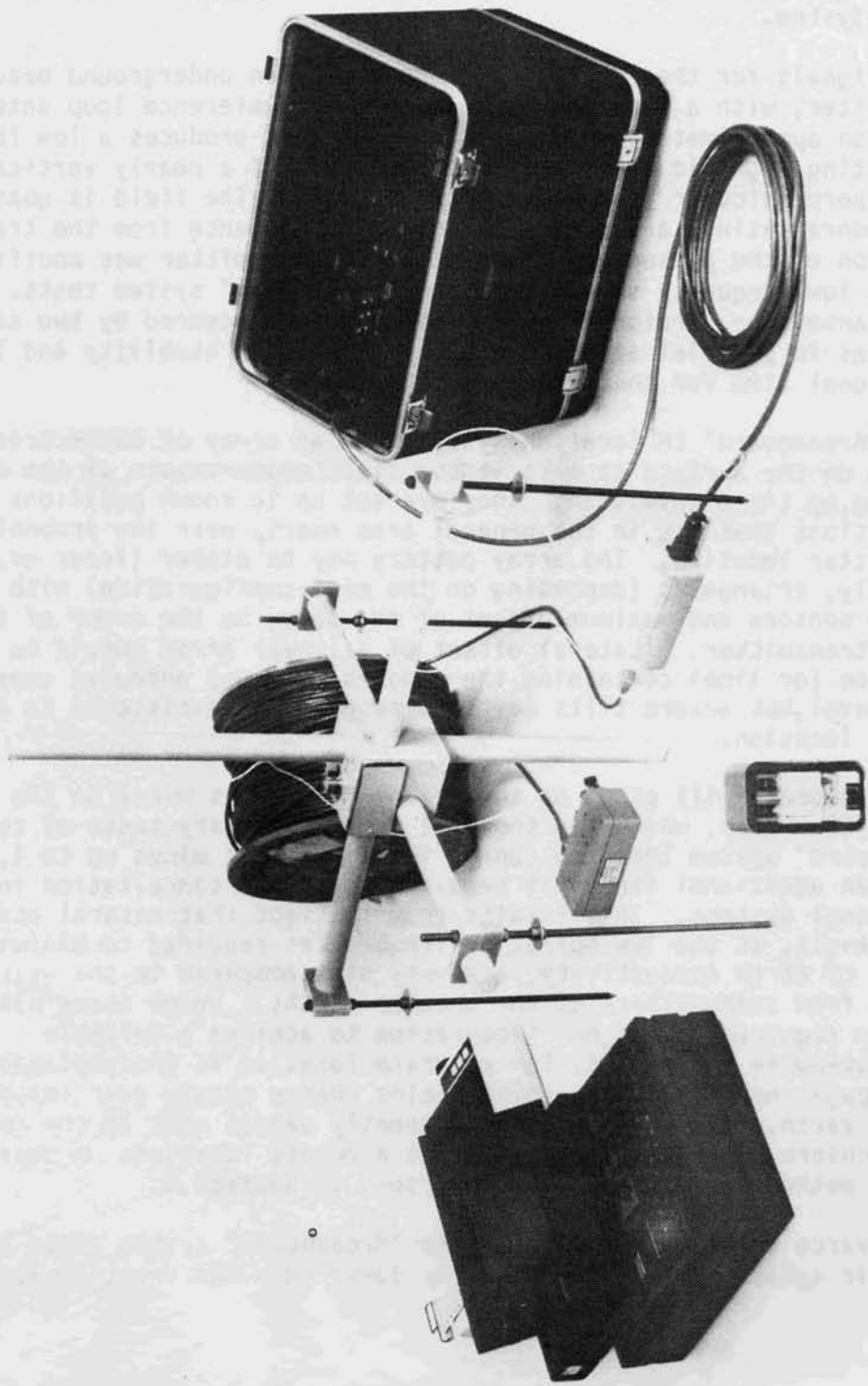


FIGURE 2-1. Breadboard Location System.

noise cancellation levels. The goal is to be able to achieve a 40- to 60-dB SNR with a signal integration time of an hour or less although longer times may be required under poorer conditions or to achieve greater accuracy. Each of the three sensors used for location are connected by a cable to a Sensor Data Unit for automatic detection of the signals and preprocessing of the data. The Location Analysis Unit (LAU) processes the measurements from the SDU's and solves for the most likely location of the transmitter.

## 2.1 SEARCH COIL SENSORS

The Model 107310 triaxial search coil specifications are given in Table 2-1 and the overall dimensions are shown in Figure 2-2. The search coils have the high degree of sensitivity and accuracy required for accurate location work in a relatively compact form. It is possible to break the structure down to elements that are easy to transport and then reassemble quickly and accurately at any required location.

Each axis of the array consists of a copper wire solenoid wound around a highly permeable core and is electrostatically shielded. The solenoid is encapsulated in a fiberglass tube which can be accurately and reproducibly aligned. The three rods required for a complete vector field measurement sensor, are held by screw clamps in a central hub. The rods are sufficiently rigid so that accurate alignment can be maintained without the need for additional struts between the ends.

In order to minimize the profile, the lower end of the vertical rod can be inserted in a hole, when circumstances permit. A rigid supporting structure can be used on hard surfaces. Mounting feet with adjustable screws are clamped on the ends of the horizontal rods for leveling the structure by using a precision bubble level mounted on the hub. The unit is roughly aligned in the preferred direction. A transit or portable laser level (construction type) is used to precisely determine azimuth by sighting on an optical mirror, mounted on the hub, and measuring the reflection angle. A secure, noncontacting wind screen must be placed over the sensor to minimize mechanical vibration.

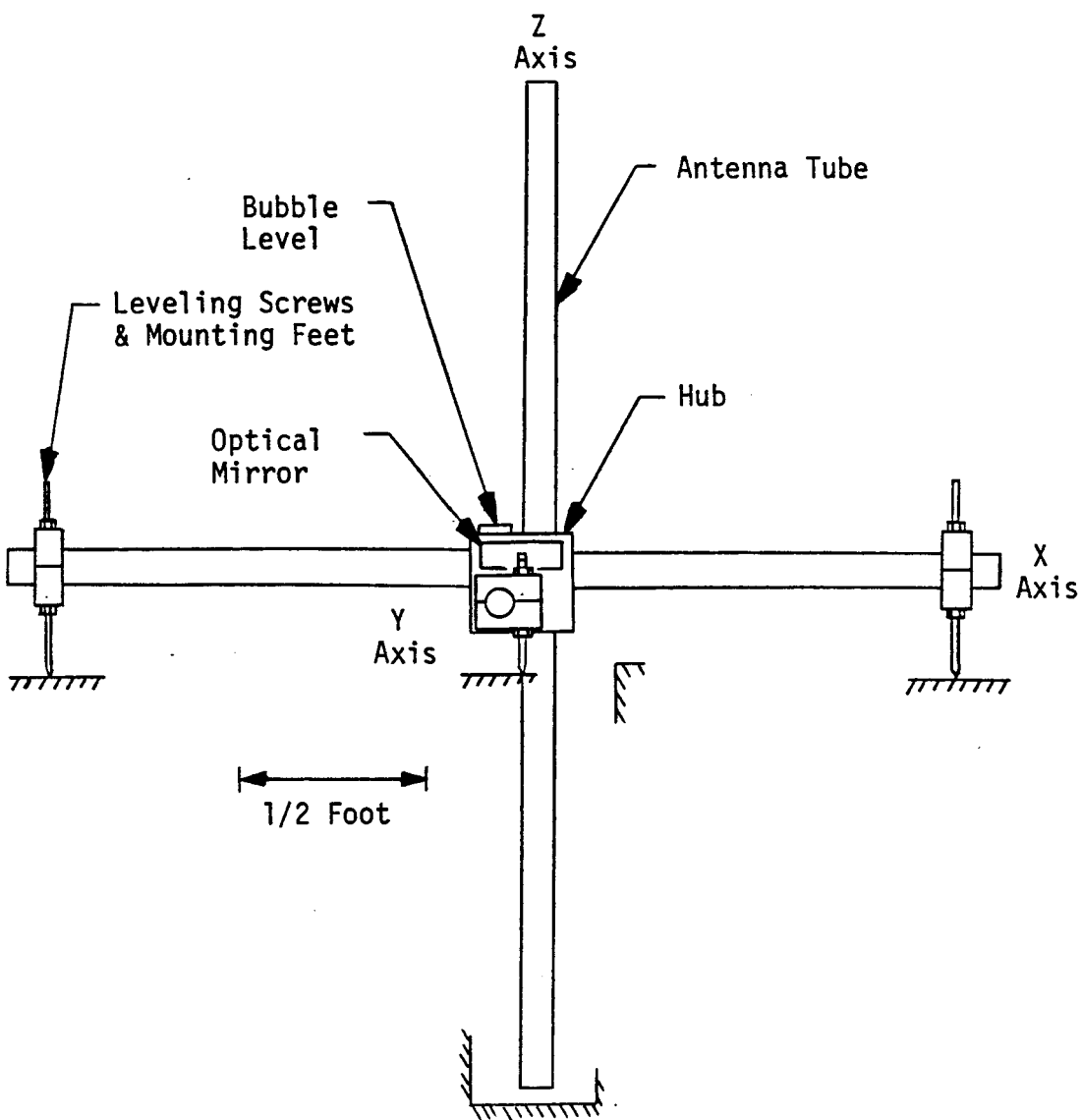
The electronics block diagram for the search coil is shown in Figure 2-3. The preamplifier and feedback circuit built into each coil rod provide a flat frequency response from approximately 0.2 Hz to 200 Hz. The preamplifier front end utilizes low noise FET's selected for a noise voltage density of approximately  $5 \text{ nV}/\sqrt{\text{Hz}}$ . The overall effective noise level of each axis of the search coil is equivalent to -156 dB Ho (or  $H_{no} = 15.9 \times 10^{-9} \text{ A/m}/\sqrt{\text{Hz}}$ ) at 10 Hz and varies approximately inversely with frequency.

A separate, so-called post detection amplifier provides additional gain, notch filtering for powerline interference, and orthogonality trimming for the 3-axis search coil assembly. It is placed close to the coil assembly to minimize possible noise pickup on the coil output lines. In the simple version used for the "breadboard" system tests (Figure 2-3),

Intrinsic Noise Level	-153 dBHo* at 10 Hz (varies approximately as 1/f)
Scale Factor	20 V/A/m (Nominal. Calibrated to an accuracy of approximately $\pm 0.1\%$ )
Maximum Linear Output Voltage	$\pm 5$ V peak
Bandwith	Approximately 0.2 to 200 Hz (before 60 Hz notch filter)
Orthogonality	$< 0.1^\circ$ (calibrated with correction in hardware)
Power Supply	Eight AA-size batteries (12 V)
Size	1-3/8 inch OD x 34 inches (each axis)
Weight	Search Coil 21 pounds; Amplifier 2 pounds
Operating Temperature	-40°C to +60°C (design goal); (-40°F to +140°F)

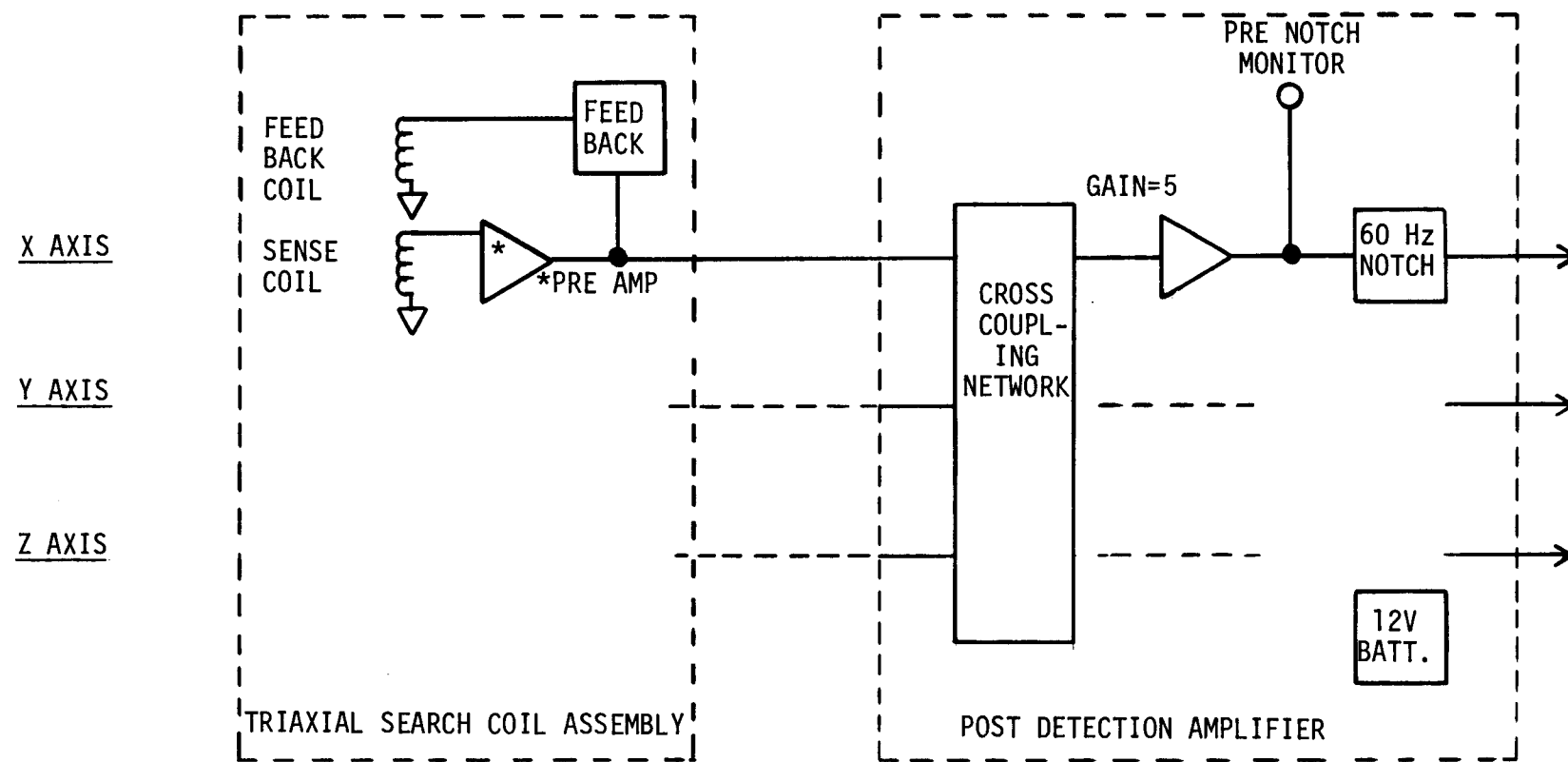
\*dBHo is relative to  $1 \text{ A}^2/\text{m}^2\text{Hz}$ .

Table 2-1. Specifications - Develco Model 107310 3-Axis Search Coil Sensor (with Model 107315 Post Detection Amplifier)



3-Axis Search Coil Sensor

FIGURE 2-2



Block Diagram  
 Search Coil and Post Detection Amplifier

FIGURE 2-3



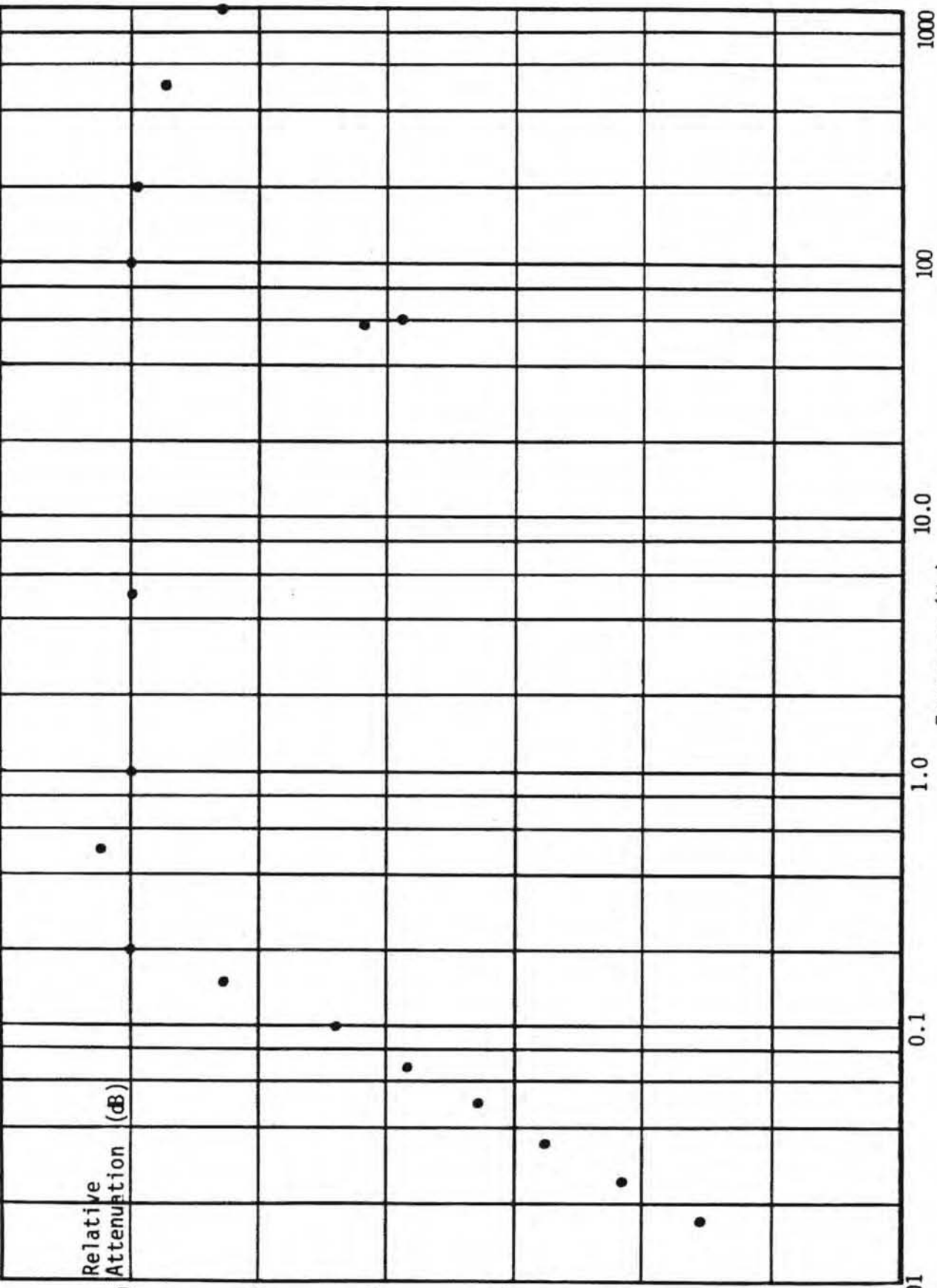


FIGURE 2-4. Search Coil Frequency Response

the gain ratio was limited to five to minimize the possibility of saturation in high level powerline fields such as in the lab and calibration tests. Also, a single 60-Hz notch filter with an attenuation of approximately 35 to 40 dB was used.

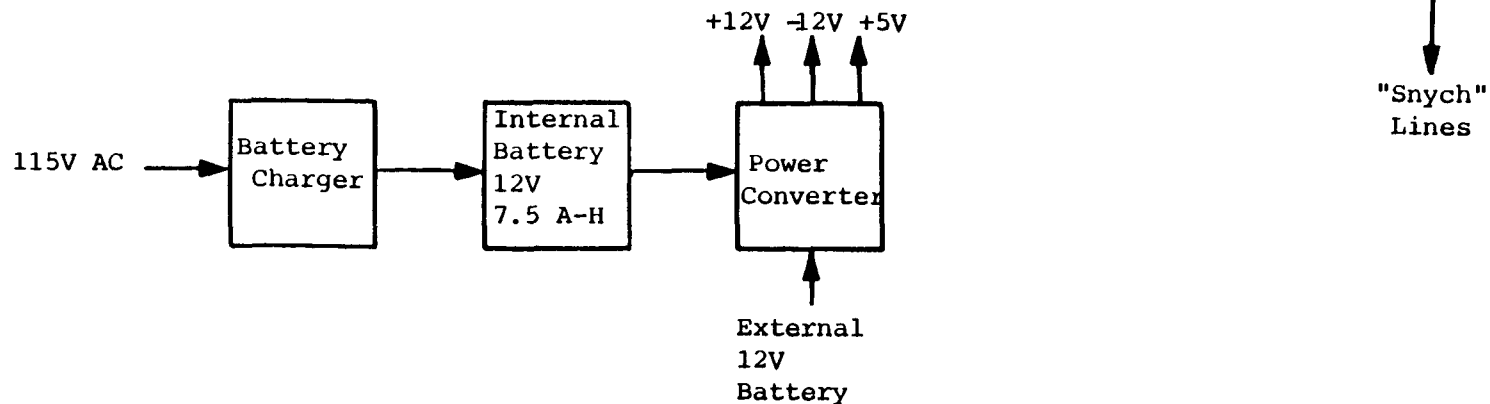
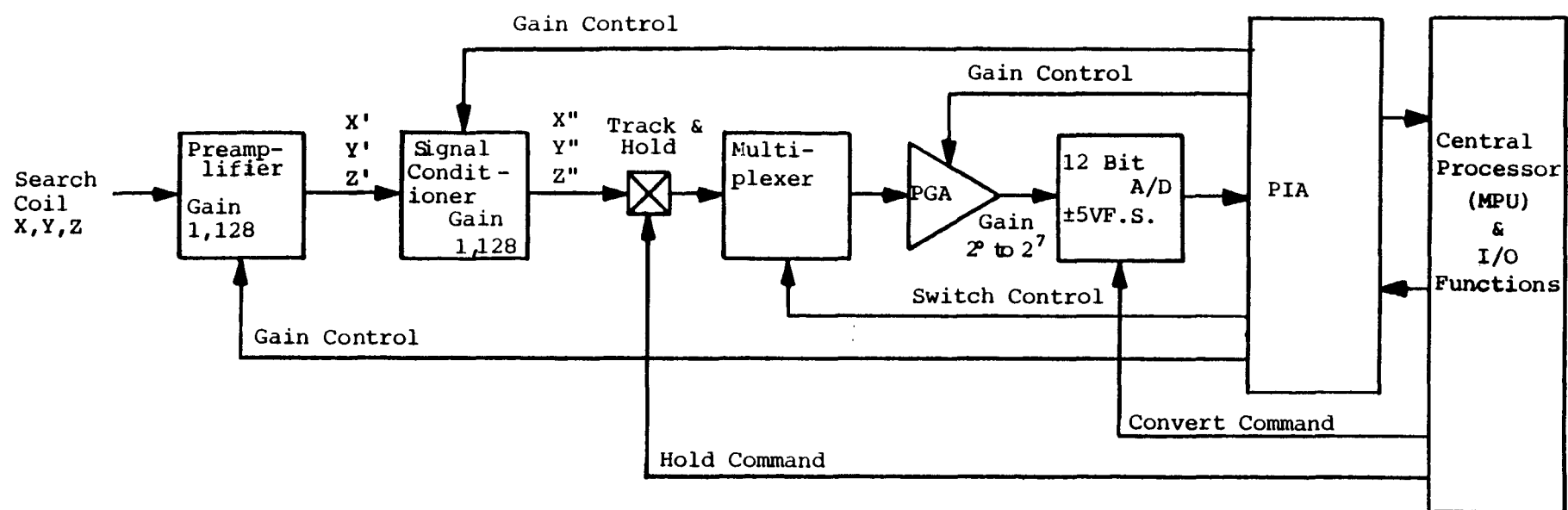
The overall frequency response of a typical search coil and post detection amplifier channel is shown in Figure 2-4. The amplifier outputs are transmitted to the receiver over a 22-gauge, three twisted shielded pair, 1,000 foot cable.

Because the triaxial search coil structure is inherently asymmetrical, there is some magnetic coupling between the axes. To achieve better than 0.1 degree orthogonality, this coupling must be carefully "trimmed" out on each unit, during the calibration process. This is done with an adjustable resistor network that supplies a small sample of signal from each axis to be subtracted from each of its transverse axes to cancel the coupling. Thus, each post detection amplifier is matched to a particular search coil assembly set. If, in the future, it is found that 1/4 degree (or so) orthogonality is adequate, then it appears that no adjustment will be required.

## 2.2 SENSOR DATA UNIT AND PREAMPLIFIER

The Sensor Data Unit (SDU), Model 107145-02, and its associated Preamplifier, Model 107096, were modified to serve as the signal receivers in the "Breadboard" location system. These units are part of a Develco proprietary electromagnetic guidance system for horizontal boring. Their basic function is to provide wideband filtering, automatic gain control and digital conversion, in hardware; and impulsive noise processing, narrow-band filtering, coherent signal detection and phase tracking, in software. The modifications for the location tests consist of minor preamplifier changes and the addition of a "Synch" function, to measure relative phase of the three SDU's, a block averaging function for long-term integration of the signal, and display of the detected field amplitudes. The nominal specifications and block diagram of functions are shown in Table 2-2 and Figure 2-5, respectively.

The combination of the external preamplifier and internal signal conditioner board provide an overall 3 dB bandwidth of from approximately 1-1/2 to 20 Hz, for anti-alias filtering and powerline frequency rejection. The input of the preamplifier was modified to provide a unity gain differential amplifier for rejecting common-mode pickup on the 1,000-foot cable to the sensor and its post detection amplifier. Notch filters were also added to reject the third harmonic of a square wave signal to prevent generation of very low beat frequencies in the impulsive noise limiting process. These beat frequencies are due to transmitter and SDU clock frequency differences and would adversely affect the long-term averaging process. Both the preamplifier and the signal conditioner have a programmable gain control of either unity or 128 ( $2^7$ ), which is automatically selected by the microprocessor unit (MPU).



Sensor Data Unit Block Diagram

FIGURE 2-5

Operating Frequency*	10-2/3 Hz
Frequency Stability	±100 ppm over the temperature range
Analog Bandwidth	Approximately 1-1/2 to 20 Hz
Powerline Frequency Rejection	>80 dB at 60 Hz >65 dB at 120 Hz >70 dB at 180 Hz
Input Voltage	±5 V max.
Total Variable Gain	1 to 2 <sup>21</sup> (126 dB) max.
Gain Calibration	±0.1%
Phase Tracking (Channel-to-channel at signal frequency)	≤2°
Noise Level (Referred to preamplifier input)	<-160 dBHo
A/D Converter	12 bit, ±5 V full scale
Track and Hold	<2-1/2 μS
Signal Input Channels	3
Power Supply	115 V or 220 V, 50/60 Hz (<50 W max) or 12 V internal battery (<4 hour operation) or 12 V external battery
Operating Temperature	-20 to +60°C
Size	SDU 13.5" Dp x 20" W x 19"H (transit case)
	PREAMP 3-1/8" W x 2-1/4" H x 6-7/8" L
Weight Approx.	SDU: 55 lbs. PREAMP: 2 lbs.

\*Default value. May also be programmed to operate at 2-2/3 and 5-1/3 Hz. A preamplifier notch filter change is also needed for satisfactory long-term integration with square wave signals.)

Table 2-2. Specifications - Develco Model 107145-02 Sensor Data Unit (with Model 107096 Preamplifier)

The software is written to accommodate four discrete signal frequencies, but only two are useful in this version because of preamplifier hardware limitations. The default operating value stored in memory (PROM) is 10-2/3 Hz and the system will automatically operate at this frequency when turned on. An operating frequency of 5-1/3 Hz may be entered by the SDU key pad. The operating frequency is derived from the MPU crystal oscillator which has a stability of  $\pm 100$  ppm over the temperature range.

Data sampling by the Analog-to-Digital (A/D) board functions is also controlled by the MPU software. Each of the three search coil axis channels are connected to individual track-and-hold circuits; these are directly controlled by the nonmaskable interrupt (NMI) process and sampled at a 170-2/3 Hz rate. The signal channels are then multiplexed, amplified by a 3-bit programmable gain amplifier (PGA) with a gain from  $2^0$  through  $2^7$ , and digitized by a 12-bit A/D converter. (In addition to the signal data, one of nine subcommutated data channels are also sampled. Three of these are used for internal housekeeping functions and A/D zero bias correction of each sample and the others are unused in this version.) A/D conversion is not NMI controlled but occurs in the interval before the next channel is multiplexed.

The signal sample data is stored along with the gain at which it was taken and other information for gain control. The gain of each of the three channels is always the same at a given time. If a gain change affects either the preamp or signal conditioner, one or two 1.5-second frames will be skipped (two for preamp) to allow for amplifier settling.

Impulsive noise processing (INP) does not occur during the first pass of the routine operation. The data samples are simply summed into the equivalent of a single cycle for processing to determine the initial estimate of the in-phase and quadrature components of the signal. Once an estimate of the signal amplitude and relative phase in each axis have been determined, each sample may then be symmetrically limited to reduce the effect of impulsive noise. This process consists of subtracting the estimated signal contribution from each sample, limiting the remainder and processing the remainder for coherent signal.

Data filtering and the second level of data processing occurs once all the raw data have been reduced. This process includes the computations of gain, filtered signal amplitude and phase, Signal-to-Noise ratio (SNR) and other variables required for impulsive noise processing. The variable computations will differ for the nonreference and reference channels. In the location application, the reference channel is automatically selected during the initial evaluation process, based on the best SNR, and used to track the phase of the SDU relative to the signal. Once selected, it remains fixed. Prior to the selection of a reference channel, all channels are treated the same and use the same computations as would a reference channel.

When the system is first turned on or is reset, it goes through a fast settling mode as part of the initial acquisition process. The required gain is determined by a successive approximation method starting with a value of  $2^{16}$ . After testing any trial gain, the process may decide that it satisfies the requirements. If a gain change would set the gain outside of the hardware limitations ( $2^0$  to  $2^{21}$ ), a warning message is displayed.

The output from the impulsive noise limiting process is low pass filtered by a second-order filter with a damping factor of 0.9 and a time constant of 15 seconds (noise bandwidth approximately 0.01 Hz). The signal output of these filters is used for all other internal receiver functions. It is also long term integrated by a simple continuous block averaging process to improve the signal-to-noise ratio (SNR) of the amplitude values displayed for use in the location calculation. The long term averaging can be reset at any time without restarting the entire signal acquisition process.

The long-term average output amplitude is displayed in RMS pico-tesla, along with phase in degrees, and SNR in db for each channel on a 40-character, electro-luminescent display. The X channel appears on the default line and the other lines are toggled with the key pad. Conversion of the SDU input voltage to equivalent field at the sensor assumes a sensor scale factor of 20 V/(A/M) and a post detection amplifier gain of five. Precise calibration ratios are applied during the location calculation process to achieve a more accurate result. The SDU and preamplifier set calibrations are given in Table 2-3. (See Section 3, Table 3-5, for the search coil values.)

The channel phases displayed are with respect to the SDU clock for the reference channel, and with respect to the reference channel for the other two channels. Ideally, the two nonreference channels will be either in phase ( $0^\circ$ ) or exactly out of phase ( $180^\circ$ ) with respect to the reference channel. A warning is issued if a phase anomaly greater than  $30^\circ$  is detected (i.e., if the nonreference channels deviate more than  $30^\circ$  from being exactly in or out of phase with the reference channel). Possible causes of phase anomalies are electrical interference, field scattering from conducting structures, very low signal levels, or problems in the equipment.

Since the phase of each of the three SDU clocks is arbitrary, they must have a common reference for use in the location calculations. This is accomplished by a so-called "Synch" cable interconnection between the units to measure the phase of two secondary units with respect to a primary unit. The primary SDU is indicated by a shorting wire in the primary cable connector connected to that SDU. Each SDU polls an I/O port which indicates that the SDU is either a primary or secondary. If it is a primary SDU then it will cause the communications lines to the two secondaries to pulse every cycle of the received signal frequency (such as 10-2/3 Hz) in synch with the primary SDU oscillator. The secondary SDU uses a high-speed counter to start at the beginning of a signal cycle, that

Channel	X	Y	Z
SDU 1 (5.3 Hz)	1.02070	1.02070	1.02030
SDU 3 (5.3 Hz)	1.02030	1.02070	1.02030
SDU 4 (5.3 Hz)	1.01300	1.01900	1.01400
SDU 1 (10.6 Hz)	1.06870	1.06330	1.06330
SDU 3 (10.6 Hz)	1.06330	1.07100	1.06730
SDU 4 (10.6 Hz)	1.05430	1.06100	1.05370

Table 2-3. Sensor data unit and preamplifier calibration ratios  
 The calibration ratio is defined as the calibrated B field divided by the measured B field displayed by the SDU.

has been shifted to be in phase with its own clock, and count until the primary SDU start of cycle is detected. The phase difference between primary and secondary SDU is then computed and displayed in degrees by the secondary SDU's. (The relative phase of the primary is necessarily zero.)

The normal default "monitor" display registers contain five lines of information including the three channels of long term average signal data. They are displayed one line at a time. The X channel signal data is the first line displayed under all default conditions. The remaining lines may be displayed by pressing the "Next" key of the keypad to go in the forward direction only. If a warning message appears, it may be cleared by pressing any key, but a warning flag (letter) will remain on the right of the display as long as the condition exists. Other system parameters and data may be displayed and some may be changed by using the keypad. In some cases, particularly when an inadvertent parameter change could affect system operation, a user identification code (UIC) may be required.

### 2.3 LOCATION ANALYSIS UNIT

The Location Analysis Unit (LAU), supplied for use in the "Breadboard" location system, consists of a GRID Compass Model 1101 portable computer, with disk and printer, and Develco Locator/DLMG<sup>®</sup> software. The key features of the GRID equipment are summarized in Table 2-4. The LAU is used to calculate the location of the transmitter that generates the fields measured by the Sensor Data Units (SDU). In the current version, data from the SDU's are entered manually at the LAU computer keyboard. All three LAU system components can be used when ac power is available, or the Compass 1101 computer can be used alone with an optional battery pack (not supplied). In either case, it gives the results on site and also saves the input data and calculated results for future examination.

Software supplied by GRID includes the operating system and demonstration programs that are stored on the hard disk and in bubble memory. The Develco Locator/DLMG<sup>®</sup> software is stored on the hard disk and in bubble memory, with a backup version on a floppy disk. The Locator software provides the following:

1. Data forms that arrange the necessary inputs to the computer program in a convenient format.
2. Initialization routines that synchronize, rotate and calibrate the raw data from the three triaxial sensor measurements to produce orthogonal vector measurements.
3. Two automatic and one manual initial estimate routines that provide the starting point for the location calculation.



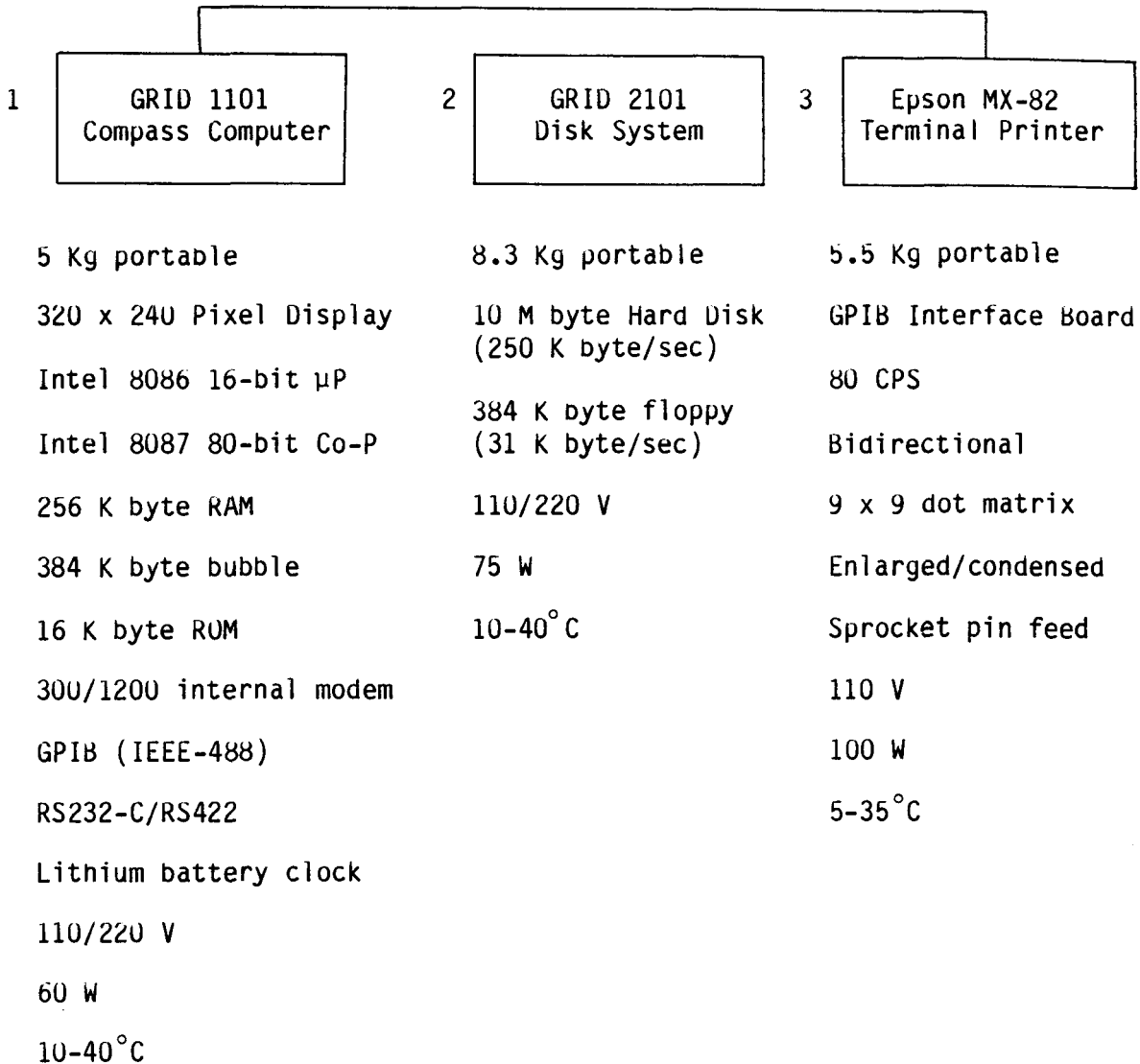


Table 2-4. Location analysis unit hardware.

4. The main Locator program to calculate the source location, orientation and magnitude based on six convergence attempts for each initial estimate.
5. A utility program to calculate fields produced by a known transmitter (for diagnostic purposes).
6. A utility program for calculation of calibration data in case recalibration is necessary.
7. Data output routines to display, store and print results in a format for easy evaluation.

Development of the location method and "Locator" software was funded by Develco for use in general underground and other location applications. The location method is based on the Develco background patent that has been applied for.<sup>4</sup> DLMG is the specific version of the "Locator" software that has been adapted for use in preliminary testing of the "Breadboard" Electromagnetic (EM) Rescue System to evaluate this method as a means of locating miners trapped in deep mines. There are a few minor limitations imposed by the specific initialization and initial estimate routines used in this version. It requires data from three sensor locations that can be at different elevations. The sensors must be leveled but the azimuthal orientation can be in any known direction. Best results will be obtained when the sensors are used in a triangular array centered over the probable transmitter location, with a sensor spacing on the same order as the transmitter depth, and the sensor or antenna plane is tilted less than 20 to 30 degrees. In cases other than these, successful source locations can be made, but the starting point for the location algorithm may have to be entered manually.

Each location project will normally have several sets of SDU measurements taken over time. The main project information is entered only once, followed by the sets of data measurements as they are recorded from the SDU's. All entries are made at the Compass keyboard in response to prompts from the Compass screen. The entered information and data are automatically stored on the hard disk (or in bubble memory); printed copies may be made if desired. All results will also be filed automatically. The amount of information displayed and printed can be controlled, i.e., the output of some diagnostic technical data (which would be filed regardless) can be inhibited.

Following the entry of the data into the LAU, the measurements are individually calibrated according to the sensors and SDU's from which they were recorded. The measurements are then synchronized in time using phase relationships among the SDU's (measured with synchronization cables). Next, the measurements are mathematically rotated so that the azimuths of the sensors are aligned with the array coordinate system. The result of these preliminary calculations are vector field measurements at each sensor; these vectors are then used in the automatic initial estimate routines and in the main Locator program.

The main location program calculates the location, orientation, and magnitude of a remote, unknown, low-frequency (quasi-static) magnetic field source. In general, it can be used to locate virtually any magnetic dipole source, based on the field measurements made at three triaxial sensors set in a triangular array at any attitude with respect to the source. Depending on the geometry of the problem, it may be possible to use fewer sensors or other array configurations (e.g., co-linear). Given sufficiently accurate measurements, the program can make the correct location over any distance, i.e., the algorithm used is independent of linear scale (within the numerical limits of the computer used).

The location program calculations employ a unique mathematical model of the source and the fields it produces. Six simultaneous equations are required to solve for the six unknowns of source position (3-X, Y, Z), orientation (2-tilt, azimuth), and strength (1). The computer program calculates the simultaneous solution to the nonlinear equations by a unique iterative search and convergence method. Computation begins with an initial estimate of the solution and then converges to a correct solution of the equations if possible. The initial estimate does not have to be accurate but must be in a suitable region that depends on the specific sensor array and transmitter geometry. Because of the complex nature of the equations, it may not be possible to reach a solution by a given route. Therefore, six attempts are made for each initial estimate.

There are multiple possible roots, or mathematically correct answers, to the original six equations with six unknowns. Only one is the correct answer to the real world problem. The nature of the equations have been investigated and modeled for an extensive variety of source and sensor configurations. Knowledge of the behavior of these functions and of the general constraints on possible source locations and orientations is used in the computer (or manual) routines to select an appropriate starting point that will, in most cases, lead to the correct solution.

A very deep starting point is generally best in the trapped miner case, which will usually involve locating a nearly vertical magnetic dipole source (horizontal loop antenna) by using sensors deployed in a nearly horizontal surface plane. The software has two routines to automatically select the starting point. The first routine selects a point below the projected intersection of the horizontal field directions at the sensors. This method works well whenever the loop antenna is nearly horizontal (most cases). The second routine selects a starting point directly beneath the centroid of the sensor array. This is more conservative and may be useful when the sensor or antenna plane is severely tilted. Starting points based on other information may also be entered by the operator. From each starting point the main Locator program attempts to find the solution.

The mathematical solution occurs when the functions are identically equal to zero. In practice, the field measurements are contaminated by noise and there may be errors in the computer calculations which either result in long computational times or prevent achieving zero. Therefore, convergence limits are used to determine when the iteration process should be terminated. This can potentially lead to false answers that may or may not be close to a real root, but are not the correct answer. Various methods are used to discard false answers. For example, very often the incorrect answers are completely unrealistic or physically impossible. In other cases, they do not produce the correct field values when the equations are inverted. To help assure arrival at the correct answer, the results from the six convergence attempts are displayed in descending order of fit to the measured data, thus the first result listed is "best".

## 2.4 BEACON TRANSMITTER

This portion of the deep mine (1,000 m) location system equipment will be similar in form and function to that used in the existing Bureau of Mines VF equipment for shallower mines (<300 m). That is, it will consist of a wire loop antenna deployed in a nearly horizontal configuration, and the electronic circuitry to drive it which may be powered by the miner's cap-lamp battery. The primary difference in the deep mine application are the need for:

1. Lower operating frequencies (1 to 10 Hz) to minimize propagation effects.
2. Higher frequency and amplitude stability to permit the longer signal integration times required.
3. Higher overall transmitter efficiency to achieve an acceptable operating time with a battery for continuous (CW) use.
4. Higher intrinsically safe moment for a given range of probable loop area possibilities.

Several conceptual alternatives for achieving the performance goals for deep mine applications were investigated as part of the Phase I work.<sup>3</sup> However, it was sufficient to simply modify the existing VF rescue transmitter to operate at low frequencies (1-10 Hz range) for the purposes of the "Breadboard" system evaluation tests.

The transmitters used were production prototypes manufactured by General Instruments Corporation, P/N 852-1476, which have optional output frequencies of 630, 1050, 1950 or 3030 Hz.<sup>7</sup> This version would normally be carried on a belt and attached to a 4-volt (4.2 to 3.5 V charge-discharge range) cap-lamp battery when needed. The standard antenna is 300 feet of #18AWG solid copper wire with a nominal resistance of  $1.9\Omega$ . The transmitter has a stable quartz crystal oscillator (30-50 kHz range) and a binary divider to generate the operating frequency. A decade divider is

used to provide a 10% duty cycle for use with audio detection methods and to extend the battery life time to greater than 40 hours with a partially discharged battery (e.g., old battery at end of shift). Continuous (CW) operation may be keyed with a pushbutton switch. The antenna is driven by a full-wave switching bridge that produces an unregulated square-wave output with a peak voltage and current proportional to the battery voltage and load. (The specified output current is 6 A with a  $0.2\Omega$ , 100  $\mu\text{H}$  load.)

The modifications consisted of bypassing the transmitter oscillator and divider circuitry with another design to produce hardwire selectable output frequencies of 2-2/3, 5-1/3 and 10-2/3 Hz. A watch crystal oscillator is used, similar to that in the original transmitter circuit, with a stability of one part in  $10^5$  and frequency of 32,768 Hz. Its output is divided to the selected frequency and drives the antenna output through the original transmitter control and switching circuitry. In addition, the CW mode was hardwired to be on continuously (i.e., the keying switch was bypassed). The changes were accomplished by "piggy-backing" the new circuitry and by making appropriate wiring changes - the original printed circuit boards were not permanently altered.

The capacity of a standard lead-acid cap-lamp battery is on the order of 12 to 15 ampere hours (A-H) with a standard 1-A lamp load. Under load conditions, the terminal voltage varies gradually from approximately 4 volts, at full charge, to approximately 3-1/2 volts near cutoff. Although the voltage drop in the transmitter switching circuit depends on voltage and the temperature, etc., the expected average transmitter current into a nominal  $2\Omega$  load, is on the order of 1.7 to 1.5 A peak square wave. Thus, under CW operating conditions, a fully charged battery will have an operating life of from approximately seven to nine hours. A partially discharged battery, such as an old one at the end of the shift, will have a useful life of approximately half that. As mentioned previously, these lifetimes are inadequate for an operational system and alternatives must be considered in the future. They are also inconvenient for the evaluation tests where it is expected the transmitter will be left on for extended periods of time.

Tests were conducted with the modified transmitter and  $2\Omega$  load connected to a standard Wheat cap-lamp battery to verify the expected voltage decay rate. With a battery that was less than fully charged, it was found the terminal voltage on this sample decreased approximately 40 to 60 mV per hour initially, and approximately the same amount per half hour at later times. The total time to complete discharge was approximately six hours and the decay rate accelerated in the last 1.5 hours. For a simple long term signal averaging scheme, such as is the case for the "Breadboard" receiver, these figures translate to an equivalent signal-to-noise ratio (SNR) of about 40 to 36 dB, respectively, when integrated over the same period of time.

Even though the signal amplitude may be changing, the receivers will provide the correct relative mean signal amplitude over a given period of time because the variation is common to all of them. However, the apparent SNR will be lower than it might otherwise be with a stable signal which makes it difficult to evaluate signal quality with the "Breadboard" system. Because of this, and the need to achieve a longer operating time, capacity was increased by using two cap-lamp batteries in parallel for the first in-mine test.

Loop current variations caused by temperature-induced changes in loop resistivity (0.4% per degree C for copper) are also possible. However, this is not expected to be a serious factor in most test situations because of the fairly stable mine environment.

The standard 300-foot wire loop antenna is to be deployed as a single turn around a 60- by 90-foot pillar for the in-mine test. The enclosed area is 5,400 square feet ( $502 \text{ m}^2$ ). This antenna configuration will generate a peak magnetic dipole moment (turns X area X current) of  $753 \text{ Am}^2$  with a nominal peak square wave current of 1.5 A. The RMS moment referred to the fundamental frequency is  $2\sqrt{2} / \pi$  times the peak square-wave value or  $678 \text{ Am}^2$ .

If the standard antenna is layed out in a one-turn square configuration (the largest probable size in actual mine installations), the enclosed area will be  $523 \text{ m}^2$  and the inductance will be  $190 \mu \text{ H}$ . If the peak energy storage ( $1/2 LI^2$ ) is limited to a conservative intrinsically safe level of  $1/2$  millijoule (mJ), then the peak current must be limited to 2.3 A, with square wave excitation. The VF transmitter output will typically be less than this when used with the 4-V battery (4.2 maximum less transmitter voltage drop) and  $1.9 \Omega$  (nominal at room temperature) antenna.

A larger loop antenna was also used for the first in-mine test to simplify initial system functional checkout. The wire was 1,000 feet of #14AWG copper wire with a nominal resistance of  $2.5 \Omega$ . It was wrapped around four pillars with a total enclosed area of approximately 52,900 square feet ( $4915 \text{ m}^2$ ). A fundamental frequency RMS moment of approximately  $6600 \text{ Am}^2$  was expected to result if a peak current of 1.5 A was achieved.

### 3.0 3-AXIS SEARCH COIL CALIBRATION

Four 3-axis search coil assemblies were calibrated at the NASA-Ames Research Center Magnetic Test Facility.<sup>6</sup> The 20-foot diameter, 3-axis Helmholtz coil facility was used in order to have minimum gradients. Although it is usually used for dc measurements, the Helmholtz coil support structure is insulated to prevent eddy currents at ac. (A large demagnetizing coil structure approximately 30 feet south from the Helmholtz center was not insulated, but it did not produce any significant effects.) All measurements except those for the Helmholtz coil transfer function were made at 5 Hz. Measurement and performance goals were:

- a) Helmholtz gradients  $< 0.1\%$  within  $\pm 15$  inches of center.
- b) Angular measurement accuracy  $< \pm 1$  m radian ( $\pm 0.1$  mr goal).
- c) Search coil orthogonality  $< \pm 1$  m radian (0.057 degrees).
- d) Search coil scale factor accuracy  $< \pm 0.1\%$ .

The Helmholtz coil gradients at 5 Hz were measured and found to be less than 0.14% over a region of  $\pm 24$  inches about the center. (The N-S axis had the maximum gradient. The E-W gradient was much less and the vertical gradient was negligible.) The transfer function of each Helmholtz coil pair (vertical, East-West, North-South) was precisely calibrated at dc by switching polarity with the results shown in Table 3-1.

The fields produced by the respective Helmholtz coil pairs were adjusted to be level (or vertical) and mutually perpendicular by means of a cross coupling network. A precision level was used to establish the horizontal plane. A visible laser source, located approximately 45 feet from the coil center and oriented parallel to the N-S axis, and an optical (reflecting) block were used to establish a repeatable reference axis and permit precise 90-degree rotations.

The 3-axis search coil assembly shown in Figure 2-2 includes a precise bubble level and front surface mirror for orientation with respect to vertical and azimuth (the laser line). Since the Helmholtz field directions were precisely adjusted, it was sufficient to leave the search coil orientation fixed and sequentially energize the Helmholtz coil pairs. The search coil X, Y, and Z axes were oriented parallel to the Helmholtz E-W, N-S (the laser line) and vertical axes, respectively.

The output of the search coil parallel to the field is proportional to its scale factor. The output of the search coils' transverse to the field is proportional to their orthogonality with respect to the first search coil. Orthogonality was electrically adjusted by means of a cross trimming network in the post detection amplifier to achieve a minimum output from the transverse search coils.

Details of the Helmholtz coil orthogonality adjustment and search coil calibration procedures are described in the following:

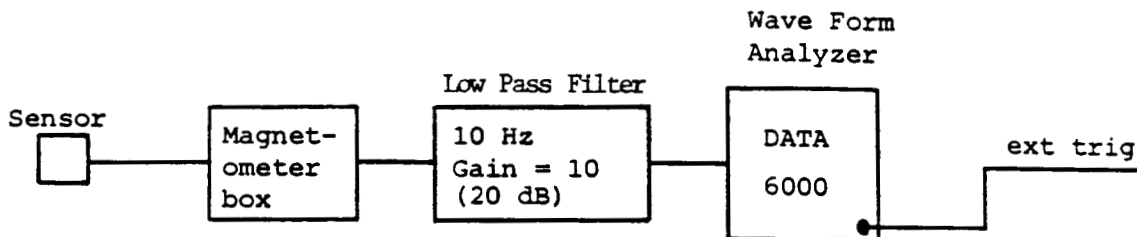
Axis	$T_H$ (Gauss/Ampere)
X (E-W)	0.4464
Y (N-S)	0.4271
Z (vertical)	0.5748

Table 3-1. Helmholtz coil transfer function calibration. Averaged for gradient over  $\pm 60$  cm about the centroid.



## A. METHOD OF MEASURING VOLTAGES

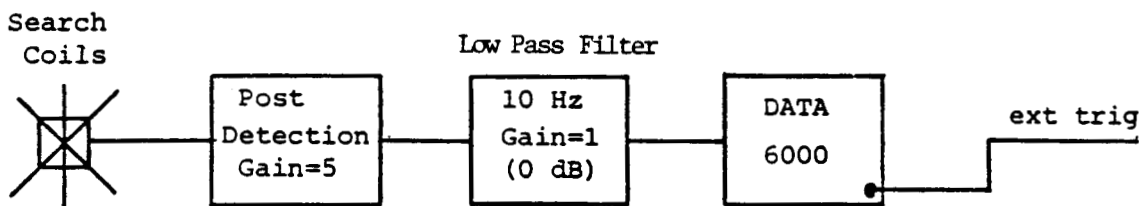
The voltage measurement setups used are shown in Figure 3-1.



TMB = 1mS, 200 points (>1/2cycle)

TRIG = ext, normal, DC

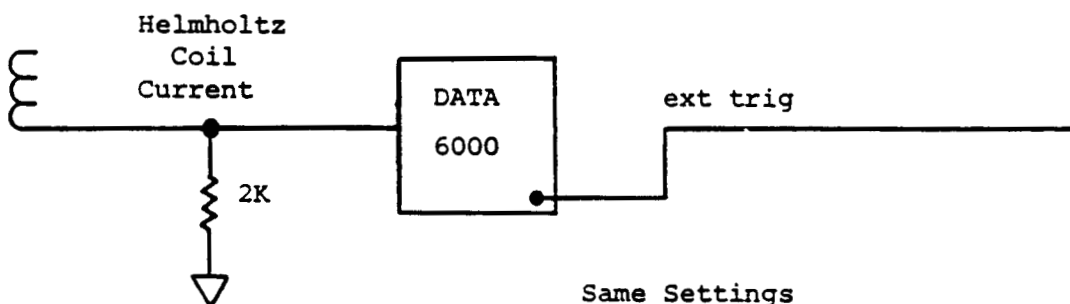
INP = DC coupled,  $\pm 500\text{mv}$



Same Settings

INP = DC,  $\pm 5\text{V}$

Stacked from 20 to 100 samples



Same Settings

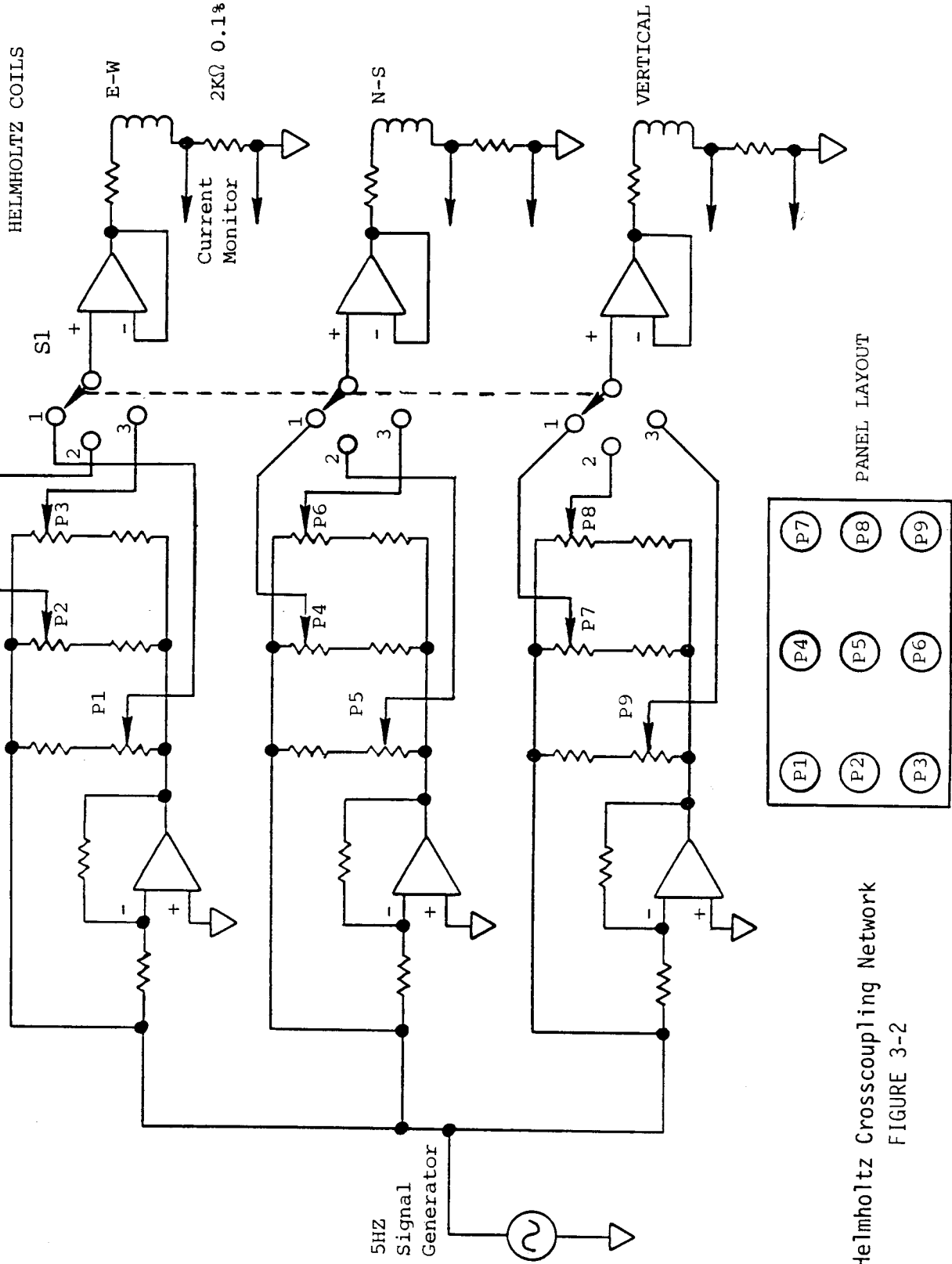
INP = DC,  $\pm 5\text{V}$  or  $\pm 50\text{V}$

(Use scope for preliminary Helmholtz adjustment.)

FIGURE 3-1. Calibration Voltage Measurements

## B. HELMHOLTZ COIL ADJUSTMENTS

- 1) The cross coupling network that was used to trim the Helmholtz coil alignment is shown in Figure 3-2. Connections to the Helmholtz coils are also shown.
- 2) A glass plate (1) was placed in the center of the coil structure as shown in Figure 3-3A.
- 3) The plate (1) was then leveled using a precision and sensitive level that was placed in the center of the plate.
- 4) A fluxgate magnetometer (2) was firmly attached to a square, mirror-coated glass prism (3).
- 5) With the vertical coil energized (rotary switch S1 in Figure 3-2 in position 3) with the maximum available current (about 20 V p-p at the generator output), P3 was adjusted to give the same magnetometer reading (amplitude and phase) when its axis pointed E or W. P6 was adjusted to give the same reading when its axis pointed N or S. At this point, the vertical field was perpendicular to the leveled plate with an estimated 0.5 m Radian accuracy.
- 6) The glass prism was rotated into a position in which the fluxgate axis is vertical. See Figure 3-3B. With the fluxgate in the position shown in Figure 3-3B and the N-S coil energized (S1 in position 2) the field reading is equal in amplitude and reversed in phase to the reading obtained after the prism is rotated 180 degrees. This is achieved by adjusting P8. The same procedure is repeated with the E-W coil energized (S1 in position 1) and adjusting P7. At this point both E-W and N-S fields lie in a horizontal plane.
- 7) The prism is brought back to its position as in Figure 3-3A. With the E-W coil energized and the fluxgate axis pointing N-S, the prism was rotated to get the minimal output. A laser visible source placed on a tripod about 45 feet away was adjusted so as to get the reflected beam (from the prism) anywhere above or below, but on a vertical line that passes through the source. With the laser source in this fixed position the prism can be rotated in precisely 90 degree steps. The fluxgate is rotated back and forth 180 degrees (to point N and S) and P4 adjusted to get the same amplitude and opposite phase.
- 8) With the N-S coil energized and the fluxgate sensor pointing E (using the laser beam for precise alignment) the same amplitude and opposite phase of the measured field is adjusted using P2 and flipping the sensor from E to W several times for repeated measurements. At this point, the E-W and N-S fields are



Helmholtz Crosscoupling Network  
FIGURE 3-2

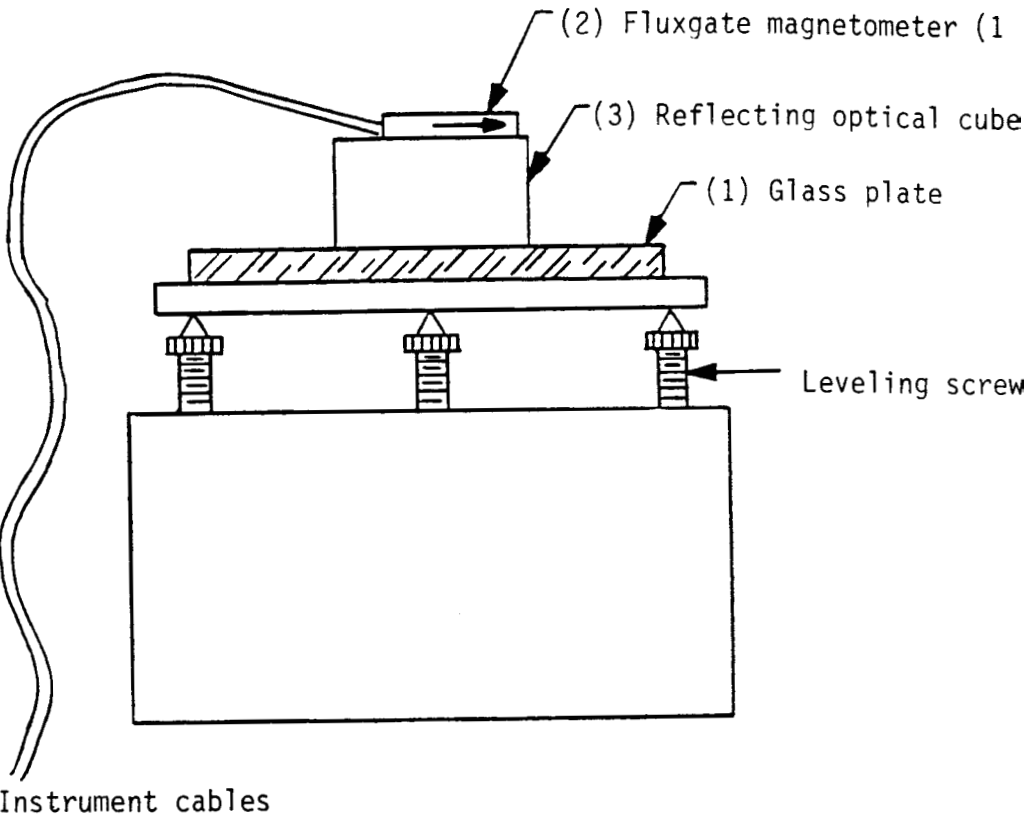


FIGURE 3-3A

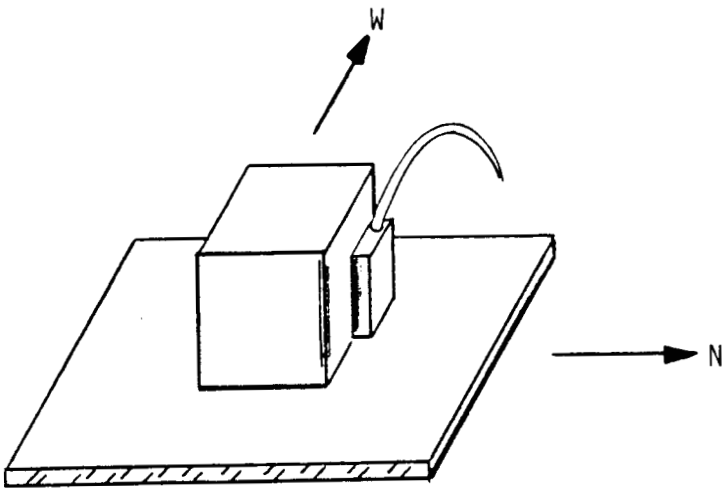


FIGURE 3-3B

orthogonal. The procedure is complete. (As a cross check, all measurements can be repeated without adjustment to make sure previous adjustments were not affected.)

### C. SEARCH COIL CALIBRATION

- 1) The search coil structure is mounted on a stand, designed to locate its center in the center of the Helmholtz structure, with leveling and azimuth adjustments. See Figure 3-4. After leveling, the search coil structure is rotated and aligned with the laser beam that is bounced off a mirror glued to the holding hub.
- 2) Energizing one axis at a time, the outputs of the cross axis are adjusted to read zero (or a minimum limited by noise).
- 3) The output of the main axis is measured as well as the voltage across the current monitoring resistor.

To avoid saturating the search coil post detection amplifier (with a gain of five), ambient field amplitudes were limited to levels on the order of 30 to 45 mA/m peak. The ambient noise fields (mostly 60 Hz and some 180 Hz) were on the order of less than 2 to 5 mA/m peak. Noise levels were reduced to less than 0.1 mA/m peak after the post detection notch and other filtering. Using the Data Precision 6000 Waveform Analyzer to digitally stack from 20 frames (for orthogonality measurements) to 100 frames (for scale factor measurements) further reduced the noise levels to 0.03 and 0.01 mA/m peak, respectively, i.e., 60 to 70 dB below the signal levels. The residual noise was mostly due to power line and other sources. The in-band noise (below 10 Hz) was approaching the atmospheric noise level limit after precautions were taken to minimize noise induced by vibration.

The search coil orthogonality measurements before and after the electrical cross trim adjustments were made are summarized in Tables 3-2 and 3-3. The "before" measurements include the effects of both electrical (e.g., cross coupling between the asymmetrically located individual search coils) and mechanical (e.g., setup, mirror, level, and individual search coil misalignments) factors. The "final" measurements were made after refining the test setup and procedure. Mechanical repeatability (i.e., without making any electrical readjustments) was checked by taking apart two of the 3-axis search coils and then reassembling them and repeating the measurements with satisfactory results. Table 3-4 illustrates the worst case misalignment errors by assuming the search coil and Helmholtz coil misalignments are additive. The maximum error of 2 milliradians or 0.1 degrees is well within the limit considered necessary for accurate location.

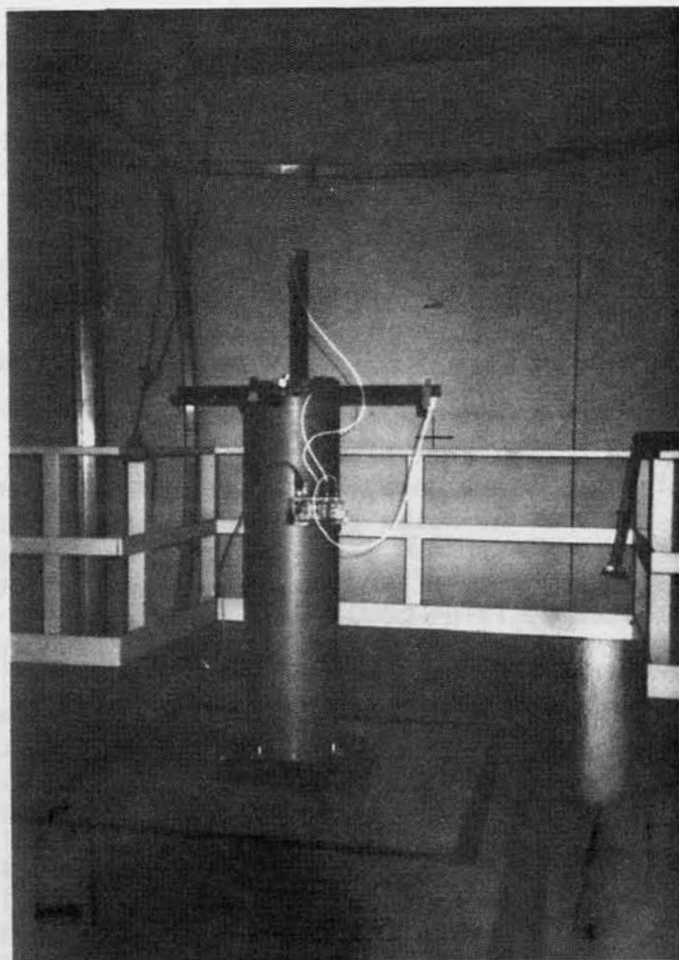


FIGURE 3-4. Search Coil in Test Stand.

Drive Axis:	EW Drive (X)		NS Drive (Y)		Vert Drive (Z)	
Output Axis:	Y	Z	X	Z	X	Y
S/N 1	2.2	1.5	1.1	1.8	2.1	2.4
S/N 2	0.9	1.2	4.2	1.9	3.0	3.4
S/N 3	0.8	0.7	3.1	4.2	0.1	0.4
S/N 4	5.0	3.4	3.3	1.3	2.4	0.3

Includes measurement and procedure errors, e.g., (1) azimuth errors with laser alignment on 25' baseline; (2) Helmholtz coil connection problem; and (3) voltage (pp) measurement errors due to noise. Procedure and setup was improved prior to the final measurements.

Table 3-2. Orthogonality measurement before adjust cross trim; i.e., pots in "0" position. (All values in milliradians.)

Drive Axis: Output Axis:	E-W Drive (X)		N-S Drive (Y)		Vert. Drive (Z)	
	Y	Z	X*	Z	X	Y
S/N 1 after final adjustment	0.33	0.16	0.70	0.17	0.26	0.26
S/N 2 after final adjustment	0.33	0.57	0.86	0.52	0.38	0.38
take apart and reassemble	1.0	0.33	1.2	0.86	0.90	1.15
S/N 3 after final adjustment	0.32	0.09	0.89	0.44	0.42	0.33
S/N 4 after final adjustment	0.51	0.34	0.92	0.36	0.33	0.26
reinstall and repeat	0.34	0.17	0.98	0.36	0.26	0.26
take apart and reassemble	0.34	0.51	1.06	0.71	0.33	0.26
Helmholtz coil calibration (approx)	.29	.37	.24	.15	---	.28---

\*Had problem with residual phase (scattering?).

Table 3-3. Final orthogonality measurements.  
(All values in milliradians.)



	Drive	X	Y	Z	Worst Axis	Combined (RSS)
Axis						
S/N 1	X		.94	.54	.94	1.08
	Y	.62		.54	.62	.82
	Z	.53	.32		.53	.62
S/N 2	X		1.10	.66	1.10	1.28
	Y	.62		.66	.66	.91
	Z	.94	.67		.94	1.15
Reassemble S/N 2	X		1.44	1.18	1.44	1.86
	Y	1.29		1.43	1.43	1.93
	Z	.70	1.01		1.01	1.23
S/N 3	X		1.13	.70	1.13	1.33
	Y	.61		.61	.61	.86
	Z	.46	.59		.59	.75
S/N 4	X		1.16	.61	1.16	1.31
	Y	.80		.54	.80	.97
	Z	.71	.51		.71	.87
Repeat S/N 4	X		1.22	.54	1.22	1.33
	Y	.63		.54	.63	.83
	Z	.54	.51		.54	.74
Reassemble S/N 4	X		1.30	.61	1.30	1.44
	Y	.63		.54	.63	.83
	Z	.88	.86		.88	1.23
Worst Case					1.44	1.93
						$(\sum x^2)^{1/2}$

Table 3-4. Total search coil and Helmholtz alignment error after trim. Values are sum of search coil and Helmholtz misalignment. (All values in milliradians.)

The calibrated scale factors for the search coil and post detection amplifier combination, as measured in the test facility, are shown in Table 3-5. The measured gain of the post detection amplifier is shown in Table 3-6 and the net scale factor calculated for the search coil alone is shown in Table 3-7.

Unit	Scale Factor (V/(A/m))		
	X Axis (EW)	Y Axis (NS)	Z Axis (Vert.)
S/N 1	91.33	91.40 (mean $91.20 \pm .29\%$ )	90.87
S/N 2	91.27	91.28 (mean $90.92 \pm .59\%$ )	90.21
S/N 3	87.73	88.28 (mean $87.97 \pm .31\%$ )	87.90
S/N 4	87.90	88.10 (mean $87.91 \pm .22\%$ )	87.72

Notes:

S/N 1 and 2 are newer units and S/N 3 and 4 are older units.

The calibration ratio for use in correcting measured data is defined as the nominal scale factor of 100 V/(A/m) divided by the calibrated scale factor.

Table 3-5. Calibrated scale factor - search-coil and post detection amplifier.

## Channel Gain Ratios

	X	Y	Z
--	---	---	---

S/N 1	4.985	4.985	4.971
S/N 2	4.975	4.977	4.964
S/N 3	4.968	4.970	4.973
S/N 4	4.974	4.962	4.977

Table 3-6. Post detection amplifier.

Unit	Scale Factor (V/(A/m))		
	X Axis (EW)	Y Axis (NS)	Z Axis (Vert.)
S/N 1	18.32	18.34 (mean 18.31 $\pm$ .16%)	18.28
S/N 2	18.35	18.34 (mean 18.29 $\pm$ .49%)	18.17
S/N 3	17.66	17.76 (mean 17.70 $\pm$ .28%)	17.68
S/N 4	17.67	17.75 (mean 17.68 $\pm$ .34%)	17.63

Note: S/N 1 and 2 are newer units, and S/N 3 and 4 are older units.

Table 3-7. Scale factor referred to search coil output.

#### 4.0 TEST OF ATMOSPHERIC NOISE CANCELLATION BY USING A REMOTE SENSOR

The ability to locate miners trapped in deep mines (1,000 m) from the surface is directly dependent on the ability to largely eliminate the effects of natural and man-made noise. There is some limited experimental evidence that natural noise can be cancelled more than 90% by using a remote sensor.<sup>5</sup>

Therefore, spatial correlation and cancellation of atmospheric noise using long baseline differences from a remote sensor was considered as a possible means for achieving one of the necessary noise reduction methods. (Impulse noise processing is also necessary, but this will only reduce high level peaks and compress the range of variation.) In this approach, the remote reference, or "far" sensor, is placed 10 times as far from the beacon transmitter (10-20 km) as the most distant "near" sensor (1-2 km) so it is exposed to a signal amplitude of less than 0.2% of that at any other sensor and can be considered a sample of pure noise.

The tests on this program were conducted to determine if a cancellation of 20 db, or down to the search coil noise limit (whichever is greater), could be achieved using amplitude correlation only.

##### 4.1 LOCATION AND SETUP

The remote sensor cancellation tests were performed at the USGS Stone Canyon Seismological Observatory, which is 15 miles (24 km) south of Hollister, California, with their cooperation and permission. The specific sites were chosen based on low cultural noise, available nearby phone drops, access and security.

The "local" sensor site was located in a field on a hill approximately 1/2 mile west of the Stone Canyon Observatory itself. An inactive powerline ended about 100 yards from the site and 60 Hz interference was normally not observable. (Leakage from a damaged cable was a problem in wet weather, but the power was subsequently turned off.)

The "remote" sensor site was situated in a field behind the California Division of Forestry fire station at Bear Valley. The distance to the fire station and the nearest powerlines was on the order of several hundred yards.

The straight line distance between the two sites was approximately five miles (8 km) and roughly parallel to the nearby (1/4 to 1/2 mile or so) San Andreas fault, in hilly terrain. The valley is agricultural and the hills are ranch land. The geology is highly faulted and irregular, so these sites should represent a "worst case", i.e., minimum correlation.

Each 3-axis sensor was mounted close to the ground with the lower half of the vertical axis in a shallow pit. Adjustable mounting feet were driven into the ground to provide stability and leveling. The horizontal

axes were oriented N-S, E-W with a hand compass. A pyramid wind screen was placed over the sensors and weighted down.

The sensors were positioned in open areas away from trees, fences, etc., to minimize the possibility of wind-induced seismic noise, but it could not be verified if this was successful. However, numerous ground squirrels at Bear Valley, the unexpected herding of cattle at Stone Canyon after installation, and the severe winter storms were definite sources of uncorrelated noise at times. This can be prevented in future operations by hardening (concrete pads, secure shelter) and area fencing.

Analog data was transmitted from the field sites over standard voice grade telephone lines by using the data grade VCO's (Voltage Controlled Oscillators) and discriminators as shown in Figures 4-1 and 4-2. Recordings were made at selected times (e.g., day and night) with a Teac R-61 Cassette Data Recorder.

The post detection amplifier, used for these tests, amplifies the search coil output and notches the powerline harmonic interference at 60, 120 and 180 Hz. It was placed close to the coil assembly to minimize possible noise pickup on the coil output cables.

Three Develco 6242 VCO units were mounted inside a weather resistant box, which also contained two 12 V "Gel-Cell" (lead acid) batteries (4.5 A-H each) and a telephone line coupler. One battery powered the search coils and post detection amplifier and the other battery powered the VCO's. The telephone coupling circuit provided off-hook simulation and a timer that maintained data transmission for 25 minutes after detection of the ring tone. It also powered two relays that connected the batteries only during data transmission.

The upper limit of the system passband frequency response is limited by the VCO-Discriminator combined transfer function which is down 3 db at approximately 20 Hz. The low frequency response is limited by the ac coupling network in front of the VCO input and is approximately 4 Hz. The overall attenuation at 60, 120 and 180 Hz was 90, 80 and 90 db, respectively. The combined channel gain of the search coil, post detection amplifier and VCO was  $12 \times 10^5$  V/(A/m) and the recorder gain was input/output = 1/0.29.

Since the recorder only had four channels, the procedure was to record one "local" (Stone Canyon) channel and all three "remote" (Bear Valley) channels at a given time. The procedure was repeated in turn for  $X_L$ ,  $Y_L$ , and  $Z_L$  for a given data set.

## 4.2 DATA ANALYSIS

Three received atmospheric noise signals from one "remote" orthogonal set of sensors and one additional "local" noise signal were recorded simultaneously and so retrieved for the following analysis. The three axes

VCO Settings

STATION	AXIS	VCO Frequency	VCO Attenuation
Bear Valley	XR	680HZ	18dB
	YR	1360HZ	18dB
	ZR	2040HZ	18dB
Stone Canyon	XL	1020HZ	18dB
	YL	1700HZ	18dB
	ZL	2380HZ	18dB

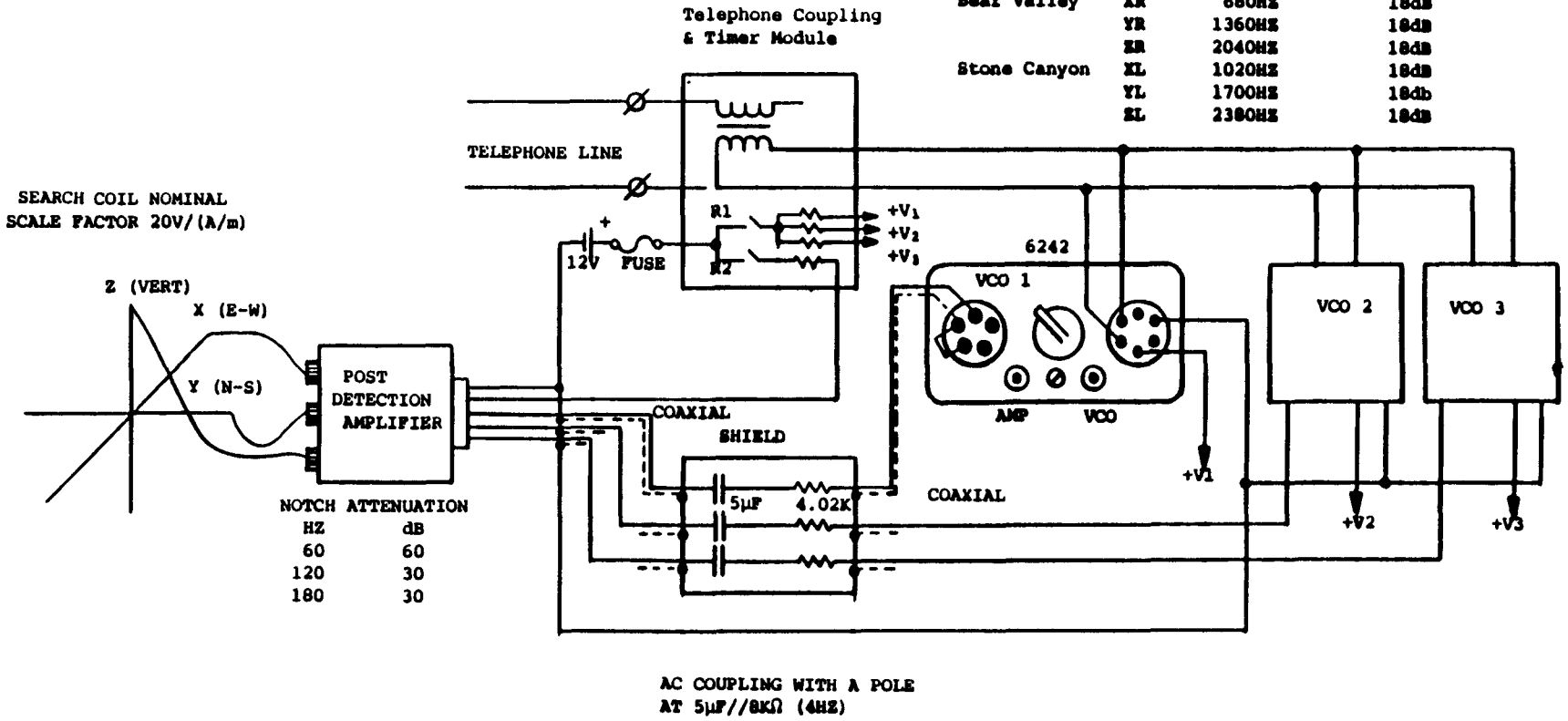
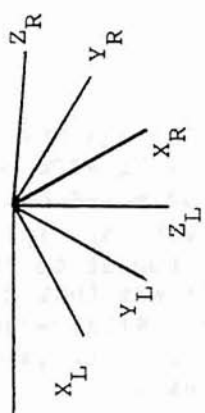
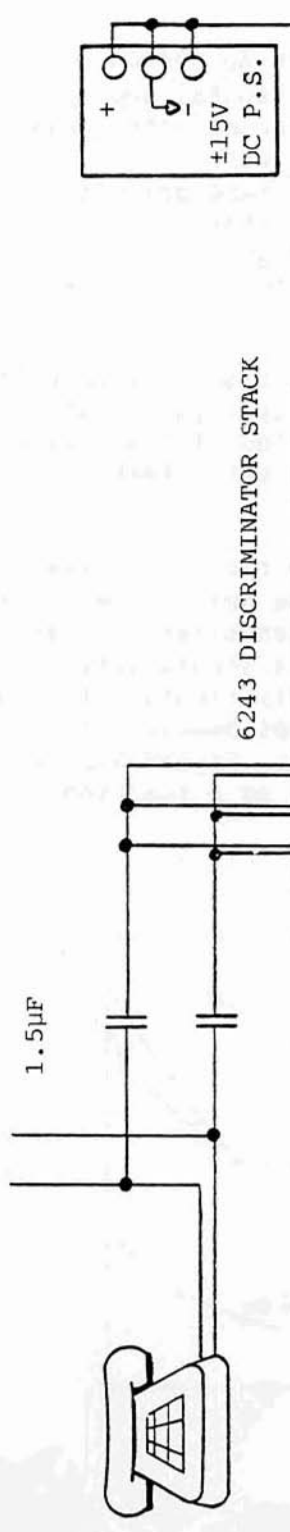


FIGURE 4-1. Noise Data Transmission Setup.

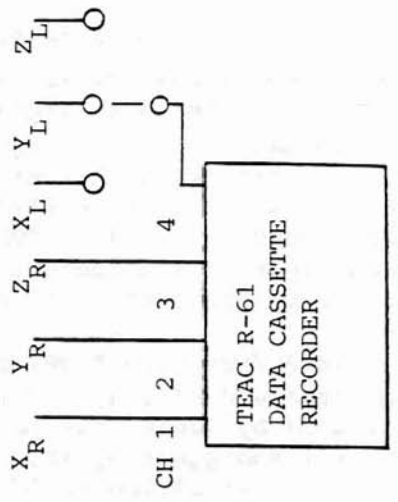
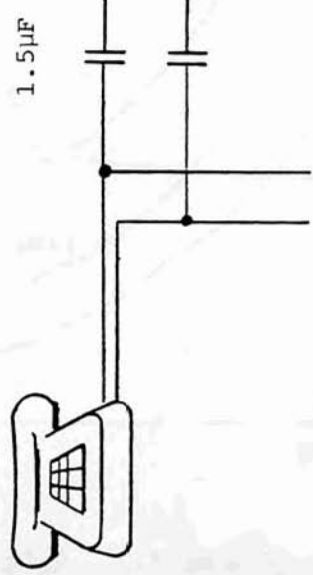


LINE 1



Outputs to tape recorder

LINE 2



Noise Data Receiving and Recording Setup

FIGURE 4-2.

of the full set were designated  $X_R$ ,  $Y_R$ , and  $Z_R$ . The  $X_R$  search coil was oriented E-W and  $Y_R$ , N-S.  $X_R$ ,  $Y_R$  were both horizontal and  $Z_R$  vertical. The local signal was selected out of a second orthogonal set designated  $X_L$ ,  $Y_L$ , and  $Z_L$ . The axes  $X_L$ ,  $Y_L$ , and  $Z_L$  were roughly aligned with a magnetic compass to have the same orientation as  $X_R$ ,  $Y_R$ , and  $Z_R$ , respectively. It was thus expected that corresponding signals from the two sites would be highly correlated and good cancellation could be achieved with gain adjustment alone, without having to add orthogonal components.

A Data Precision Model 6000 Waveform Analyzer was used to take FFT's of the data and display the results in terms of power spectral density. This was done by Taking 512 samples, with a sampling period of 5 ms, performing the FFT and squaring it. This was repeated and the data stacked (summed) on the order of 200 to 400 times (see Appendix I).

From measurement of the full bandwidth RMS of the recorded noise, it was verified that there was no significant change in the noise power during a period of one recording (40 minutes). Thus, in a cancellation measurement it is possible to minimize the residual noise with a single setting of gain compensation, assuming only that the the spectral distribution is stable. This gain will be different for different frequencies because of differential gain and phase shifts between channels. Figure 4-3 shows the residual noise level  $Y_L - KY_R$  (not in the same scale) as a function of K for a particular data set.

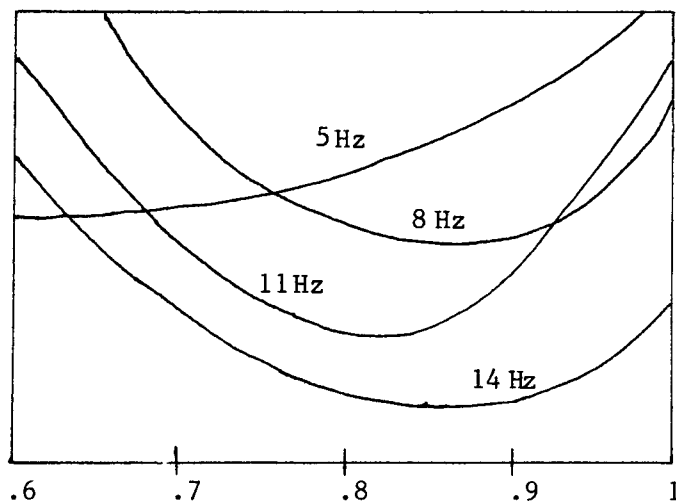


FIGURE 4-3. Relative gain (K).

As is clearly seen it is possible to choose a gain that will give satisfactory results for a span of frequencies and this gain may also be found by:

$$K = \frac{Y_L(\text{RMS})}{Y_R(\text{RMS})}$$

It was confirmed that direct subtraction, with appropriate gain adjustment, of parallel axes did indeed produce the best result, since no apparent improvement could be achieved by cross coupling orthogonal amplitude components into the summing network (e.g.,  $\pm K_X X_R$  and  $\pm K_Z Z_R$  into  $Y_R$ ). This indicates the correlated noise field direction was essentially the same at both locations.

Some representative results for ambient and cancelled atmospheric noise levels are shown in Table 4-1, where the values are in dBH<sub>0</sub> relative to 1 A<sup>2</sup>/m<sup>2</sup> Hz, and Figures 4-4 through 4-6. Note the Schumann resonance maximums at 8, 14 and 20 Hz and minimums at 5, 11 and 17 Hz, are clearly visible on the horizontal components. The results obtained with recorded data are consistent with both earlier preliminary measurements and the FFT's from real-time signals.

The best cancellation results were achieved by subtraction of the Y-channel amplitudes from the two sites. Table 4-1 illustrates that the results could be duplicated at different times of day and on different days. At 5 and 11 Hz the cancelled amplitudes are approaching the search coil noise limit. These levels are approximately 30 dB below the Develco 1/f noise model and approximately 20 dB below the typical levels for temperate zones (e.g., Maxwell and Stone's Malta data).<sup>11</sup> The apparently uncorrelated residual atmospheric noise at the Schumann resonance peaks (8, 14 and 20 Hz) is probably simply due to the higher amplitude at these frequencies, which is of no consequence since the operating frequency will be at a minimum.

The cancelled results for the X (horizontal), in particular, and Z (vertical) axes were not as good but are within the goal for the expected noise level due to cancellation alone. In the case of the X axis, it is suspected that the higher noise level may have been a system problem since the noise level of the X axis used at the remote site became very high after the recording work was completed, and had to be repaired. Also, better results had been obtained for the X axis during preliminary tests prior to the recording phase.

The nominal ambient levels of the vertical (Z axis) fields are on the order of 10 to 20 dB lower than the horizontal fields, as is expected in regions with horizontally stratified earth conductivity. For the data illustrated in Figure 4-5A, there is some evidence of the resonance at 8 Hz. However, there is clearly some additional interference at the remote site. Cancellation did not result in any substantial reduction in this case, probably because the level is already approaching the search coil noise, which is low enough.

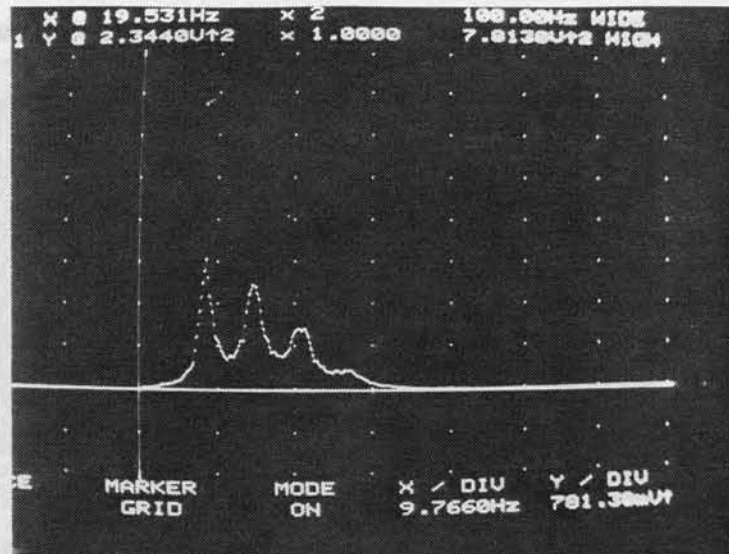
$f$ (Hz)*	5	8	11	14	17	20	Remarks
$Y_R$ $Y_L - 0.88 Y_R$	-140.1 -147.1	-130.3 -146.6	-136.9 -152.1	-129.7 -150.7	-134.7 -153.2	-132.6 -151.4	from 6:20 a.m. recording on 1/11/83
$X_R$ $X_R - 0.88 X_L$	-140 -143	-131.7 -142.2	-141.3 -144.7	-137 -144.4	-143.2 -147.4	-140.9 -147.4	from 5:30 a.m. recording on 1/11/83
$Y_R$ $Y_L - 0.87 Y_R$	-141 -147.6	-130 -144.6	-136.3 -152.7	-132.6 -150.8	-136 -153.2	-133.4 -149.9	from 7:30 p.m. recording on 1/12/83
$Z_R$ $Z_L$	-144.8 -146.2	-142.4 -139.7	-147.2 -147.2	-148.4 -143.6	-149.2 -148.9	-149.2 -149.2	from 10:20a.m. recording on 1/7/83
Bucked	No substantial reduction even with gain adjustment.						

\*The figures correspond to minimas and maximas. The actual frequencies at which they occur deviate from the above frequencies up to about  $\pm 0.2$  Hz.

Table 4-1. Summary of cancellation results (in dBH<sub>0</sub> relative to 1 A<sup>2</sup>/m<sup>2</sup> Hz).

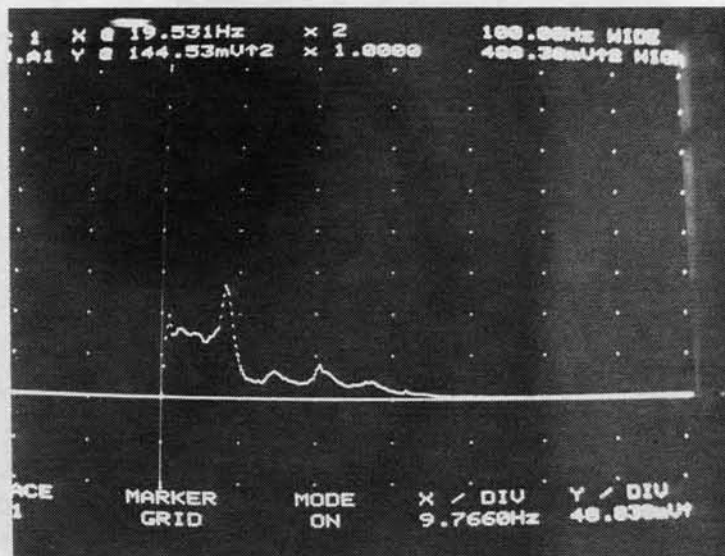
Figure 4-4. Typical Spectral Display for a Horizontal Coil

## A. Individual Remote Site



$Y_R$ , sum of 250 squared FFT's, 512 samples each, 5 ms sampling interval from 7:30pm recording on 1/12/83.

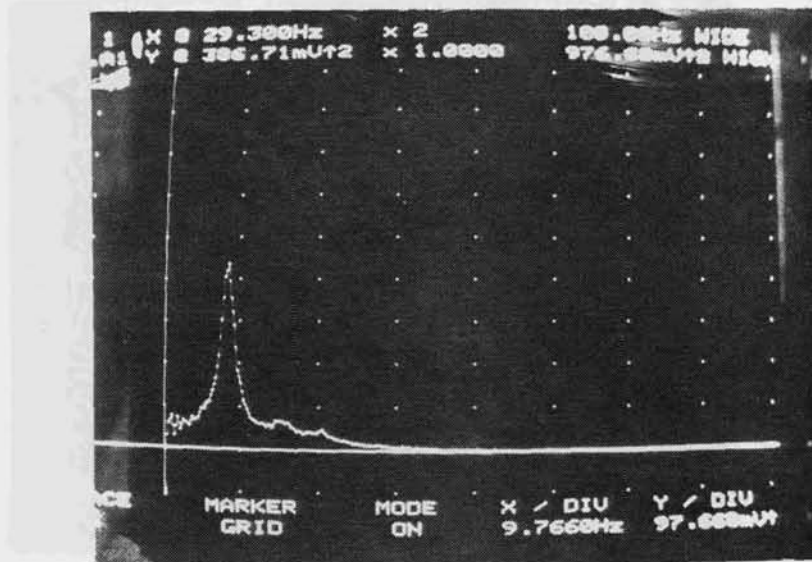
## B. Noise Residue after Cancelling



$Y_L = 0.87Y_R$ , sum of 400 squared FFT's, 512 samples each, 5 ms sampling interval from 7:30pm recording on 1/12/83.

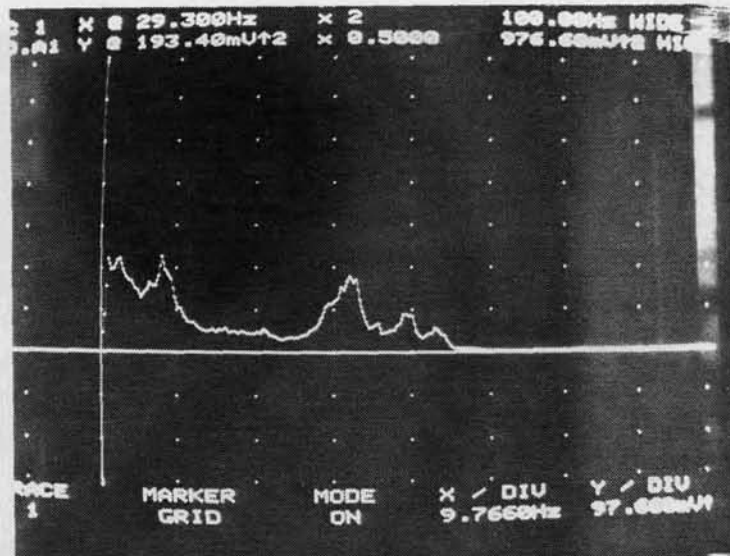
Figure 4-5. Typical Spectral Display for Vertical Coils

## A. Local Site



$Z_L$ , sum of 405 squared FFT's, 512 samples each, 5 ms sampling interval from 10:20am recording on 1/7/83.

## B. Remote Site (note differences between the two sites.)



$Z_R$ , details same as above.

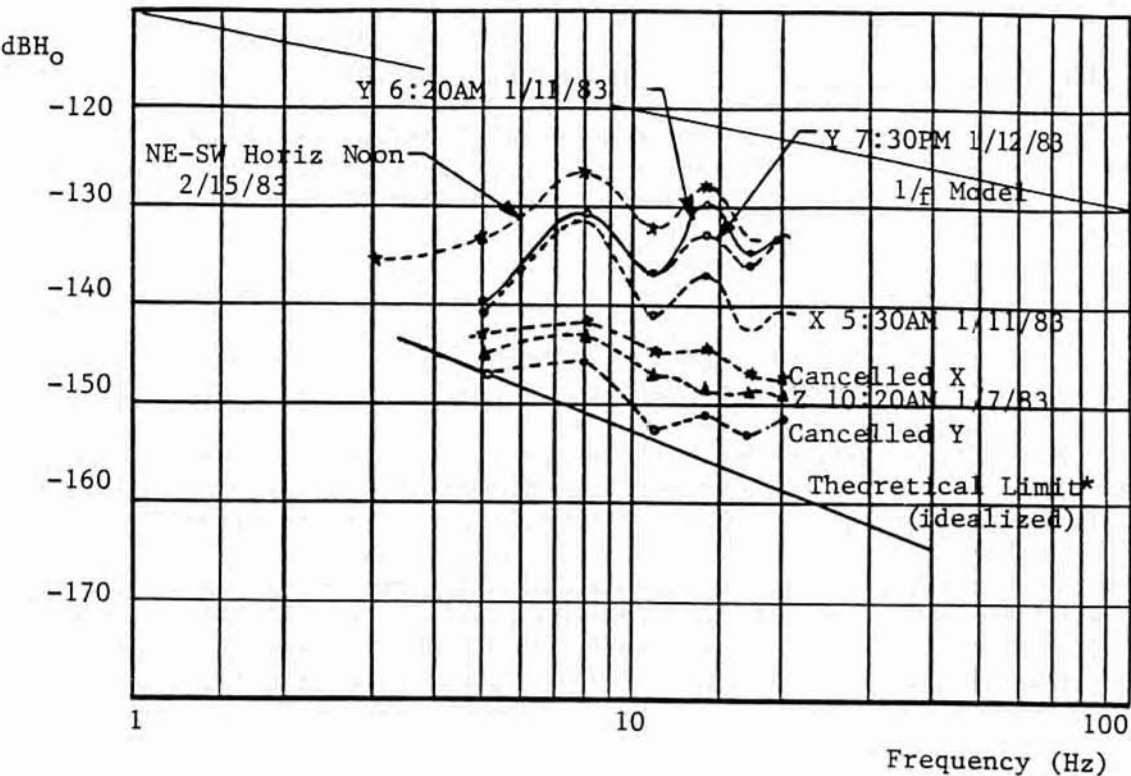


FIGURE 4-6. Comparison of Results with Theoretical Noise Limit.

\* The theoretical noise reduction limit for cancellation is approximately -153 dBH<sub>0</sub>, or an intrinsic noise level of -156 dBH<sub>0</sub> per coil, at 10 Hz.

In summary, this limited test and evaluation has shown that the desired noise levels can be achieved with cancellation. Even though the actual ambient noise levels were 10 to 20 dB lower than the "Develco Model", the cancelled result is approaching the search coil noise limit particularly at the 11 Hz minimum (for the specific gain constant, K, used in this case). This suggests that the uncorrelated noise due to geological, seismic and electronic factors is sufficiently low that similar cancellation levels can be achieved even under conditions of higher ambient atmospheric noise levels.

### 4.3 CONCLUSION

The experiment described above, although limited in scope, clearly demonstrates the expected properties of remote cancellation, and has achieved adequate noise levels for location of a trapped miner at a depth of 1 km, through overburden with an average conductivity of 0.01 S/m. For instance, with a transmitter vertical moment of 700 Am<sup>2</sup>RMS at 5.3 Hz, the field at the surface within a horizontal radius of 500 meters of the transmitter's vertical projection will be at least  $7 \times 10^{-8}$  A/m, or -143 dBH. From Table 4-1, the worst case measured noise density at this frequency after cancellation is -143 dBH<sub>0</sub> on the X-axis. The signal-to-noise ratio is therefore 0 dB in 1 Hz bandwidth. For N dB improvement by time averaging, the required time is  $T = 1/2 \cdot 10^{(N/10)}$ . Thus, a 40 dB SNR can be achieved in 5,000 seconds, or about 1.4 hours. If the X-axis amplifier was excessively noisy as suspected, the required averaging time could be reduced by as much as one-half.

It should also be noted that this experiment did not take advantage of phase correction, axis alignment correction, or impulse noise processing after cancellation. Each of these refinements, as shown by Raab<sup>9</sup> and Develco<sup>3</sup> can potentially provide further noise reduction. In particular, impulse processing has been shown by Evans<sup>10</sup> and others to have increased effectiveness when the impulsiveness of the noise increases, such as might result from nearby thunderstorm activity.

The season and locale of the remote cancellation tests resulted in relatively low absolute noise levels, masking the available improvement that might be afforded by the above techniques. Therefore, it is recommended that operational systems incorporate fully adaptive amplitude, phase, and alignment cancellation, and that impulse noise processing be incorporated in the signal chain following cancellation.



## 5.0 IN-MINE LOCATION TEST

### 5.1 SITE DESCRIPTION

The field test was conducted at the Kerr-McGee potash facility near the town of Hobbs in the flat Permian Basin area of southwestern New Mexico. The mine has a single level extending laterally over some 80 square miles, sloping 1-2 degrees down to the northeast. The test site was in the southwest area of the mine, where the depth below surface is about 1,250 feet. The surface conditions in this area include reddish-brown soil with a hardpan layer 1-2 feet down; the only vegetation supported are low, sometimes dense, brush, grass, and cactus.

The site had been designated by the mine engineer as a relatively flat area on the surface at some distance (1,000-2,000 feet) from the nearest power line and with convenient access to several areas of the tunnel network below. Four stations (D-1 through D-4) were surveyed about 500 feet apart in a pattern that would allow the surface sensors to be installed in either a colinear or triangular array (Figure 5-1). The ground slopes from the area of the stations down into a canyon to the northwest. Two preliminary loop positions were selected down in the mine, one large (LP-1) and one small (LP-2). The surface station positions were measured by the mine engineer in the mine coordinate system, which arbitrarily designates the production hoist tower as 50,000 feet N and 50,000 feet E. The mine coordinates were tied to the surface through section markers. The coordinate system actually used in the location tests had its origin (0 N, 0 E) translated to mine coordinates 46,000 N, 44,000 E to reduce the magnitude of the sensor and transmitter coordinates, since a preliminary run using the actual mine coordinates was apparently hampered by the large linear dimensions (this deficiency in the software has since been corrected). Station D-3 was arbitrarily set at zero elevation (Z=0).

### 5.2 SENSOR SYSTEM INSTALLATION

The basic scheme for installing the sensors was to place and orient the sensors approximately as desired and then measure the exact placement and orientation of the sensors in a known coordinate system. Because of time constraints, the only array shape used in the field test was colinear, with sensors A, B, and C installed at stations D-1, D-4, and D-3, respectively. The basis for positioning the sensors were large survey stakes that were placed by the mine engineer at the stations; the exact position of the stakes was known in the mine coordinate system. The sensors were installed roughly along the baseline between the stations, but brush surrounding the actual surveyed stake positions required the positions of the sensors to be 10-15 feet away along this baseline. The Y-axes of the sensors were aligned approximately along the baseline, with the positive Y-axes to the northeast. Since the stake positions were known within the mine coordinate system, the sensor positions had only to be determined locally with reference to the stakes. Some of the local measurements were made using a battery-operated auto-leveling construction

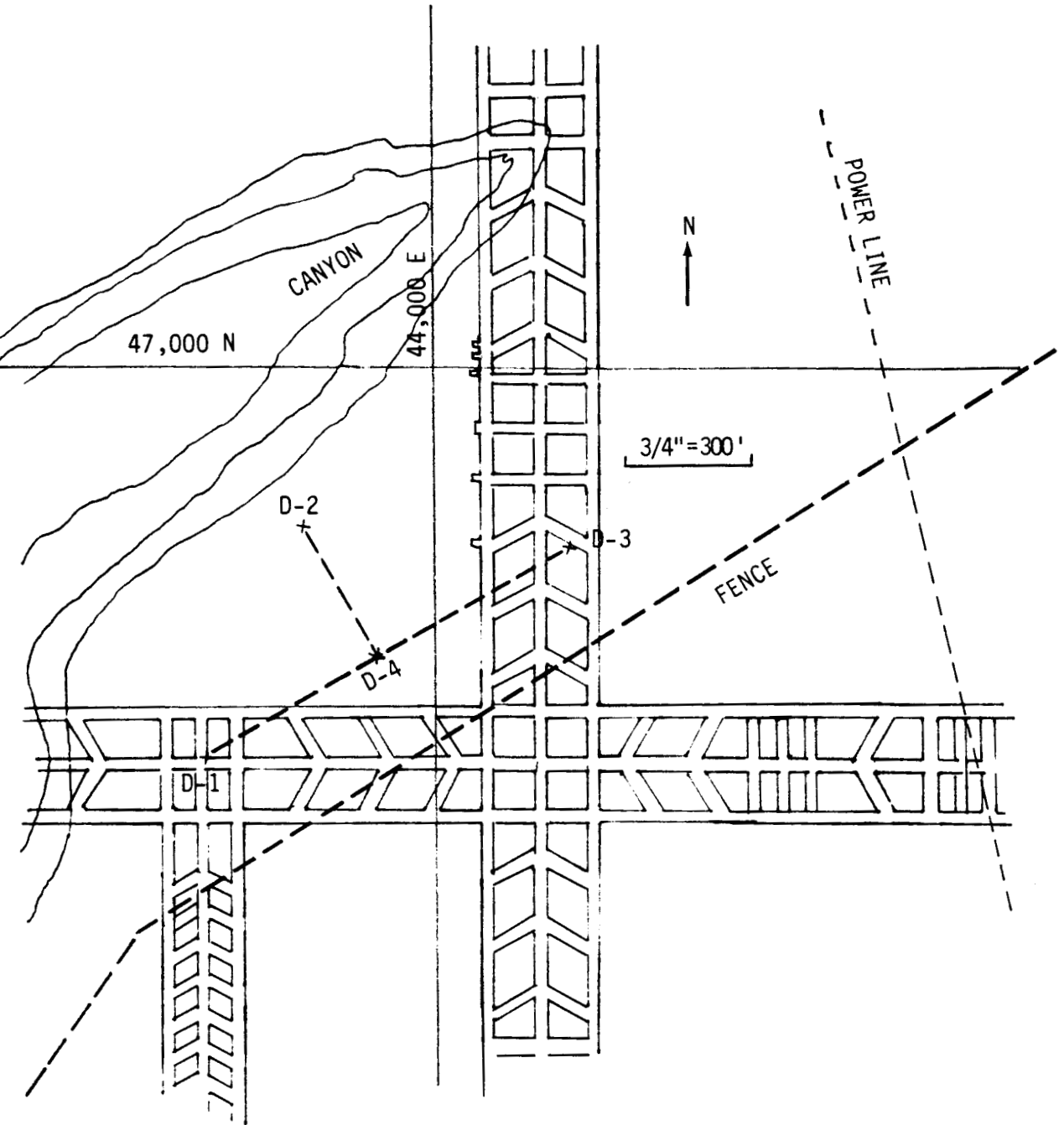


FIGURE 5-1. Plan View of In-Mine Test Location.

laser with a head that rotates 360 degrees about a horizontal axis; this allows the beam to be aimed anywhere in a vertical plane perpendicular to the rotation axis.

A shallow (1-2 foot) hole was dug for the lower Z-axis of each search coil assembly (Figure 5-2). The four horizontal axes (+X, -X, +Y, -Y) are designed to be held in place by fiberglass clamps mounted on brass stakes. First, two stakes were driven into the ground to support one arm of the search coil on the lower half of the brackets; the brackets were adjusted until the arm was resting level. The two remaining stakes were then driven in alongside the remaining arm and the lower half of the brackets adjusted to support the arm in a level position without lifting the other arm out of its brackets. Once the search coil was resting level and firmly on all brackets, the upper part of each bracket was clamped down to hold the arms securely in position.

At each sensor position, a local baseline was set up by using a transit to position a small stake on each side of the large stake at a distance of about 20 feet along the baseline. The survey laser was then placed exactly along this local baseline by lining up its beam with the two stakes; it could then be used to establish the baseline at any point in its 360-degree arc. By measuring from the sensor over to this baseline and then along the baseline to the large stake, the displacement of the sensor from the large stake could be resolved into its components in the mine coordinate system, thus determining the horizontal position of the sensor (Table 5-1). The vertical position of each sensor was simply estimated, since no accurate data were available. Sensor C at station D-3 was arbitrarily set at zero elevation ( $Z=0$ ). A very gradual slope to the west suggested that sensor B (Station D-4) was at perhaps -3 feet and Sensor A (Station D-1) was at -6 feet.

The azimuthal bearing of the positive X-axis of each sensor was measured in degrees clockwise from north (Table 5-1). This was done by positioning the laser at the same height as the mirror mounted on the sensor, aligning the laser beam parallel to the baseline, deflecting the beam off the mirror and back to the laser position, measuring the distance subtended by the beam at the laser position, dividing that distance by the distance from the laser to the mirror, taking the arctangent of the result to get the subtended angle, dividing the subtended angle in half to get the deflection angle, adding (or subtracting) the deflection angle to the azimuthal direction of the baseline to get the azimuthal direction of the positive Y-axis of the sensor, and then adding 90 degrees to get the direction of the positive X-axis. In two cases the mirror was close enough to the baseline (1-2 inches) and the laser was at the right height to leave the laser in the position used earlier to locate the sensor position. In the third case, the mirror was about 20 inches off of the baseline, so another line was set up on line with the mirror and parallel to the baseline. The deflection angle was measured as before to obtain the azimuthal orientation of the X-axis.

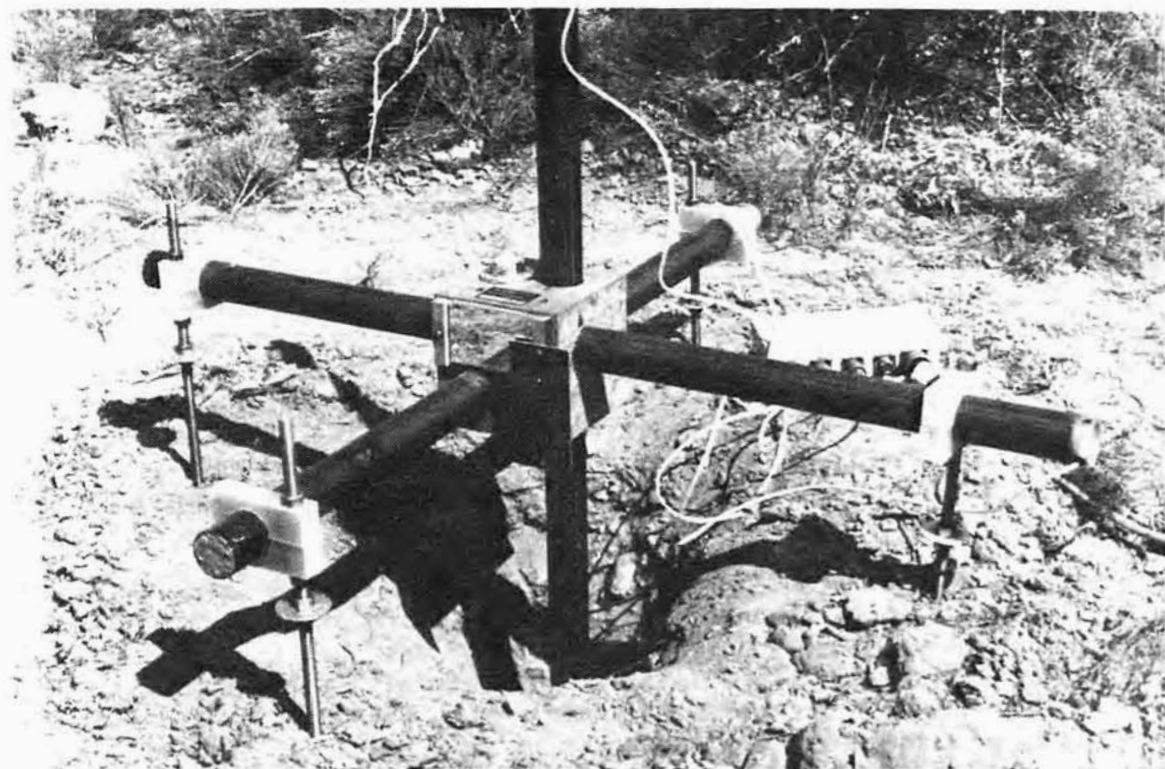


FIGURE 5-2. Three-axis search coil surface sensor measures signals from transmitter-loop in mine.

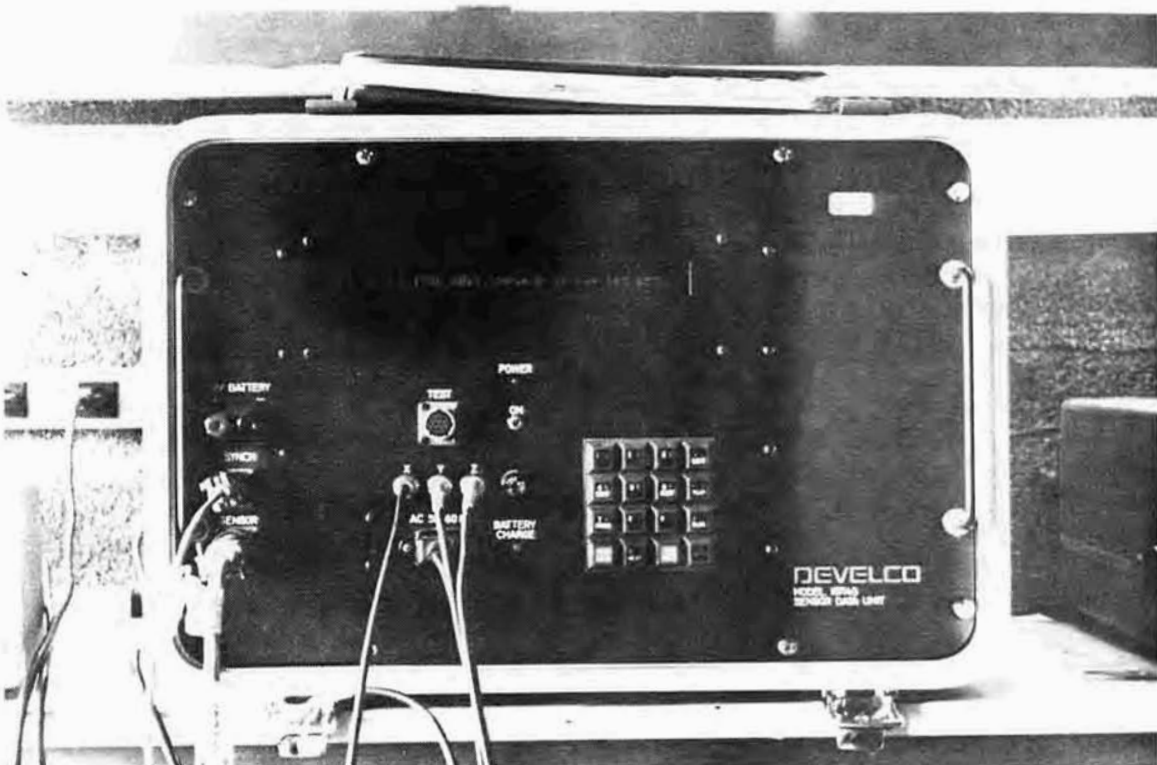


FIGURE 5-3. Sensor Data Unit processes signals and displays amplitude and phase information.

As an experimental procedure, the sensor orientations were also measured using a hand-held compass. The pertinent bearing is the direction of the positive X-axis of the sensor measured in degrees clockwise from north. Two sightings were taken on each sensor, one sighting down along the positive X-axis and the other back along the negative X-axis. Each pair of measurements agreed to within 1.5 degrees; the averages of the pairs were used as the sensor orientations in a trial location calculation (see data set 11 under Location Test Data).

<u>Station</u>	<u>Sensor</u>	<u>X-Pos (ft)</u>	<u>Y-Pos (ft)</u>	<u>Z-Pos (ft)</u>	<u>X-Az (deg)</u>
D-1	A	-576.75	50.88	-6.0	144.2
D-4	B	-128.57	308.62	-3.0	151.0
D-3	C	295.67	552.18	0.0	147.5

Table 5-1. Sensor positions and azimuthal orientations.

Positions are measured in a translated version of the mine coordinate system. Azimuths are measured clockwise from north.

To complete the installation of each sensor, the search coil leads were then connected to the post detection amplifier. After unreeling the 1,000' cable and connecting it to the post detection amplifier, the packing crate was set upsidedown over the search coil as a windscreen, with only a small tunnel opening at its base for the cable to exit and for access to the switch on the amplifier. Three burlap bags were filled with about 80 pounds each of dirt and set on top of the crate with as low a profile as possible. Each 1,000' cable was then connected to a preamplifier, which was then connected over a short cable to its matching Sensor Data Unit (SDU, Figure 5-3).

The SDU's were placed in an equipment van (Figure 5-4) along with the Location Analysis Unit (computer, disk system, and printer) and a 14-track Honeywell recorder. The van was parked along a road that runs just north of the fence line (Figure 5-1), about 300 feet south of Station D-4. Ac power was supplied by a trailer-mounted generator parked about 30 feet from the van.

Two kinds of tape recordings were made for future analysis; signal plus noise during the location tests and noise only at various times. The 14-track Honeywell 101B FM Recorder used was set up for  $\pm 1$  V maximum deviation, 54 kHz center frequency, and IRIG WB Group I, 15 ips operation. The tape SNR was approximately 44 to 49 dB relative to the maximum record level. The typical signal plus noise level was on the order of +50% full scale, with occasional higher peaks (recorder clipping would occur at about 20-40% over full scale). Ideally, all three SDU's should be run in the fixed-gain mode but this was found to be unnecessary since the front-end gain ratio stayed at a constant level of 128; in addition, the gain should

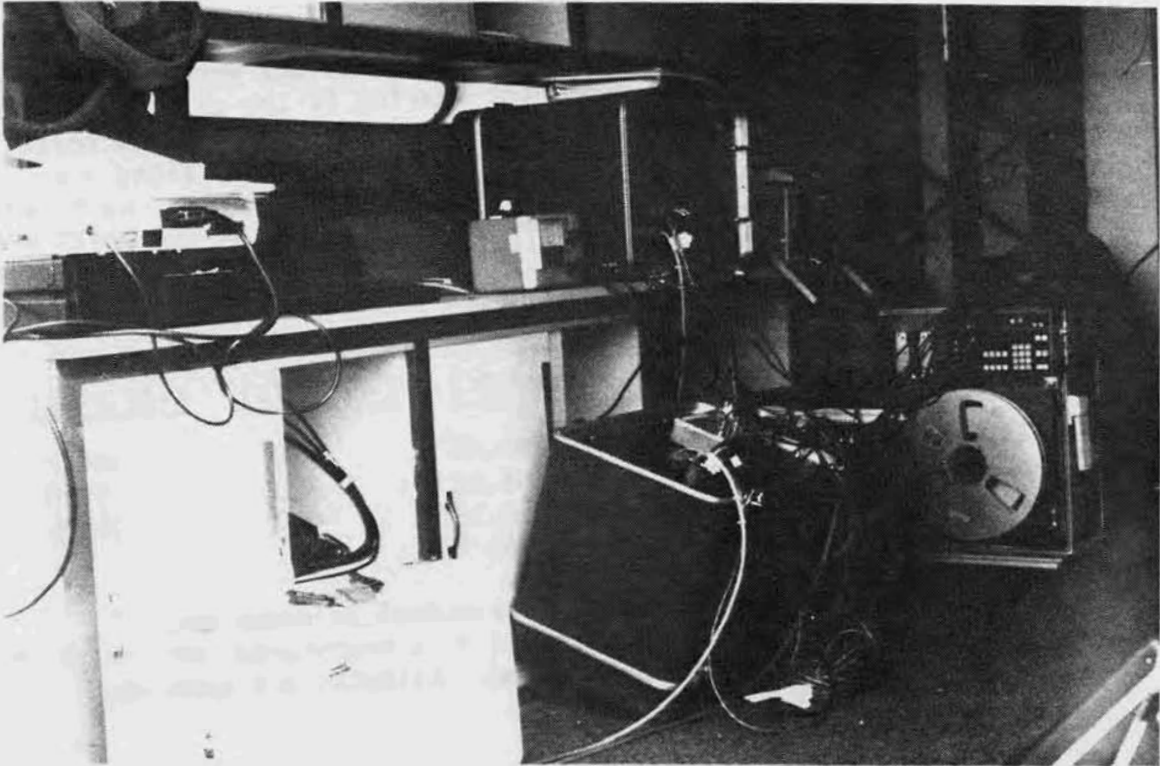


FIGURE 5-4. Equipment van holds (left to right) computer system, Sensor Data Units, and tape recorder.



FIGURE 5-5. Computer calculates transmitter location based on information

not be fixed when acquiring location data. Recordings were made of all nine sensor channels at the analog outputs of the three SDU's, along with a stable 25 kHz reference frequency for playback speed control.

### 5.3 TRANSMITTER INSTALLATION

Three transmitter-loop positions were used during the location tests (Figure 5-6), with a project name assigned to each position as follows: a 920' circumference loop at LP-1 was Project KMO2, a 470' loop at LP-2 was Project KMO3, and a 380' loop at the spontaneously selected position LP-3 was Project KMO4 (Project KMO1 was assigned to the system checkout below). Each loop was laid out along the perimeter of one or more pillars and connected to the modified transmitter; the transmitter was powered by two cap-lamp batteries connected in parallel. Loop deployment and transmitter operation were done just prior to each test on a prearranged schedule, since there was no communication with the surface test site. Operating time was limited by the necessary preparations before each test and the hoist operating schedule in the afternoon. The duration of transmission ranged from 25 minutes to two hours (Table 5-2), with an average battery discharge rate of about 50 mV/hour. Loop current was measured with a small portable oscilloscope and a low-value series resistor. The transmitter operating frequency was 10-2/3 Hz. The gauge and length of the wire used varied between the three loop positions to keep the resistance close to the nominal 2-ohm standard (Table 5-3).

The estimated moments ranging from 4,868 to 759 Am<sup>2</sup> were calculated from the measured currents and the enclosed loop areas as scaled from the mine map. The differences between these estimated moments and the mean moments from the location calculations are probably due mainly to errors in scaling the loop dimensions from the map. Since the measuring equipment has been accurately calibrated, the moments from the location calculations are probably correct. Although a standard 300' loop was not installed, the calculated moment of 678 Am<sup>2</sup> for a standard loop (Section 2.4) is on the same order as that actually obtained from the 380' loop used at LP-3 because of the higher resistance and thus lower current.

### 5.4 SYSTEM FUNCTIONAL CHECKOUT

Sample atmospheric noise measurements were made to verify the stability of the sensor installations and that the noise levels would be low enough for proper location system operation. A narrow bandpass filter with a center frequency of 8 Hz, a noise bandwidth of 2 Hz, and a gain ratio of 45 was connected to the broadband analog output of each of the three SDU's in turn. The front-end gain ratio of each SDU was 128. Voltage measurements were made with an HP403 low-frequency RMS voltmeter. The conversion to equivalent field assumed a combined sensor and post detection amplifier scale factor of 100 V/A/m.

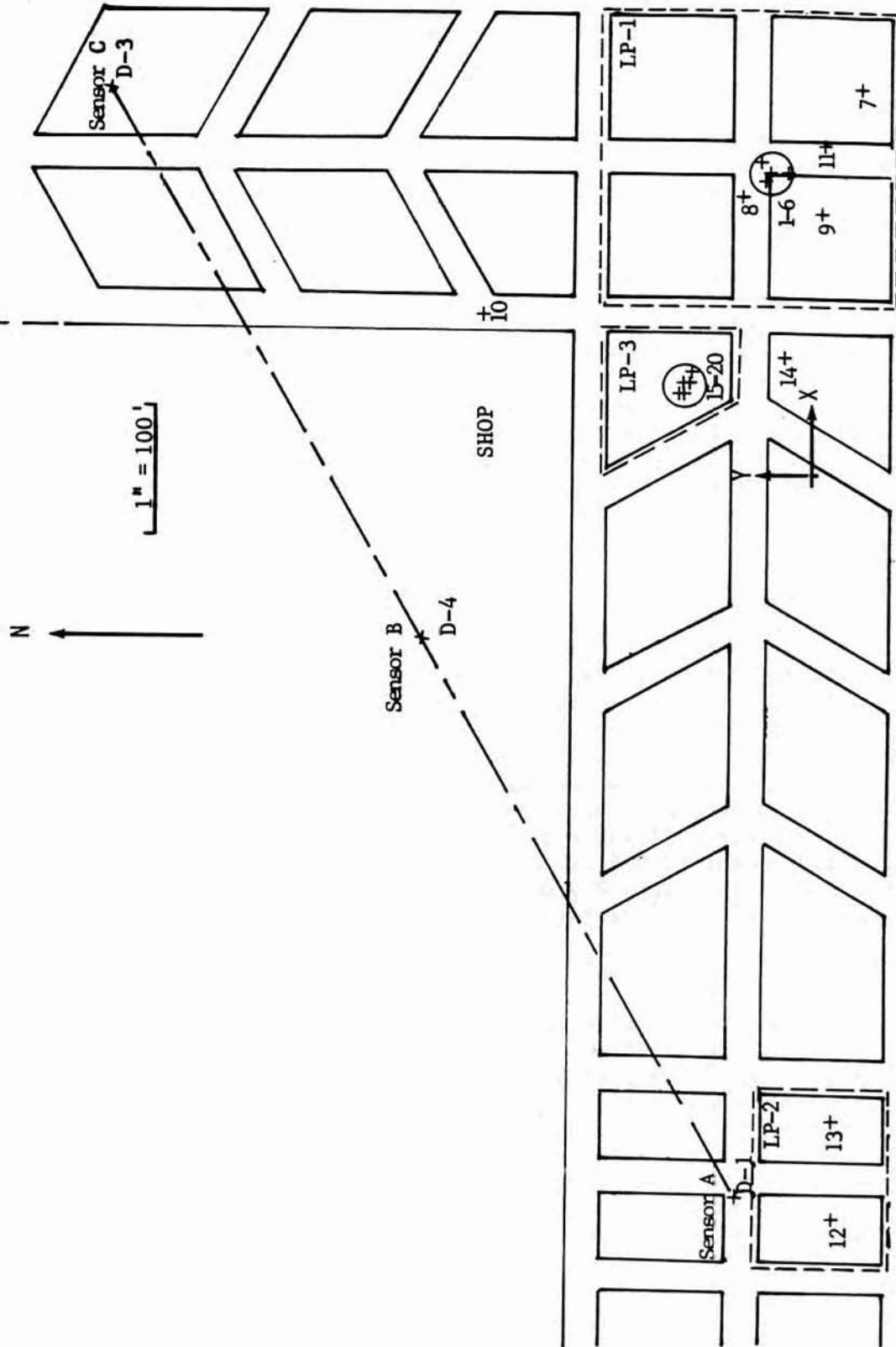


FIGURE 5-6. Location results from in-mine field test. A number beside a cross indicates the set of data that resulted in that particular horizontal location; where the crosses are too densely clustered, the cluster is circled and the range of data sets given. The depth (or Z-location) of each result appears in Table 5-5, along with the tilt and moment for each result.



		Position 1 4-Pillar (Init/Final)	Position 2 2-Pillar (Init/Final)	Position 3 1-Pillar (Init/Final)
Loop resistance <sup>1</sup>	ohms	2.8/---	3.5/---	2.7/---
Battery voltage				
No load	V	4.194/4.105	4.100/-----	4.210/4.045
Load	V	4.052/4.106	4.041/4.014	4.090/3.986
Loop current (pk) <sup>2</sup>	A	1.10 /1.10	0.90 /0.90	1.11 /1.11
Duration	min	--/60	--/25	---/120

<sup>1</sup>Does not include 0.1-ohm resistor used for current measurements.

<sup>2</sup>Measured using the 0.1-ohm series resistor, which is always in the circuit during transmission.

Table 5-2. Transmitter parameter measurement summary.

	Units	Position 1 4-Pillar	Position 2 2-Pillar	Position 3 1-Pillar
Loop Dimensions <sup>1</sup>	feet	230x230	135x100	110x100x55 <sup>2</sup>
Loop Circumference	feet	920	470	380
Enclosed Area	ft <sup>2</sup>	52900	13500	8250
	m <sup>2</sup>	4915	1254	766
Wire Gauge	AWG	#14	#18	#18
Wire Length	feet	~1000	~480	~400
Wire Resistance <sup>3</sup>	ohms	2.8	3.5	2.7
Peak Current <sup>3</sup>	A	1.1	0.9	1.1
Peak Moment <sup>4</sup>	Am <sup>2</sup>	5406	1129	843
RMS Moment <sup>5</sup>	Am <sup>2</sup>	4868	1016	759
Mean Moment	Am <sup>2</sup>	4923	853	698

<sup>1</sup>Based on scaled dimensions from mine map.

<sup>2</sup>Trapezoidal pillar, see Figure 5-6.

<sup>3</sup>Measured values.

<sup>4</sup>RMS moment referred to the fundamental for a square-wave is

$$m_0(\text{RMS}) = \frac{2\sqrt{2}}{\pi} NAI_{pk}$$

<sup>5</sup>Based on results of location calculations (RMS).

Table 5-3. Transmitter-loop parameters and moments.

These atmospheric noise measurements were made in the late morning on October 10, before the sets of signal measurements for location projects KM02 and KM03. The results were essentially identical on each corresponding axis at each sensor station (Table 5-4) and are consistent with expected atmospheric noise levels based on previous measurements. In addition, the vertical field is approximately 20 dB lower than the horizontal field, as is expected in regions with horizontally stratified earth conductivity. The weather conditions at the time of the measurements were mildly breezy and partially overcast, although it was cloudier to the southwest and there could have been distant thunderstorms. It was concluded that the windscreens placed over the sensors were adequate.

<u>Axis</u>	<u>Average*</u>	<u>Horizontal Total</u>	<u>Expected</u>
X (horiz)	-129 to -126	-121 to -119	-126
Y (horiz)	-121 to -120		
Z (vert)	-144 to -138		-146

\* This is the mean of the typical levels, as determined by observing the meter over some period of time. Occasional impulses can cause considerable variation. In this case, the Y-axis was the most variable with occasional fluctuations of  $\pm 6$  dB.

Table 5-4. Typical measured atmospheric noise levels at 8 Hz.  
All values are in dBH<sub>0</sub> relative to 1A<sup>2</sup>/m<sup>2</sup>/Hz.

Since the search coil sensor stations were within 2,000 feet of a surface high-voltage powerline (within 1,000 feet at D-3, the closest station) and approximately 1,200 feet from underground powerlines, 60 Hz interference was of potential concern. However, measurements made near D-3 showed the pre-60-Hz notch filter levels on all three sensor axes were approximately two orders of magnitude below the search coil post detection amplifier saturation level (5 V referred to the output). Typical values were less than 300 micro A/m peak or -70 dBH. The horizontal axis perpendicular to the surface powerline had the highest value. The vertical axis value was about 2 dB less and the orthogonal horizontal axis value about 6 dB less.

After the 920-foot loop was installed around the four pillars at position LP-1, a preliminary test was conducted to check system functions and verify that signal and noise levels were suitable for location measurements. The data obtained for this case were designated as Project KM01, even though the data were not used in any location calculations (ensuing location tests were designated as Projects KM02 through KM04).

One of the SDU's had a minor display malfunction that was not repaired until the following day, so that only two units were available for taking data on October 9. The system checkout was continued meanwhile with one of the two good SDU's being used to monitor two of the three sensors by switching the sensor cables back and forth. This switching of the cables (in effect, multiplexing) defeats the long-term integration of the data, which might adversely affect the results of a location calculation, but the method was sufficient to verify expected signal and noise levels during the functional checkout.

The measured signal and noise levels compared well with those expected for the configuration, with one exception: one of the channels from sensor C was found to have a signal level far below even the expected atmospheric noise levels. This problem was traced to holes in the cable that had evidently been chewed by some small animal(s), e.g., pack rats. The damaged section was removed and the cable fittings reconnected. Less extensive damage to the other two cables required only minor repair. Mine personnel suggested that chewing animals are particularly attracted by salty sweat residue deposited during handling of the cable, although the insulation itself is, in many instances, the objective.

## 5.5 LOCATION TEST DATA

The coordinate system used in the field test was right-handed and orthogonal, with the Z-Axis positive upward and the positive X-Axis pointing at 90 degrees clockwise from north. The origin of this coordinate system (Figure 5-6) is located at mine coordinates 46,000N and 44,000E. Sensor C was arbitrarily set at zero elevation ( $Z = 0$ ).

Fifteen complete sets of sensor data were recorded, at 10- to 15-minute intervals, from the three different loop positions. Each loop position was designated as a separate project; these were named KM02, KM03, and KM04 (Project KM01 designates the checkout of the system functions). These three projects have six, two, and seven sets of sensor data, respectively. One set of sensor data (No. 2) from Project KM02 was modified in various ways to create five experimental additional sets of sensor data (Nos. 7-11). All of the sheets containing the project information and sensor data are given in the appendix.

Project KM02 designates data collected on October 10, 1984, from the 920' loop at LP-1 (Figure 5-6). The first six sets of sensor data (Nos. 1-6) were collected from 12:33 to 13:30. The Sensor Data Units were reset before the first set of data was taken and reset again before the third set. The data sheets for these six sets follow the project information sheet for Project KM02 in the appendix.

The next three sets of sensor data (Nos. 7-9) are modified versions of the set of sensor data collected at 12:45 (No. 2). These three sets represent, in turn, the omission of data from sensors A, B, and C, so that data from only two sensors are used in each case. This was done to

evaluate the performance of a two-sensor system. The project information had to be changed to reflect the omission of the one sensor in each case, so that three new projects were designated KMBC, KMAC, and KMAB, respectively. The project information sheets and corresponding sensor data sheets appear in the appendix following the sheets for data sets 1-6.

Sensor data sets 10 and 11 represent modifications in the azimuthal directions of the sensors, using the data collected at 12:45 (No. 2). Set 10 discarded the local rotations of the sensors from the sensor baseline, or, in other words, it assumed that all sensors were pointing in exactly the same direction of 150.1 degrees clockwise from north. This introduced angular rotation errors of +4.9, -0.9, and +2.6 degrees at sensors A, B, and C to evaluate the sensitivity of the system to such errors. This required a revision in the project information, so that a project information sheet and sensor data sheet for a project named KMNR have been included in the appendix. Set 11 introduced the same kinds of rotational errors, but in this case the azimuthal values represent readings from a hand-held compass used to sight along the sensor. The angular errors in this case were +1.2, +0.6, and +1.5 degrees; these data appear in the appendix under project KMCR.

Project KM03 designates data collected on October 10, 1984, from the 470' loop at LP-2 (Figure 5-6). The two sets of sensor data (Nos. 12 and 13) were collected at 13:45 and 13:55, starting two minutes after a reset of the Sensor Data Units. The data sheets for these two sets follow the project information sheet for project KM03 in the appendix.

Project KM04 designates data collected on October 11, 1984, from the 380' loop at LP-3 (Figure 5-6). The seven sets of sensor data (Nos. 14-20) were collected from 10:50 to 12:25; the first set (No. 14) was taken within two minutes of resetting the Sensor Data Units. The data sheets for these seven sets follow the project information sheet for project KM04 in the appendix.

## 5.6 LOCATION RESULTS

Each set of sensor data (along with its corresponding project information) was entered into the computer running the Locator/DLMG software (Figure 5-5). The result from each set of data is an X, Y, Z-location of the source transmitter-loop, the tilt of the loop in degrees from horizontal, and the moment of the loop in amperes-squared ( $\text{Am}^2$ ) (Table 5-5). The horizontal location of each result is generally very close to the center of its corresponding loop position (Figure 5-6). The notable exceptions are data sets 7-11 (the modified sets) and data set 14.

The location results from the unmodified sets of data (Nos. 1-6) are tightly grouped near the geometric center of the loop at LP-1 (Figure 5-7), with a mean depth of -1,241 feet. The mean location is offset from the center of the loop by about 10 feet to the south and seven feet to the west. The approximate depth in this area was given by the mine

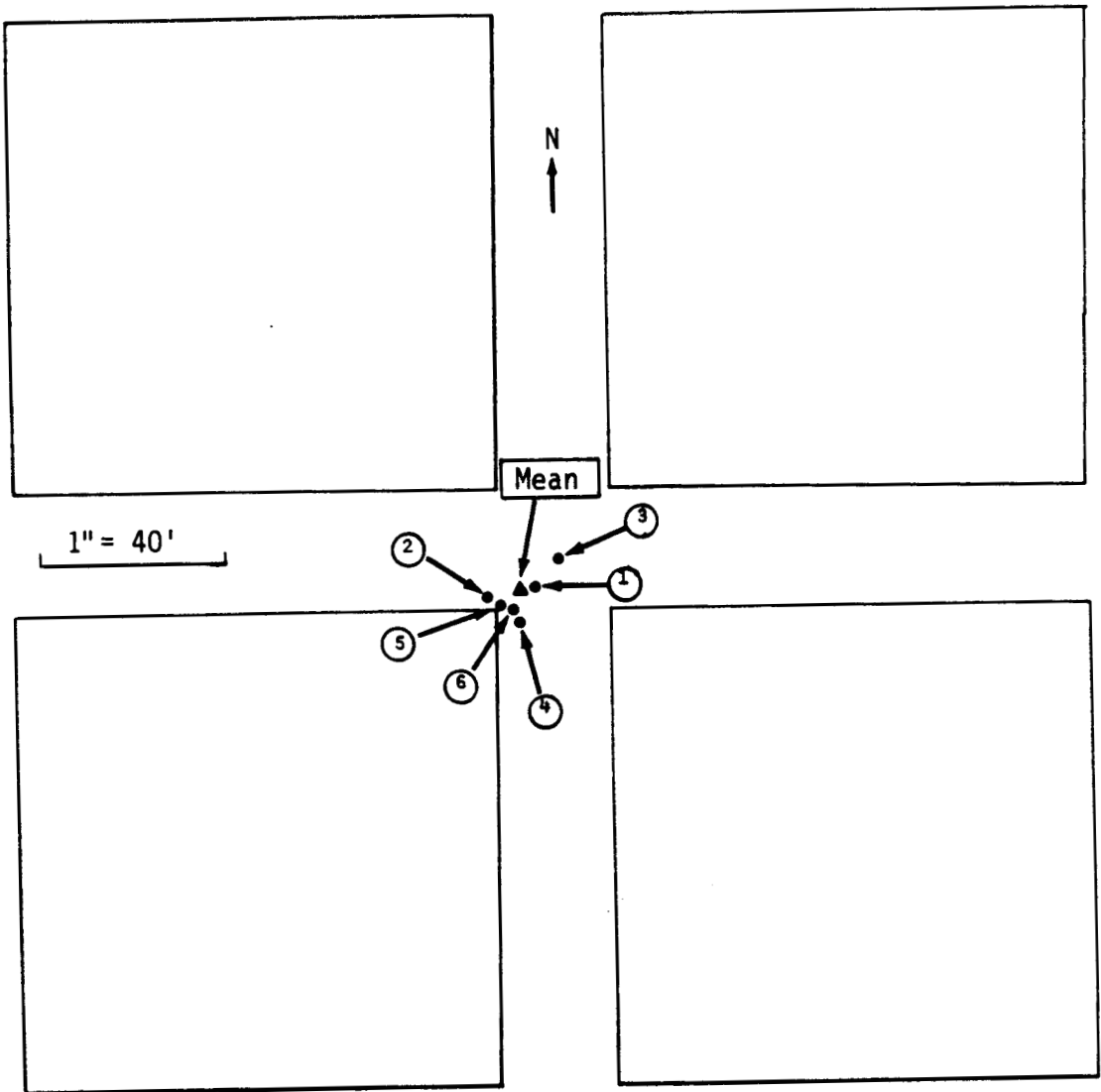


FIGURE 5-7. Location Results from Data Sets 1-6. Dots represent individual results; the mean is shown as a triangle.

engineer as -1,250 feet. The standard deviation of the location results is about five feet in the horizontal direction and seven feet in the vertical direction. The mean tilt value is three degrees from horizontal; the mean moment is about 4,900  $\text{Am}^2$ .

The location results from the sets of data using two sensors (sets 7-9) are scattered somewhat farther from the center of the loop (Figure 5-6), but still fall within its perimeter, with depths ranging from -1224 to -1240 feet. The farthest off of these is set 7, which uses only the data from Sensors B and C. It should be noted that, in this case, the transmitter-loop is located close to the vertical plane of ambiguity which bisects the line between the two sensors being used. In addition to increasing the error in the resulting location, being close to this plane produces an unusually high tilt value of 11 degrees from horizontal. Using the data from sensors A and C (set 8) or Sensors A and B (set 9) produces location results that are closer to the center of the loop and have more reasonable tilt values (5-6 degrees).

The location results from set 10 are the worst of any, lying 250 feet to the northwest of the loop center (Figure 5-6). The tilt indicated is 29 degrees from horizontal. Although the rotational errors introduced in this case by assuming that the sensors are aligned with the baseline (see Location Test Data) cause a significant deviation in the location result, the result might well be satisfactory as a first quick estimate. The location results from set 11 are much better than those from set 10, in accordance with the lower rotational errors introduced by using the compass readings for the azimuthal directions of the sensors (see Location Test Data). The horizontal location is about 40 feet from the cluster of results from data sets 1-6. The depth is -1227 feet, with a tilt of six degrees and a moment of about 4900  $\text{Am}^2$ .

The location results from data sets 12 and 13 are well within the perimeter of the loop at LP-2 (Figure 5-8), although they are more scattered than the results from sets 1-6. The sensor data used here are somewhat noisier than for the previous position because of the smaller loop size; the readings from Sensor C are particularly noisy because of the fall-off in signal strength. The mean of the two location results is 12 feet to the south and one foot to the east from the center of the loop. The mean depth is -1196 feet; the mine engineer indicated a depth of about -1225 feet in this area. The standard deviation of the location results is about 30 feet in the horizontal direction and 25 feet in the vertical direction. The mean tilt value is five degrees from horizontal; the mean moment is about 850  $\text{Am}^2$ .

The only exception to the small cluster of location results near the center of the loop at LP-3 is the result from data set 14 (Figure 5-6). The horizontal location is over 100 feet south from the center of the loop, the indicated depth is nearly 65 feet shallower than the nominal depth, and the indicated tilt is about 15 degrees steeper than the nearly-level mine floor. This data set was the first recorded after resetting the Sensor Data Units; it was taken after only two minutes of long-term integration.

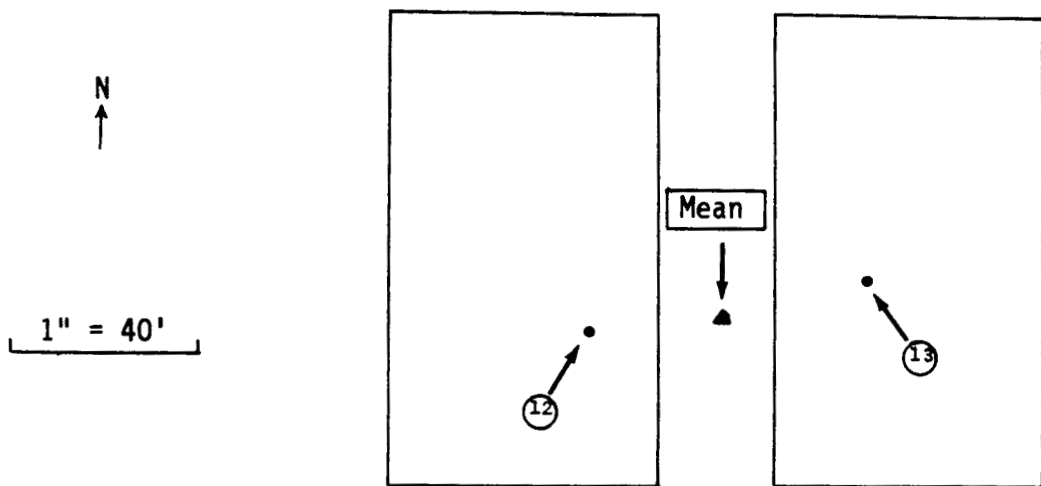


FIGURE 5-8. Location Results from Data Sets 12 and 13.

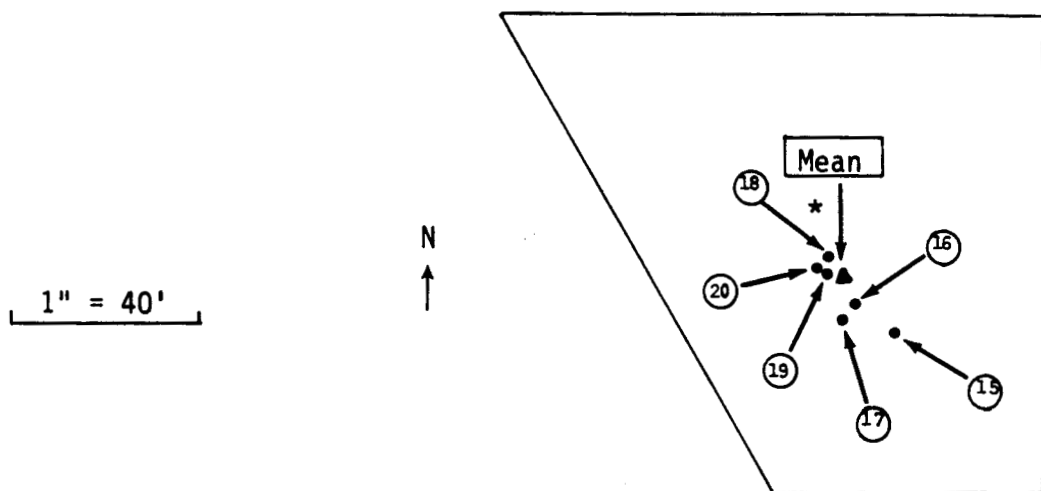


FIGURE 5-9. Location Results from Data Sets 15-20. Dots represent individual results; the mean is shown as a triangle. The asterisk indicates the geometric center of the loop.

In the case of this smaller and noisier transmitter, a longer integration time was apparently necessary to achieve good results. The location results from data sets 15-20 have a mean horizontal location about 11 feet to the south and two feet to the east of the loop center (Figure 5-9), with a mean depth of -1223 feet. The standard deviation of the location results from sets 15-20 is about six feet in both the horizontal and vertical directions. The mean tilt value is two degrees from horizontal; the mean moment is about 700 ampeters-squared.

Loop position 1 -----		Project: KM02 -----			10/10/84		
<u>Data set</u>	<u>Time</u>	<u>X-Feet</u>	<u>Y-Feet</u>	<u>Z-Feet</u>	<u>Tilt</u>	<u>Moment</u>	<u>Comments</u>
1	12:33	240.3	42.3	-1232	2	4844	reset
2	12:45	234.2	41.5	-1239	3	4916	
3	13:00	246.4	49.1	-1253	1	5047	reset
4	13:10	238.7	37.7	-1239	3	4913	
5	13:20	236.6	41.0	1240	3	4913	
6	13:30	237.8	41.4	1240	3	4906	
7	12:45	305.4	-34.0	-1224	11	5005	without A
8	12:45	217.2	55.5	1233	5	4852	without B
9	12:45	210.9	17.6	-1240	6	4904	without C
10	12:45	111.4	265.0	1243	29	4883	no rot.
11	12:45	252.2	2.6	-1227	6	4884	compass

mean results and standard deviations from data sets 1-6

	239.0	42.1	1241	3	4923
	<u>+3.8</u>	<u>+3.4</u>	<u>+7</u>	<u>+1</u>	<u>+61</u>

estimated actual loop parameters

	245.8	52.5	-1250	1	4868
--	-------	------	-------	---	------

Loop position 2 ----- Project: KM03 ----- 10/10/84

<u>Data set</u>	<u>Time</u>	<u>X-Feet</u>	<u>Y-Feet</u>	<u>Z-Feet</u>	<u>Tilt</u>	<u>Moment</u>	<u>Comments</u>
12	13:45	-586.4	-33.9	-1220	5	909	reset
13	13:55	-527.8	-25.2	-1171	5	797	

mean results and standard deviations from data sets 12 and 13

	-557.1	-29.6	-1196	5	853
	<u>+29.3</u>	<u>+4.3</u>	<u>+25</u>	<u>+0</u>	<u>+56</u>

estimated actual loop parameters

	-556.2	-16.8	-1225	1	1016
--	--------	-------	-------	---	------

Table 5-5. Location results from in-mine field test. Comments are explained under Location Test Data.



Loop position 3 -----		Project: KM04 -----			10/10/84		
<u>Data set</u>	<u>Time</u>	<u>X-Feet</u>	<u>Y-Feet</u>	<u>Z-Feet</u>	<u>Tilt</u>	<u>Moment</u>	<u>Comments</u>
14	10:50	76.7	23.2	-1186	15	672	reset
15	11:05	77.8	98.7	-1217	3	692	
16	11:25	68.4	104.4	-1223	2	700	
17	11:40	66.7	108.9	-1223	2	699	
18	11:55	63.1	115.2	-1225	2	699	
19	12:10	62.6	113.8	-1226	1	699	
20	12:25	60.6	114.4	-1226	2	699	
mean results and standard deviations from data sets 15-20							
		66.5	109.2	-1223	2	698	
		<u>+5.7</u>	<u>+6.0</u>	<u>+3</u>	<u>+1</u>	<u>+3</u>	
estimated actual loop parameters							
		64.3	98.6	-1250	1	759	

Table 5-5. Location results from in-mine field test.  
Comments are explained under Location Test  
Data.--Continued

## 5.7 DISCUSSION OF RESULTS

The mean location results agree quite well with the estimated actual loop positions (Table 5-5). The difference between the results and the actual loop positions is generally less than 1% of the distance from the loop positions to the sensors. Also, the standard deviation of the results is as low as 0.5% of the mean range. This level of error compares well with the short-term system SNR values of the measured data, which were generally 35-45 dB (40 dB is equivalent to one percent). The exact relationship, however, between noise in the measurements and error in the results is not known and is probably not linear.

There is a suggestion of a consistent bias in the mean location results of about 10 feet to the south from the center of each loop position (with varying offsets to the east or west). The mine engineer estimates an overall error of less than five feet in the mine survey used to locate the horizontal sensor positions, but survey errors in the vertical direction may be greater. The eyeball assumption, for example, that sensor B is at -3 feet depth (relative to sensor C at zero depth) and that sensor A is at -6 feet depth may well be off by several feet. If there is a systematic error in the survey, it would produce a consistent offset in the results. In addition to errors in the location results introduced by noise and by survey errors, there are position and orientation errors made when installing the sensors.

The location calculation results appear better than would be suggested by the conditions and trends in the SNR values in Table 5-6. The elapsed time given is the approximate time since the last reset of the long-term block averaging after the signal had been acquired (measurements could not be made simultaneously, but were within several minutes of the event and each other). The short-term SNR is measured at the output of the SDU lowpass filter, which has a time constant of 15 seconds and a noise bandwidth of 0.01 Hz (second-order filter). In most cases, it is in rough agreement with the expected SNR based on calculations using the estimated transmitter moment and an assumed atmospheric noise level of  $-126 \text{ dBH}_0$  with the same bandwidth. This suggests that system operation is at or near the atmospheric noise limit.

Project Name	Elapsed <sup>1)</sup> Time (m)	Sensor A SNR	Sensor B SNR	Sensor C SNR
		L-term/S-term	L-term/S-term	L-term/S-term
KM02	0	48/44	46/54	38/39
	10	34/39	41/50	34/30
	20	32/43	41/46	35/36
	30	32/42	41/51	35/47
	expected	--/43	--/47	--/46
KM03	0	32/36	25/34	20/30
	10	25/40	25/34	20/31
	expected	--/36	--/34	--/28
KM04	0	15/19	29/43	23/40
	15	14/20	26/40	24/40
	35	15/19	27/38	25/37
	60	15/16	27/45	25/40
	65	15/21	27/39	26/39
	80	16/27	27/41	26/37
	95	16/27	27/37	26/35
	expected	--/31	--/33	--/31

1) Approximate, i.e., within a few minutes.

Table 5-6. System Signal-to-Noise Ratio vs. time.  
All values in dB except as noted.

The long-term SNR is measured at the output of the SDU block-averaging process that operates continuously since the time of the last reset. For gaussian noise, averaging should increase the SNR by 10 dB for every ten-fold increase in the averaging time. If there is any deterministic change in the transmitted signal amplitude, it will be interpreted as a variance and included in the SNR calculation. The decrease in transmitter moment amplitude caused by the decay of the

cap-lamp battery voltage (Section 2.4) or transmitter current ripple are examples of why the long-term SNR's might appear somewhat lower than the short-term and not improve significantly with time. In this case, the gaussian noise would be averaged and the correct relative mean signal amplitudes will be obtained even though the displayed SNR value is low. A correct geometrical location answer will result but the calculated transmitter moment will be in error. The reason why the displayed long-term SNR values appear to be about 10 dB lower than the short-term values, as well as inconsistent with the good location results, is not understood at this time.

In reviewing the long-term SNR data in detail, it was observed that anomalously high noise conditions existed on the Y-channel of sensor A and the Z-channel of sensor C for project KMO2, as well as the Y- and Z-channels of sensor A for Project KMO4. These spurious levels appeared to be on the order of 6-10 dB higher than the level on a normal horizontal channel. The heavy impact of the last case on the system SNR is shown clearly in Table 5-6. In addition, an intermittent noise problem on the vertical (Z) channel of sensor C was observed in the field before and after project KMO4. This was later identified as a ground lead problem in the sensor preamplifier and corrected. Ground connections in the other sensor units were also inspected and secured. Other possible causes of the spurious noise levels in the other cases are problems from the cable damage, other grounding problems, or condensation. These noise problems did not seem to seriously affect the location results, possibly because the levels were still relatively low and only two of nine channels were involved in each of the affected tests.

The question of whether long-term averaging provides improvement of the location results is answered by observing the trend in the location results from data sets 14-20 (Figures 5-6, 5-9). There is a marked advance toward the center of the loop, starting with the first data following a reset (set 14) and ending with the data that were averaged for up to an hour and a half.

Overall, the location results show good consistency and accuracy. The low scatter in the results from project KMO2 shows the precision that can be expected from a source with a fairly large moment or high SNR. Results from Project KMO3 show the greater scatter expected from noisier measurements (from a smaller loop) made over a short time. Project KMO4 again showed low scatter, due in part to the longer block-averaging time.

## 6.0 CONCLUSIONS AND RECOMMENDATIONS

The basic goal of Phase II of this program was to test the key features that would be needed in an electromagnetic system that uses 3-4 stationary 3-axis sensors on the surface to locate a magnetic loop antenna of limited size deployed by a miner trapped in a deep mine (1,000m). The major objectives were to verify:

- a) sensor sensitivity
- b) noise cancellation feasibility (in a separate test)
- c) location method operation

Practical, relatively compact 3-axis search coil sensors with an intrinsic noise level approximately 3 orders of magnitude lower than nominal atmospheric noise levels have been built and tested. These sensors have been used to demonstrate the expected properties of remote noise cancellation. This limited experiment achieved adequate noise levels for location of a trapped miner at a depth of 1 km through an overburden with an average conductivity of 0.01 S/m. The experiment did not take advantage of phase corrections, axis alignment corrections, or impulse noise processing after cancellation. Each of these refinements can potentially lead to further noise reduction.

A breadboard location system was supplied to this program in order to evaluate the proposed location method in shallower mines prior to building an operational prototype for use in deep mines (1,000m). In addition to the sensors, the system consists of 3 Sensor Data Units, which serve as receivers, and a Location Analysis Unit, which is a portable computer with unique software for location calculation. The location method developed by Develco has proven effective over a variety of sensor array configurations and conditions in computer simulations, scaled lab-array tests, and the in-mine test. The in-mine test without noise cancellation conducted on this program demonstrated that an accuracy of less than 1% of depth could be achieved in a 380m deep mine with a colinear array.

It is recommended that the Bureau of Mines conduct additional tests with the breadboard location system. At first, these should be under controlled, nominal circumstances at a shallow research mine to fully evaluate the basic procedures and functions. The emphasis should be on the methods and reproducibility of the surveying and sensor emplacement in the field. Then tests should be conducted at a variety of deep mines, including some greater than 400m, to gain experience with effects such as electrical interference and scattering in different environments. Additional investigations into noise cancellation should emphasize algorithm development and testing with noise data obtained under a variety of conditions.

It should then be possible to fully determine the requirements for a complete prototype operational deep-mine location system using noise cancellation. This version might incorporate the following general features:

- 1) A fourth sensor for noise cancellation which can be installed at a large distance (10-15 km) from the other three sensors to measure noise only for remote cancellation.
- 2) Compact, low power signal acquisition/digitizing equipment.
- 3) RF data links to transmit signal information from the sensors and eliminate the need for long cables.
- 4) Wideband, fully adaptive noise cancellation and narrowband impulsive noise processing in software.
- 5) A direct serial digital data link between the signal acquisition equipment and the computer used to make the location calculations. This would speed the collection of measured data and reduce the chance of recording errors.
- 6) High-efficiency, constant level sine wave transmitters for miners would eliminate harmonic interference and signal decay, and extend battery life.

## Appendix I. Summary of method used to determine power spectral density for cancellation tests.

Program used for the summation of FFTs on the Data 6000 Wave Analyzer (Data Precision, Analogic Corp.):

```
10 MAGCA1 = FFT (Buf A1,,0,0,0,3)
20 SQ.A1 = SQ (MAGCA1)
30 ADD.A1 = ADD.A1 + SQ.A1
```

Calculating the power spectral density:

$$\text{PSD} = \frac{R * \Delta t * N}{2 * N_1} \quad \text{in } V^2/\text{Hz}$$

R = reading on display (cursor "ON")  
 $\Delta t$  = sampling interval (5 ms in this analysis)  
 N = number of samples (512 in this analysis)  
 $N_1$  = number of squared FFTs summed.

$$\text{dBHo} = 10 \log \frac{\text{PSD}}{G^2}$$

G = channel gain, including recorder, in V/(A/m).

## Appendix II. Location Test Data Sheets.

The following abbreviations are used in the Sensor Data of the Sensor Data Unit data tables, in order:

- CHAN - the channel (X,Y, or Z) corresponding to the following three entries.
- Ampl - the displayed signal amplitude in pictoteslas.
- p - the displayed phase in degrees. For a reference channel (see below), phase is relative to the SDU clock. For a non-reference channel, phase is relative to reference channel.
- SNR - the long-term signal-to-noise ratio in decibels of the individual channel.
- REF - the reference channel of the SDU. This is selected automatically according to the strongest signal.
- SNRS - the long-term system signal-to-noise ratio in decibels.
- T - the elapsed time in seconds since system reset.
- PM - the phase difference in degrees between the SDU's reference channel and the primary SDU's reference channel.
- SNRS - the short-term system signal-to-noise ratio in decibels.
- T - the low-pass filter time constant in seconds.

----- PROJECT NAME (4 CHAR) -----

-----  
KM02  
-----

===== DATE & TIME (25 CHAR) =====

OCTOBER 10, 1984

Wednesday P.M.

===== MINE LOCATION (25 CHAR) =====

K-M, HOBBS, NEW MEXICO

===== COMMENTS (25 CHAR) =====

POSITION 1 - 1000' LOOP

===== COORDINATE SYSTEM BASIS (25 CHAR) =====

TRANSLATED MINE COORDINATES

COORDINATE X--AZIMUTH	BASELINE UNITS	SIGNAL FREQUENCY	PRIMARY SDU
90	F	10.6	B
(0-360 DEG)	(F/M)	(HZ)	(A/B/C)

===== EQUIPMENT SERIAL NUMBERS =====

SDU A: 1

SENSOR A: 1

SDU B: 4

SENSOR B: 4

SDU C: 3

SENSOR C: 3

===== SENSOR PLACEMENT DATA =====

SEN	X-LOC	Y-LOC	Z-LOC	X-AZM
A	-576.75	50.88	-6.0	144.2
B	-128.57	308.62	-3.0	151.0
C	295.67	552.18	0.0	147.5



TIME (HH:MM)	12:33	PROJECT	KM02
EXPECTED CURRENT (AMPS)	TIMES / \	EXPECTED AREA (SQ-METERS)	EQUALS ---
			EXPECTED MOMENT (AMP×M×M) 4916

## SENSOR DATA UNIT A

CHAN	Amp1 (pT)	P (DEG)	SNR		
X	0.3706 E01	-172	36		
Y	0.5211 E01	-171	30		
Z	0.4616 E01	168	39		
REF	SNRS	T	PM	SNRS	T
Z	30	93	-108	36	15

## SENSOR DATA UNIT B

CHAN	Amp1 (pT)	P (DEG)	SNR		
X	0.5564 E01	-175	38		
Y	0.2815 E01	-179	33		
Z	0.1016 E02	80	52		
REF	SNRS	T	PM	SNRS	T
Z	41	314	-0	56	15

## SENSOR DATA UNIT C

CHAN	Amp1 (pT)	P (DEG)	SNR		
X	0.5000 E01	178	33		
Y	0.3742 E01	111	37		
Z	0.9429 E01	-6	35		
REF	SNRS	T	PM	SNRS	T
Y	35	420	-24	42	15

TIME (HH:MM)	12:45	PROJECT	KM02
EXPECTED CURRENT (AMPS)	TIMES	EXPECTED AREA (SQ-METERS)	EQUALS
			---
			---
			4200
			(AMP×M×M)

## SENSOR DATA UNIT A

CHAN	Amp1 (pT)	P (DEG)	SNR
X	0.3750 E01	-170	34
Y	0.5238 E01	-173	28
Z	0.4644 E01	-180	44
REF	SNRS	T	PM
Z	31	590	-87

## SENSOR DATA UNIT B

CHAN	Amp1 (pT)	P (DEG)	SNR
X	0.5566 E01	-175	39
Y	0.2836 E01	-178	33
Z	0.1016 E02	105	53
REF	SNRS	T	PM
Z	42	720	-0

## SENSOR DATA UNIT C

CHAN	Amp1 (pT)	P (DEG)	SNR
X	0.5001 E01	179	35
Y	0.3726 E01	157	38
Z	0.9430 E01	-5	37
REF	SNRS	T	PM
Y	36	819	-43

TIME (HH:MM)	13:00	PROJECT	KM02
EXPECTED CURRENT (AMPS)	TIMES	EXPECTED AREA (SQ-METERS)	EQUALS
			4900
			(AMP×M×M)

## SENSOR DATA UNIT A

CHAN	Amp1 (pT)	P (DEG)	SNR
X	0.3737 E01	-171	49
Y	0.5105 E01	-171	50
Z	0.4777 E01	-169	59
REF	SNRS	T	PM
Z	48	38	-42

## SENSOR DATA UNIT B

CHAN	Amp1 (pT)	P (DEG)	SNR
X	0.5544 E01	-175	43
Y	0.2814 E01	-177	38
Z	0.1015 E02	159	67
REF	SNRS	T	PM
Z	49	96	0

## SENSOR DATA UNIT C

CHAN	Amp1 (pT)	P (DEG)	SNR
X	0.4955 E01	179	39
Y	0.3703 E01	-117	41
Z	0.9419 E01	-8	37
REF	SNRS	T	PM
Y	38	140	-78

TIME (HH:MM)	13:10	PROJECT	KM02
EXPECTED CURRENT (AMPS)	TIMES	EXPECTED AREA (SQ-METERS)	EQUALS
			5000

## SENSOR DATA UNIT A

CHAN	Amp1 (pT)	P (DEG)	SNR
X	0.3708 E1	-171	34
Y	0.5202 E1	-171	31
Z	0.4640 E1	-164	50
REF	SNRS	T	PM
Z	34	585	-14

## SENSOR DATA UNIT B

CHAN	Amp1 (pT)	P (DEG)	SNR
X	0.5549 E1	-175	38
Y	0.2836 E1	-175	31
Z	0.1014 E2	-168	57
REF	SNRS	T	PM
Z	41	633	0

## SENSOR DATA UNIT C

CHAN	Amp1 (pT)	P (DEG)	SNR
X	0.4979 E1	-178	34
Y	0.3689 E1	-59	36
Z	0.9406 E1	-6	34
REF	SNRS	T	PM
Y	34	681	-104

TIME (HH:MM)	13:20	PROJECT	KM02
EXPECTED CURRENT (AMPS)	TIMES	EXPECTED AREA (SQ-METERS)	EQUALS
			5000
			(AMP×M×M)

## SENSOR DATA UNIT A

CHAN	Amp1 (pT)	P (DEG)	SNR		
X	0.3721 E1	-171	33		
Y	0.5197 E1	-169	29		
Z	0.4635 E1	-161	46		
REF	SNRS	T	PM	SNRS	T
Z	32	1170	17	43	15

## SENSOR DATA UNIT B

CHAN	Amp1 (pT)	P (DEG)	SNR		
X	0.5553 E1	-175	38		
Y	0.2824 E1	-178	31		
Z	0.1013 E2	-133	58		
REF	SNRS	T	PM	SNRS	T
Z	41	1220	0	46	15

## SENSOR DATA UNIT C

CHAN	Amp1 (pT)	P (DEG)	SNR		
X	0.4978 E1	177	34		
Y	0.3694 E1	6	35		
Z	0.9398 E1	-7	35		
REF	SNRS	T	PM	SNRS	T
Y	35	1262	-133	36	15

TIME (HH:MM)	13:30	PROJECT	KM02
EXPECTED CURRENT (AMPS)	TIMES	EXPECTED AREA (SQ-METERS)	EQUALS
	\ /		---
	-   -		---
	/ \		
			4913
			(AMP×M×M)

## SENSOR DATA UNIT A

CHAN	Amp1 (pT)	P (DEG)	SNR
X	0.3715 E1	-172	34
Y	0.5187 E1	-171	30
Z	0.4632 E1	-158	45

REF	SNRS	T	PM	SNRS	T
Z	32	1614	41	42	15

## SENSOR DATA UNIT B

CHAN	Amp1 (pT)	P (DEG)	SNR
X	0.5547 E1	-175	39
Y	0.2816 E1	-177	31
Z	0.1012 E2	-106	56

REF	SNRS	T	PM	SNRS	T
Z	41	1688	0	51	15

## SENSOR DATA UNIT C

CHAN	Amp1 (pT)	P (DEG)	SNR
X	0.4976 E1	177	34
Y	0.3694 E1	58	35
Z	0.9390 E1	-7	35

REF	SNRS	T	PM	SNRS	T
Y	35	1736	-157	47	15

----- PROJECT NAME (4 CHAR) -----

-----  
KMBC  
-----

===== DATE & TIME (25 CHAR) =====

OCTOBER 10, 1984

Wednesday P.M.

===== MINE LOCATION (25 CHAR) =====

K-M, HOBBS, NEW MEXICO

===== COMMENTS (25 CHAR) =====

SENSORS B AND C ONLY

===== COORDINATE SYSTEM BASIS (25 CHAR) =====

TRANSLATED MINE COORDINATES

COORDINATE X--AZIMUTH	BASELINE UNITS	SIGNAL FREQUENCY	PRIMARY SDU
90	F	10.6	A
(0-360 DG)	(F/M)	(HZ)	(A/B/C)

===== EQUIPMENT SERIAL NUMBERS =====

SDU A: 4

SENSOR A: 4

SDU B: 3

SENSOR B: 3

SDU C: 4

SENSOR C: 4

===== SENSOR PLACEMENT DATA =====

SEN	X-LOC	Y-LOC	Z-LOC	X-AZM
A	-128.57	308.62	-3.0	151.0
B	295.67	552.18	0.0	147.5
C	-128.57	308.62	-3.0	151.0

TIME (HH:MM)	12:45	PROJECT	KMBC
EXPECTED CURRENT (AMPS)	TIMES	EXPECTED AREA (SQ-METERS)	EQUALS
			4200
			(AMP×M×M)

## SENSOR DATA UNIT A

CHAN	Amp1 (pT)	P (DEG)	SNR
X	0.5566 E1	-175	39
Y	0.2836 E1	-178	33
Z	0.1016 E2	105	53

REF	SNRS	T	PM	SNRS	T
Z	42	710	-0	53	15

## SENSOR DATA UNIT B

CHAN	Amp1 (pT)	P (DEG)	SNR
X	0.5001 E1	179	35
Y	0.3726 E1	157	38
Z	0.9430 E1	-5	37

REF	SNRS	T	PM	SNRS	T
Y	36	819	-43	45	15

## SENSOR DATA UNIT C

CHAN	Amp1 (pT)	P (DEG)	SNR
X	0.5566 E1	-175	39
Y	0.2836 E1	-178	33
Z	0.1016 E2	105	53

REF	SNRS	T	PM	SNRS	T
Z	42	710	-0	53	15



PROJECT NAME (4 CHAR)

KMCA

DATE & TIME (25 CHAR)

OCTOBER 10, 1984

Wednesday P.M.

MINE LOCATION (25 CHAR)

K-M, HOBBS, NEW MEXICO

COMMENTS (25 CHAR)

SENSORS A & C

COORDINATE SYSTEM BASIS (25 CHAR)

TRANSLATED MINE COORDINATES

COORDINATE X--AZIMUTH	BASELINE UNITS	SIGNAL FREQUENCY	PRIMARY SDU
90	F	10.6	A
(0-360 DG)	(F/M)	(HZ)	(A/B/C)

EQUIPMENT SERIAL NUMBERS

SDU A: 1	SENSOR A: 1
SDU B: 3	SENSOR B: 3
SDU C: 3	SENSOR C: 3

SENSOR PLACEMENT DATA

SEN	X-LOC	Y-LOC	Z-LOC	X-AZM
A	-576.8	50.88	-6.0	90
B	295.7	552.20	0.0	90
C	295.7	552.20	0.0	90

TIME (HH:MM)	12:45	PROJECT	KMCA
EXPECTED CURRENT (AMPS)	EXPECTED TIMES	EXPECTED AREA (SQ-METERS)	EXPECTED MOMENT (AMP×M×M)
	\\ /		5000
	- -		
	/ \		

## SENSOR DATA UNIT A

CHAN	Amp1 (pT)	P (DEG)	SNR		
X	-7.538	0	34		
Y	-0.0262	0	28		
Z	5.434	0	44		
REF	SNRS	T	PM	SNRS	T
Z	31	590	0	44	15

## SENSOR DATA UNIT B

CHAN	Amp1 (pT)	P (DEG)	SNR		
X	0.5520	0	35		
Y	7.546	0	38		
Z	11.45	0	37		
REF	SNRS	T	PM	SNRS	T
Y	36	819	0	45	15

## SENSOR DATA UNIT C

CHAN	Amp1 (pT)	P (DEG)	SNR		
X	0.5520	0	35		
Y	7.546	0	38		
Z	11.45	0	37		
REF	SNRS	T	PM	SNRS	T
Y	36	819	0	45	15

----- PROJECT NAME (4 CHAR) -----

=====

KMAB

-----

=====

DATE & TIME (25 CHAR)

-----

OCTOBER 10, 1984

Wednesday P.M.

-----

=====

MINE LOCATION (25 CHAR)

-----

K-M, HOBBS, NEW MEXICO

-----

=====

COMMENTS (25 CHAR)

-----

SENSORS A & B ONLY

-----

=====

COORDINATE SYSTEM BASIS (25 CHAR)

-----

TRANSLATED MINE COORDINATES

-----

COORDINATE X--AZIMUTH	BASELINE UNITS	SIGNAL FREQUENCY	PRIMARY SDU
90	F	10.6	B
(0-360 DG)	(F/M)	(HZ)	(A/B/C)

=====

EQUIPMENT SERIAL NUMBERS

-----

SDU A: 1

SENSOR A: 1

SDU B: 4

SENSOR B: 4

SDU C: 4

SENSOR C: 4

-----

=====

SENSOR PLACEMENT DATA

-----

SEN	X-LOC	Y-LOC	Z-LOC	X-AZM
A	-576.75	50.88	-6.0	90
B	-128.57	308.62	-3.0	90
C	-128.57	308.62	-3.0	90

TIME (HH:MM)	12:45	PROJECT	KMAB
EXPECTED CURRENT (AMPS)	TIMES	EXPECTED AREA (SQ-METERS)	EQUALS
	\ /		---
	-   -		---
	/ \		
			4800
			(AMP x M x M)

## SENSOR DATA UNIT A

CHAN	Amp1 (pT)	P (DEG)	SNR
X	-7.538	0	34
Y	-0.0262	0	28
Z	5.434	0	44
REF	SNRS	T	PM
Z	31	590	0

## SENSOR DATA UNIT B

CHAN	Amp1 (pT)	P (DEG)	SNR
X	-6.212	0	39
Y	4.207	0	33
Z	12.20	0	53
REF	SNRS	T	PM
Z	42	710	0

## SENSOR DATA UNIT C

CHAN	Amp1 (pT)	P (DEG)	SNR
X	-6.212	0	39
Y	4.207	0	33
Z	12.20	0	53
REF	SNRS	T	PM
Z	42	710	0

----- PROJECT NAME (4 CHAR) -----

=====

KMNR

-----

DATE & TIME (25 CHAR)

OCTOBER 10, 1984

Wednesday P.M.

MINE LOCATION (25 CHAR)

K-M, HOBBS, NEW MEXICO

COMMENTS (25 CHAR)

NO ROTATIONS FROM BASELINE

COORDINATE SYSTEM BASIS (25 CHAR)

TRANSLATED MINE COORDINATES

COORDINATE X--AZIMUTH	BASELINE UNITS	SIGNAL FREQUENCY	PRIMARY SDU
90	F	10.6	B
(0-360 DG)	(F/M)	(HZ)	(A/B/C)

EQUIPMENT SERIAL NUMBERS

SDU A: 1	SENSOR A: 1
SDU B: 4	SENSOR B: 4
SDU C: 3	SENSOR C: 3

SENSOR PLACEMENT DATA

SEN	X-LOC	Y-LOC	Z-LOC	X-AZM
A	-576.75	50.88	-6.0	150.1
B	-128.57	308.62	-3.0	150.1
C	295.67	552.18	0.0	150.1

TIME (HH:MM)	12:45	PROJECT	KMNR
EXPECTED CURRENT (AMPS)	TIMES	EXPECTED AREA (SQ-METERS)	EQUALS
			4200

SENSOR DATA UNIT A

CHAN	Amp1 (pT)	P (DEG)	SNR
X	0.3750 E01	-170	34
Y	0.5238 E01	-173	28
Z	0.4644 E01	-180	44

REF	SNRS	T	PM	SNRS	T
Z	31	590	-87	44	15

SENSOR DATA UNIT B

CHAN	Amp1 (pT)	P (DEG)	SNR
X	0.5566 E01	-175	39
Y	0.2836 E01	-178	33
Z	0.1016 E02	105	53

REF	SNRS	T	PM	SNRS	T
Z	42	710	-0	53	15

SENSOR DATA UNIT C

CHAN	Amp1 (pT)	P (DEG)	SNR
X	0.5001 E01	179	35
Y	0.3726 E01	157	38
Z	0.9430 E01	-5	37

REF	SNRS	T	PM	SNRS	T
Y	36	819	-43	45	15

----- PROJECT NAME (4 CHAR) -----

=====

KMCR

-----

=====

DATE & TIME (25 CHAR)

-----

OCTOBER 10, 1984

Wednesday P.M.

-----

=====

MINE LOCATION (25 CHAR)

-----

K-M, HOBBS, NEW MEXICO

-----

=====

COMMENTS (25 CHAR)

-----

COMPASS READING FOR AZIM

-----

=====

COORDINATE SYSTEM BASIS (25 CHAR)

-----

TRANSLATED MINE COORDINATES

-----

COORDINATE X--AZIMUTH	BASELINE UNITS	SIGNAL FREQUENCY	PRIMARY SDU
90	F	10.6	B
(0-360 DG)	(F/M)	(HZ)	(A/B/C)

=====

EQUIPMENT SERIAL NUMBERS

-----

SDU A: 1

SENSOR A: 1

SDU B: 4

SENSOR B: 4

SDU C: 3

SENSOR C: 3

-----

=====

SENSOR PLACEMENT DATA

-----

SEN	X-LOC	Y-LOC	Z-LOC	X-AZM
A	-576.75	50.88	-6.0	143.0
B	-128.57	308.62	-3.0	149.5
C	295.67	552.18	0.0	147.0

-----

TIME (HH:MM)	12:45	PROJECT	KMCR
--------------	-------	---------	------

EXPECTED CURRENT (AMPS)	TIMES	EXPECTED AREA (SQ-METERS)	EQUALS	EXPECTED MOMENT (AMP×M×M)
				4200

SENSOR DATA UNIT A

CHAN	Amp1 (pT)	P (DEG)	SNR
X	0.3750 E01	-170	34
Y	0.5238 E01	-173	28
Z	0.4644 E01	-180	44

REF	SNRS	T	PM	SNRS	T
Z	31	590	-87	44	15

SENSOR DATA UNIT B

CHAN	Amp1 (pT)	P (DEG)	SNR
X	0.5566 E01	-175	39
Y	0.2836 E01	-178	33
Z	0.1016 E02	105	53

REF	SNRS	T	PM	SNRS	T
Z	42	710	-0	53	15

SENSOR DATA UNIT C

CHAN	Amp1 (pT)	P (DEG)	SNR
X	0.5001 E01	179	35
Y	0.3726 E01	157	38
Z	0.9430 E01	-5	37

REF	SNRS	T	PM	SNRS	T
Y	36	819	-43	45	15



PROJECT NAME (4 CHAR)

KM03

DATE & TIME (25 CHAR)

OCTOBER 10, 1984

Wednesday P.M.

MINE LOCATION (25 CHAR)

K-M, HOBBS, NEW MEXICO

COMMENTS (25 CHAR)

POSITION 2- 480' LOOP

COORDINATE SYSTEM BASIS (25 CHAR)

TRANSLATED MINE COORDINATES

COORDINATE X--AZIMUTH	BASELINE UNITS	SIGNAL FREQUENCY	PRIMARY SDU
90	F	10.6	B
(0-360 DG)	(F/M)	(HZ)	(A/B/C)

EQUIPMENT SERIAL NUMBERS

SDU A:	1	SENSOR A:	1
SDU B:	4	SENSOR B:	4
SDU C:	3	SENSOR C:	3

SENSOR PLACEMENT DATA

SEN	X-LOC	Y-LOC	Z-LOC	X-AZM
A	-576.75	50.88	-6.0	144.2
B	-128.57	308.62	-3.0	151.0
C	295.67	552.18	0	147.5

TIME (HH:MM)	13:45	PROJECT	KM03
EXPECTED CURRENT (AMPS)	TIMES	EXPECTED AREA (SQ-METERS)	EQUALS
			680
			(AMP×M×M)

## SENSOR DATA UNIT A

CHAN	Amp1 (pT)	P (DEG)	SNR
X	0.2094 E0	167	19
Y	0.7755 E-1	58	8
Z	0.3030 E1	-65	46
REF	SNRS	T	PM
Z	32	75	105
SNRS	T	SNRS	T
		36	15

## SENSOR DATA UNIT B

CHAN	Amp1 (pT)	P (DEG)	SNR
X	0.1142 E0	-155	12
Y	0.1197 E1	6	20
Z	0.1742 E1	40	54
REF	SNRS	T	PM
Z	25	125	-0
SNRS	T	SNRS	T
		34	15

## SENSOR DATA UNIT C

CHAN	Amp1 (pT)	P (DEG)	SNR
X	0.1457 E-1	-133	**
Y	0.9325 E0	-98	21
Z	0.5173 E0	-16	33
REF	SNRS	T	PM
Y	20	171	142
SNRS	T	SNRS	T
		30	15

TIME (HH:MM)	13:55	PROJECT	KM03
--------------	-------	---------	------

EXPECTED CURRENT (AMPS)	TIMES	EXPECTED AREA (SQ-METERS)	EQUALS	EXPECTED MOMENT (AMP×M×M)
	\ /		---	900
	-   -		---	
	/ \			

## SENSOR DATA UNIT A

CHAN	Amp1 (pT)	P (DEG)	SNR
X	2280 E0	-171	9
Y	6969 E-1	-132	-7
Z	3004 E1	-57	40

REF	SNRS	T	PM	SNRS	T
Z	25	624	136	40	15

## SENSOR DATA UNIT B

CHAN	Amp1 (pT)	P (DEG)	SNR
X	1569 E0	172	6
Y	1201 E1	7	22
Z	1736 E1	78	50

REF	SNRS	T	PM	SNRS	T
Z	25	683	0	34	15

## SENSOR DATA UNIT C

CHAN	Amp1 (pT)	P (DEG)	SNR
X	1615 E-1	81	**
Y	9571 E0	-32	23
Z	5106 E0	-17	28

REF	SNRS	T	PM	SNRS	T
Y	20	717	112	31	15

----- PROJECT NAME (4 CHAR) -----

===== KM04 =====

===== DATE & TIME (25 CHAR) =====

OCTOBER 11, 1984

Thursday A.M.

===== MINE LOCATION (25 CHAR) =====

K-M, HOBBS, NEW MEXICO

===== COMMENTS (25 CHAR) =====

POSITION 3 - SMALL 400' LOOP

===== COORDINATE SYSTEM BASIS (25 CHAR) =====

TRANSLATED MINE COORDINATES

COORDINATE X--AZIMUTH	BASELINE UNITS	SIGNAL FREQUENCY	PRIMARY SDU
90	F	10.6	B
(0-360 DG)	(F/M)	(HZ)	(A/B/C)

===== EQUIPMENT SERIAL NUMBERS =====

SDU A:	1	SENSOR A:	1
SDU B:	4	SENSOR B:	4
SDU C:	3	SENSOR C:	3

===== SENSOR PLACEMENT DATA =====

SEN	X-LOC	Y-LOC	Z-LOC	X-AZM
A	-576.8	50.88	-6.0	144.2
B	-128.6	380.60	-3.0	151.0
C	295.7	552.2	0.0	147.5

TIME (HH:MM)	10:50	PROJECT	KM04
EXPECTED CURRENT (AMPS)	TIMES	EXPECTED AREA (SQ-METERS)	EQUALS
	\ /		---
	-   -		---
	/ \		
			700
			(AMP×M×M)

## SENSOR DATA UNIT A

CHAN	Amp1 (pT)	P (DEG)	SNR
X	0.4353 E0	-123	23
Y	0.9589 E0	-1	17
Z	0.1073 E1	163	15
REF	SNRS	T	PM
X	15	119	176
			SNRS
			19
			T
			15

## SENSOR DATA UNIT B

CHAN	Amp1 (pT)	P (DEG)	SNR
X	0.5946 E0	-175	22
Y	0.2020 E0	-174	14
Z	0.1956 E1	-134	55
REF	SNRS	T	PM
Z	29	170	0
			SNRS
			43
			T
			15

## SENSOR DATA UNIT C

CHAN	Amp1 (pT)	P (DEG)	SNR
X	0.4431 E0	-177	13
Y	0.8140 E0	7	22
Z	0.1428 E1	34	40
REF	SNRS	T	PM
Z	23	207	-170
			SNRS
			40
			T
			15

TIME (HH:MM)	11:05	PROJECT	KM04
--------------	-------	---------	------

EXPECTED CURRENT (AMPS)	TIMES	EXPECTED AREA (SQ-METERS)	EQUALS	EXPECTED MOMENT (AMPxMxM)
	\ /		---	
	-   -		---	700
	/ \			

## SENSOR DATA UNIT A

CHAN	Amp1 (pT)	P (DEG)	SNR
X	0.4795 E0	-148	17
Y	0.8883 E0	23	13
Z	0.1060 E1	-172	15

REF	SNRS	T	PM	SNRS	T
X	14	933	-146	20	15

## SENSOR DATA UNIT B

CHAN	Amp1 (pT)	P (DEG)	SNR
X	0.6269 E0	-167	18
Y	0.1955 E0	-176	10
Z	0.1948 E1	-102	49

REF	SNRS	T	PM	SNRS	T
Z	26	977	0	40	15

## SENSOR DATA UNIT C

CHAN	Amp1 (pT)	P (DEG)	SNR
X	0.4419 E0	-175	15
Y	0.7974 E0	7	22
Z	0.1432 E1	99	44

REF	SNRS	T	PM	SNRS	T
Z	24	1013	157	40	15

TIME (HH:MM)	11:25	PROJECT	KM04
EXPECTED CURRENT (AMPS)	TIMES	EXPECTED AREA (SQ-METERS)	EQUALS
			---
			---
			700
			(AMP×M×M)

## SENSOR DATA UNIT A

CHAN	Amp1 (pT)	P (DEG)	SNR
X	0.4876 E0	-159	18
Y	0.8893 E0	10	13
Z	0.1065 E1	-170	16

REF	SNRS	T	PM	SNRS	T
X	15	2156	-87	19	15

## SENSOR DATA UNIT B

CHAN	Amp1 (pT)	P (DEG)	SNR
X	0.6283 E0	-179	19
Y	0.2017 E0	-178	10
Z	0.1946 E1	-57	49

REF	SNRS	T	PM	SNRS	T
Z	27	2196	0	38	15

## SENSOR DATA UNIT C

CHAN	Amp1 (pT)	P (DEG)	SNR
X	0.4447 E0	-174	16
Y	0.7938 E0	8	22
Z	0.1429 E1	-167	44

REF	SNRS	T	PM	SNRS	T
Z	25	2237	107	37	15

TIME (HH:MM)	11:40	PROJECT	KM04
--------------	-------	---------	------

EXPECTED CURRENT (AMPS)	TIMES	EXPECTED AREA (SQ-METERS)	EQUALS	EXPECTED MOMENT (AMP×M×M)
	\ /		---	700
	- -		---	
	/ \			

## SENSOR DATA UNIT A

CHAN	Amp1 (pT)	P (DEG)	SNR
X	0.4898 E0	-171	19
Y	0.8891 E0	-7	13
Z	0.1063 E1	-173	16

REF	SNRS	T	PM	SNRS	T
X	15	3050	-43	16	15

## SENSOR DATA UNIT B

CHAN	Amp1 (pT)	P (DEG)	SNR
X	0.6286 E0	175	19
Y	0.1984 E0	-179	10
Z	0.1944 E1	-23	47

REF	SNRS	T	PM	SNRS	T
Z	27	3090	0	45	15

## SENSOR DATA UNIT C

CHAN	Amp1 (pT)	P (DEG)	SNR
X	0.4476 E0	-167	17
Y	0.7951 E0	5	22
Z	0.1428 E1	-96	44

REF	SNRS	T	PM	SNRS	T
Z	25	3125	70	40	15



TIME (HH:MM)	11:55	PROJECT	KM04
EXPECTED CURRENT (AMPS)	TIMES	EXPECTED AREA (SQ-METERS)	EQUALS
	\ /		---
	-   -		---
	/ \		
			700
			(AMP×M×M)

## SENSOR DATA UNIT A

CHAN	Amp1 (pT)	P (DEG)	SNR
X	0.4908 E0	-174	19
Y	0.8860 E0	-3	14
Z	0.1061 E1	175	16

REF	SNRS	T	PM	SNRS	T
X	15	4082	10	21	15

## SENSOR DATA UNIT B

CHAN	Amp1 (pT)	P (DEG)	SNR
X	0.6261 E0	175	19
Y	0.1983E0	-174	11
Z	0.1940 E1	18	44

REF	SNRS	T	PM	SNRS	T
Z	27	4182	0	39	15

## SENSOR DATA UNIT C

CHAN	Amp1 (pT)	P (DEG)	SNR
X	0.4463 E0	-175	17
Y	0.7929 E0	8	23
Z	0.1425 E1	-3	43

REF	SNRS	T	PM	SNRS	T
Z	26	4281	20	39	15

TIME (HH:MM)	12:10	PROJECT	KM04
EXPECTED CURRENT (AMPS)	TIMES	EXPECTED AREA (SQ-METERS)	EQUALS
	\ /		---
	-   -		---
	/ \		
			700
			(AMP×M×M)

## SENSOR DATA UNIT A

CHAN	Amp1 (pT)	P (DEG)	SNR		
X	0.4900 E0	179	19		
Y	0.8861 E0	-7	15		
Z	0.1060 E1	169	17		
REF	SNRS	T	PM	SNRS	T
X	16	4898	52	27	15

## SENSOR DATA UNIT B

CHAN	Amp1 (pT)	P (DEG)	SNR		
X	0.6247 E0	179	20		
Y	0.2005 E0	-167	11		
Z	0.1937 E1	48	44		
REF	SNRS	T	PM	SNRS	T
Z	27	4946	0	41	15

## SENSOR DATA UNIT C

CHAN	Amp1 (pT)	P (DEG)	SNR		
X	0.4455 E0	-178	17		
Y	0.7905 E0	6	23		
Z	0.1424 E1	56	42		
REF	SNRS	T	PM	SNRS	T
Z	26	4980	-10	37	15

TIME (HH:MM)	12:25	PROJECT	KM04
--------------	-------	---------	------

EXPECTED CURRENT (AMPS)	TIMES / \	EXPECTED AREA (SQ-METERS)	EQUALS ---	EXPECTED MOMENT (AMPxMxM)
				300

## SENSOR DATA UNIT A

CHAN	Amp1 (pT)	P (DEG)	SNR
X	.4897 E0	167	19
Y	.8866 E0	-5	15
Z	.1059 E1	170	17

REF	SNRS	T	PM	SNRS	T
X	16	5706	+94	27	15

## SENSOR DATA UNIT B

CHAN	Amp1 (pT)	P (DEG)	SNR
X	.6230 E0	-176	20
Y	.2005 E0	-154	11
Z	.1935 E1	80	43

REF	SNRS	T	PM	SNRS	T
Z	27	5757	0	37	15

## SENSOR DATA UNIT C

CHAN	Amp1 (pT)	P (DEG)	SNR
X	.4446 E0	-177	17
Y	.7887 E0	5	22
Z	.1423 E1	124	42

REF	SNRS	T	PM	SNRS	T
Z	26	5799	-47	35	15

## REFERENCES

1. Sacks, H. Kenneth, "Trapped Miner Location and Communication Systems," Underground Mine Communications (Part 4), Bureau of Mines Information Circular #8745, U.S. Department of the Interior, 1977, pp. 31-43.
2. Durkin, John, "Performance Evaluation of Electromagnetic Techniques for the Location of Trapped Miners," Bureau of Mines Report of Investigations #8711, U.S. Department of the Interior, 1982.
3. Rorden, L.H., et. al., "Phase 1 - Development of System Concept for Location of Trapped Miners in Deep Mines by an Electromagnetic Method," Phase 1 Report, U.S. Department of the Interior Bureau of Mines Contract J0199009, Develco, Inc., October 1979.
4. Rorden, L.H., et. al., "Methods and Apparatus Employing an Alternating Magnetic Field for Determining Location," (Patent applied for).
5. Morrison, H.F., et. al., "Experience with the EM-60 Electromagnetic System for Geothermal Exploration in Nevada," Geophysics, Vol. 48, No. 8 (August 1983), p. 1093.
6. Moore, T.C., et. al., "Borehole Location System Concept Demonstration Tests," Final Report (1132-780505), U.S. Department of the Interior Bureau of Mines Contract J0177074, Develco, Inc., May 1978.
7. Simmons, C.H., "Development and Prototype Production of a Trapped Miner Signalling Transmitter/Transceiver," U.S. Department of the Interior Bureau of Mines Contract J03950017, NTIS #PB82-24426U, June 1981.
8. Iufer, E.J., "20 Ft. Helmholtz Coil Calibration Report," Contract No. LA28H9450F, E.J. Iufer & Associates Inc., Los Altos, CA, January 5, 1984.
9. Raab, F.H., "Adaptive-Noise-Cancellation Techniques for Through-the-Earth Electromagnetics, Volume III," U.S. Department of the Interior, Bureau of Mines Contract J0318070, Green Mountain Radio Research Company, February 1984.
10. Evans, J.E., et. al., "Design of a Sanguine Noise Processor Based Upon Worldwide Extremely Low Frequency (ELF) Recordings," IEEE Transactions on Communications, Vol. Com-22, No. 4, pp. 528-539, April 1974.
11. Maxwell, E. and Stone, D., "Natural Fields from 1 cps to 100 kc," IEEE Transactions on Antennas and Propagation, Vol. AP11, No. 3, pp. 339-343, May 1963.